Quantum nuclear many-body dynamics and related aspects

Denis Lacroix

Quantum nuclear many-body dynamics and related aspects

Denis Lacroix*

GANIL, CEA and IN2P3, Boîte Postale 5027, 14076 Caen Cedex, France

This review article is devoted to a compilation of recent advances in the nuclear many-body dynamical problem. The building block of any microscopic model is the nuclear mean-field theory, designed to provide proper description of one-body observables. Important aspects related to mean-field and its relation to observables evolutions are presented. Currently applied nuclear mean-field theories are formulated within a Density Functional Theory (DFT) framework, the so-called Energy Density Functional (EDF) theory. In addition, beyond mean-field approaches, that are introduced to account for direct nucleon-nucleon collisions, pairing and/or configuration mixing, are strongly guided by the theory of Open Quantum Systems (OQS). Both DFT and OQS are interdisciplinary concepts that play a key role in the nuclear many-body problem and are discussed in this review. Beyond mean-field theories are illustrated to fusion, transfer and break-up reactions. Finally, more phenomenological approaches dedicated to multifragmentation reactions and low energy spallation reactions are introduced.

Contents

*Electronic address: lacroix@ganil.fr

I. INTRODUCTION

This review, called "Habilitation à diriger les recherches" in France, summarizes ten years of research performed by myself and my collaborators in nuclear physics. When writing it, I was hesitating between two options (i) giving a summary and/or highlights from specific publications as it is done sometimes or (ii) providing a more detailed discussion of my different research interests starting from first principles and ending with the current discussion and status in different fields. I found more useful for myself, and I hope for the reader, to choose the second option. For this reason some aspects discussed here are introduced in a rather academic way.

Atomic nuclei belong to the class of strong interacting Many-Body systems and share many features with other systems studied in condensed matter physics, atomic physics and chemistry. Nuclei are extraordinary objects that enable to study quantum mechanics, equilibrium and non-equilibrium thermodynamic in mesoscopic systems. Although I belong to the nuclear physics community, most of the discussions presented below are not specific to nuclear physics and could easily

be translated to other areas of physics like electrons transport in metals, dynamics of Bose-Einstein condensates, etc. These fields have been tremendously stimulated by numerous observations in laboratory. General aspects of physics related to Open-Quantum systems, Many-Body physics and density functional theory will be discussed below.

One of the main objectives of my research was to provide quantum transport theories able to describe the richness of Many-Body dynamics. A guideline as well as a short motivation for the topics covered in this review are given below:

- **Open Quantum System Theory:** Transport theories developed for the many-body problem are strongly guided by the theory of Open Quantum System. To fully understand this connection, I summarize in chapter II some general aspects concerning Open Quantum System theory as well as some advances made recently.

- **N-body Transport theories:** Similarly to other fields, nuclear physics faces the complexity of the many-body problem. As a consequence, the so-called independent-particle (also called mean-field) approximation is a key concept at the heart of many actual applications. Most of the work dedicated to transport theories is devoted to going "beyond" the independent particle approximation and introduce physical effects like pairing, direct two-body collisions and/or configuration mixing. Some aspects of the mean-field approximation are given in section III, whereas an introduction to theories beyond mean-field are given in section IV.

- **Energy Density Functional theory (EDF):** Application of transport theories in nuclear systems have been completely dissociated from their formal introduction. The reason is rather simple and comes from the fact that, strictly speaking, theories introduced in section III and IV cannot be applied to realistic problems due to the complexity of the bare nuclear Hamiltonian. Instead, Hamiltonian-based theories are usually replaced by Functional-based theories. An introduction to the so-called Energy Density Functional theory and its similarities/differences with the Density Functional Theory are given in section V. Recent discussions of the so-called "beyond mean-field approach" within EDF theory for static properties of nuclei are outlined.

- **Time-Dependent Energy Density Functional Theory:** Guided by the Hamiltonian based framework given in section IV, several theories that extend the independent-particle picture have been recently applied to describe the nuclear dynamics: collective motion, fusion/transfer reactions and break-up. These applications are discussed in section VI.

- **Phenomenology of Fermi energy nuclear reactions:** it is shown in section VII that many phenomena occurring during violent reactions can be described using very simple rules. Applications of these simple rules have led to the development of phenomenological models dedicated to Heavy-Ion and nucleon-Ion reactions.

The different chapters of this review are written in such a way that they can be red independently from each other. Therefore, the reader who is less interested in some of the aspects developed here can directly jump to the desired section.

II. PREAMBLE: OPEN QUANTUM SYSTEM THEORY

A. Introduction

Most of the systems present in nature are too complex to be exactly integrable. Their complexity is generally due to the large number of degrees of freedom to be considered. This prevents from solving the problem exactly. It should also be kept in mind that most often the full description of a complex quantum system is rarely required since its microscopic equation contains in general much more information than one is really willing to have or, said differently, that one can observe in practice. Then, only a reduced description where few selected degrees of freedom of interest is searched.

This simplification leads sometimes to rather schematic but most often very useful models to understand physical phenomena. Scientists however face the following dilemma: on the one hand, one needs to reduce at maximum the complexity of a problem to make it tractable and useful, on the other hand, most of the interesting aspects stem from the interaction of the selected degrees of freedom with the environment which has been recognized as non-relevant. Therefore if one completely isolates the degrees of freedom of interest, most of the important aspects will be missed. To incorporate them properly, the system should be considered as open to its surrounding and the coupling with irrelevant degrees of freedom should be at least approximately accounted for.

Numerous concepts in our understanding of quantum mechanics have emerged from the understanding and description of a system coupled to an environment: measurement, decoherence, appearance of classical world, irreversible processes and dissipation... All these phenomena which are often encompassed in the "theory of open quantum systems", bridge different fields of physics and chemistry (Breuer and Petruccione, 2002; Gardiner and Zoller, 2000; Joos *et al.*, 2003; Weiss, 1999). The principal motivation of treating the theory of open quantum system in this document is the crucial role it has and continues to play in the development of transport theories in correlated many-body systems (see section IV). Here, the goal is not to present an exhaustive review on all methods used to treat open quantum dynamics, but to give some highlights on theories that have their counterpart in many-body physics. In addition, a discussion on non-Markovian effects, that are of actual interest, is given. Standard approaches based on projection operator theory are first introduced. New approaches based on quantum Monte-Carlo and able to describe exactly the dynamics of an Open Quantum System (OQS) are then discussed.

B. Open Quantum Systems : general aspects and approximations

The starting point of open quantum system theories is a system (S) interacting with a surrounding environment (E). We assume here that the total system (S+E) is described by the Hamiltonian

$$H = H_S + H_E + V. \tag{1}$$

H_S (resp. H_E) acts on the system (resp. env.) only while V induces a coupling between the two sub-systems. A pictorial view of the system+environment total space is presented in Fig. 1. Starting from an initial total density $D(0)$, the dynamical evolution is given by the Liouville von-Neumann equation on the density:

$$i\hbar \frac{dD(t)}{dt} \;=\; [H, D(t)]. \tag{2}$$

In many physical situations, the total number of degrees of freedom to follow in time prevents from solving exactly this equation and only a sub-class of the degrees of freedom (called hereafter relevant) associated to the system are of direct interest. One of the leitmotivs of OQS theory is to find accurate approximations for the system evolution without following explicitly irrelevant degrees of freedom associated to the environment and therefore reduce the complexity of the initial problem. An overview of the "standard" approximations made from Eq. (2) is given below. This overview will be helpful to introduce basic concepts and quantities used in OQS.

Introducing the interaction picture, densities and operators (denoted generically by X) are given by

$$D_I(t) \;=\; U^\dagger(t,0) D(t) U(t,0), \qquad X_I(t) = U^\dagger(t,0) X U(t,0), \tag{3}$$

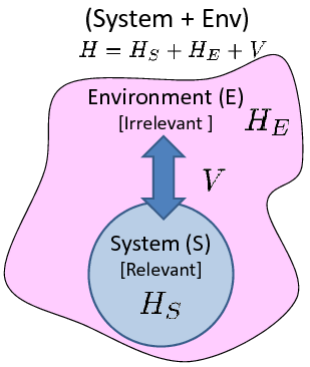

FIG. 1: *Schematic representation of a system coupled to an environment. The total system is closed while each subsystem is open with respect to its counterpart. As a consequence of the coupling, the evolution of each subsystem is not unitary leading to energy gain or loss. Here, we consider the separation into system and environment in a wide sense where the system can be regarded as selected relevant degrees of freedom in opposition to the rest of the total system called hereafter environment or irrelevant degrees of freedom.*

where $U(t,0)$ denotes the propagator associated to $H_S + H_E$. Eq. (2) transforms into $i\hbar\partial_t D_I(t) = [V_I(t), D_I(t)]$ and can be formally integrated as

$$D_I(t) = D_I(0) + \frac{1}{i\hbar}\int_0^t [V_I(s), D_I(s)]ds. \tag{4}$$

Reporting this expression into the equation of motion of D_I, leads to [1]

$$\frac{dD(t)}{dt} = -\frac{1}{\hbar^2}\int_0^t [V_I(t), [V_I(s), D(s)]]ds. \tag{5}$$

This equation is still exact. In order to reduce the complexity, a closed equation of motion of the system degrees of freedom only is searched. All the information on the system is contained in its reduced density $\rho_S(t) \equiv \mathrm{Tr}_E(D(t))$ where $\mathrm{Tr}_E(.)$ denotes the partial trace on the environment. The equation of motion of the system then reads

$$\frac{d\rho_S(t)}{dt} = -\frac{1}{\hbar^2}\int_0^t \mathrm{Tr}_E[V_I(t), [V_I(s), D(s)]]ds, \tag{6}$$

where the contribution of $D(0)$ is neglected. Above expression is still not closed since it involves the total density in the integral. In addition, the evolution of ρ_S at time t depends on the full history of the system+environment density, this is what will be called hereafter *memory effect*. The complexity often arises from the fact that, even if initially the total density writes in a simple separable form ($D = \rho_S(0) \otimes \rho_E(0)$), $D_I(s)$ becomes highly mixed as the time increases.

1. Born, Markov approximation and Redfield equation

To simplify the initial problem, two approximations are generally made: (i) the density remains separable $D(t) = \rho_S(t) \otimes \rho_E(t)$, (ii) in most cases, the environment degrees of freedom cannot be followed in time and $\rho_E(t)$ is replaced by a stationary density $\rho_E(t) \equiv R_E$. The stationary density choice depends on the physical situation, it is generally taken as a Gibbs thermal equilibrium density. Approximations (i) and (ii) are known as the *Born* and *Markov* approximations and are expected to be valid in the weak coupling limit for an environment with a number of degrees of freedom much larger than those of the system of interest. The equation of motion for ρ_S becomes:

$$\frac{d\rho_S}{dt} = -\frac{1}{\hbar^2}\int_0^t \mathrm{Tr}_E[V(t), [V(s), \rho_S(s) \otimes R_E]]ds. \tag{7}$$

---

[1] In the following, when no confusion is possible, D_I will simply be replaced by D to simplify notations.

Hereafter, it is assumed that the coupling is separable: $V = Q \otimes B$ where Q and B act on the system and environment respectively. To discuss the non-locality in time of the environment effect on the system, it is convenient to introduce the two-times correlation functions [2]:

$$D(t,s) \equiv i\langle[B, B(t-s)]\rangle_E \quad \text{and} \quad D_1(t,s) \equiv \langle\{B, B(t-s)\}_+\rangle_E, \tag{9}$$

where we have used the convention $\langle . \rangle_E \equiv \mathrm{Tr}_E(.R_E)$. Since the environment density has been replaced by a stationary density, the two memory functions only depends on $(t-s)$, such that the system density evolves in the Schrödinger picture according to the equation

$$\begin{aligned} i\hbar\frac{d\rho_S}{dt} &= [H_S, \rho_S] + \frac{1}{2i\hbar^2}\int_0^t ds D(t,s)[Q, \{Q(t-s), \rho_S(s)\}_+] \\ &\quad -\frac{1}{2\hbar^2}\int_0^t ds D_1(t,s)[Q, [Q(t-s), \rho_S(s)]]. \end{aligned} \tag{10}$$

This equation is a closed equation for the system density. It is however highly non-local in time and depends a priori on the full history of the system state. The importance of memory depends on the typical time τ_E over which D and D_1 decay out. This time scale is characteristic of the environment. Assuming that system degrees of freedom evolve much slowly than τ_E, one can neglect memory effects and replace the system density at time s by the its value at time t:

$$\frac{d\rho_S}{dt} = -\frac{1}{\hbar^2}\int_0^t \mathrm{Tr}_E[V_I(t), [V_I(s), \rho_S(t) \otimes R_E]]ds. \tag{11}$$

This approximation, known as *Markov* approximation leads to the so-called *Redfield Equation*. A further simplification can be made by extending the integral to infinity leading to the so-called *Markovian master equation*. When this approximation is not made, the theory is called *Non-Markovian*. In the following, an illustration of different levels of approximation is given using the Caldeira-Leggett model (Caldeira and Leggett, 1983). This model has been retained here not only because it is a pedagogical example but also for its role in the understanding of dissipation in quantum systems.

2. Illustration with the Caldeira-Leggett model

The Caldeira-Leggett model (Caldeira and Leggett, 1983) corresponds to a single harmonic oscillator coupled to an environment of harmonic oscillators initially at thermal equilibrium, i.e.

$$H_S = H_c + \frac{P^2}{2M} + \frac{1}{2}M\omega_0^2 Q^2, \qquad H_E = \sum_n \left(\frac{p_n^2}{2m_n} + \frac{1}{2}m_n\omega_n^2 x_n^2\right) \tag{12}$$

and $B \equiv -\sum_n \kappa_n x_n$ (Breuer and Petruccione, 2002). Here, $H_c = Q^2 \sum_n \frac{\kappa_n^2}{2m_n\omega_n^2}$ is the counter-term insuring that the physical frequency is ω_0. In that case, D and D_1 identify with the standard times correlation functions:

$$D(\tau) = 2\hbar\int_0^{+\infty} d\omega J(\omega)\sin(\omega\tau), \tag{13}$$

$$D_1(\tau) = 2\hbar\int_0^{+\infty} d\omega J(\omega)\coth(\hbar\omega/2k_BT)\cos(\omega\tau), \tag{14}$$

---

[2] With this definition

$$\langle B(t)B(s)\rangle_E = \frac{1}{2}(D_1(t,s) - iD(t,s)), \qquad \langle B(s)B(t)\rangle_E = \frac{1}{2}(D_1(t,s) + iD(t,s)). \tag{8}$$

where $J(\omega) \equiv \sum_n \frac{\kappa_n^2}{2m_n\omega_n}\delta(\omega-\omega_n)$ denotes the spectral density (Breuer and Petruccione, 2002; Leggett *et al.*, 1987). Due to the quadratic nature of the Hamiltonian, all the information on the system is contained in the first and second moments of P and Q operators. To illustrate the different philosophy used in open quantum system, equations of motion of $(\langle P\rangle, \langle Q\rangle)$ obtained respectively from Eq. (7) or (11) are given below.

Evolution of $(\langle P\rangle, \langle Q\rangle)$

Born Approximation	*Redfield Equation*
$\partial_t \langle Q(t)\rangle = \frac{\langle P(t)\rangle}{M}$	$\partial_t \langle Q(t)\rangle = \frac{\langle P(t)\rangle}{M}$
$\partial_t \langle P(t)\rangle = -M\omega_0^2 \langle Q(t)\rangle + \frac{1}{\hbar}\int_0^t D(t-s)\langle Q(s)\rangle ds$	$\partial_t\langle P\rangle = -M\langle Q(t)\rangle\left(\omega_0^2 - \frac{1}{\hbar M}\int_0^t \cos(\omega_0 s)D(s)ds\right) - \frac{1}{M\hbar\omega_0}\langle P(t)\rangle\int_0^t \sin(\omega_0 s)D(s)ds$

(15)

These equation significantly differs from each other. To solve the Born case, one should keep the memory of the expectation value of Q along the trajectory. In the Redfield case, all the memory effect are contained in the time dependence of transport coefficients and only the state of the system at time t needs to be known. Last, extending the integrals to infinity in the Redfield equation, gives

$$\frac{d\langle P(t)\rangle}{dt} = -M\omega_0'\langle Q(t)\rangle - \frac{\gamma}{M}\langle P(t)\rangle \tag{16}$$

where the standard dissipative equation in classical mechanics is recognized.

C. Standard Approximation for non-Markovian dynamics

The description of OQS given above fails in some cases to account for non-Markovian effects. Constructive frameworks that systematically extend theories presented above have been proposed. Two strategies, already illustrated by the Born and Redfield limit, are summarized here. In one case, similarly to the Born approximation, equation of motion for the system density that are non-local in time (Nakajima-Zwanzig (NZ) theory) are searched while in the other case time-local equations are found (Time-Convolution-Less (TCL) theory).

1. Liouville super-operators

As discussed above, degrees of freedom are separated into two classes associated with the relevant and irrelevant space. The projectors onto the relevant sub-space, denoted by $\mathcal{P}$, can be defined by introducing a fixed (time-independent) environment density R_E through

$$\mathcal{P}D(t) \equiv \rho_S(t)\otimes R_E. \tag{17}$$

The projector $\mathcal{Q}$ onto the irrelevant space is just defined through $\mathcal{Q}+\mathcal{P}=1$. Under the condition that $\mathrm{Tr}_E R_E = 1$, $\mathcal{P}/\mathcal{Q}$ verifies all projector properties. These projectors that act in the density space (Liouville space) are generally called super-operators and are written in Liouville notation. Similarly, it is convenient to introduce the super-operator $\mathcal{L}(t)$ associated with the density evolution

$$\frac{dD}{dt} = \frac{1}{i\hbar}[V_I(t), D(t)] \equiv \mathcal{L}(t)D(t), \tag{18}$$

as well as the associated super-propagator

$$\mathcal{G}_{\pm}^{\mathcal{X}}(t,s) = T_{\pm} e^{\int_s^t \mathcal{X}\mathcal{L}(s)ds}, \tag{19}$$

where T_+ (resp. T_-) denotes the chronological (resp anti-chronological) time ordering operators (i.e. forward propagation). Here, $\mathcal{X}$ corresponds to $\mathcal{X} = \mathcal{P}$, $\mathcal{X} = \mathcal{Q}$ or $\mathcal{X} = \mathcal{P} + \mathcal{Q} = 1$. In the latter case, we just write $\mathcal{G}_{\pm}(t,s)$. The interest of the Liouville notation is to provide compact notations for formal manipulation. For instance, the exact density at time t writes

$$D(t) \;=\; \mathcal{G}_{\pm}(t,0)D(0). \tag{20}$$

2. Time-non local vs time-local equations: Nakajima-Zwanzig (NZ) vs Time-Convolution-Less (TCL) method

The NZ method is a very general theory leading to an "a priori" exact closed expression for the relevant degrees of freedom. The strategy is now to incorporate the irrelevant degrees of freedom action by first integrating the equation of motion of the irrelevant degrees of freedom and then report their integrated action onto the relevant subspace. Starting from the evolution of the total system, gives the two coupled equations:

$$\partial_t \mathcal{P}D(t) \;=\; \mathcal{P}\mathcal{L}(t)(\mathcal{P}+\mathcal{Q})D(t), \tag{21}$$
$$\partial_t \mathcal{Q}D(t) \;=\; \mathcal{Q}\mathcal{L}(t)(\mathcal{P}+\mathcal{Q})D(t). \tag{22}$$

In the following, the notation $D_{\mathcal{P}}(t) \equiv \mathcal{P}D(t)$ and $D_{\mathcal{Q}}(t) \equiv \mathcal{Q}D(t)$ are introduced for the density respectively projected onto the the relevant and onto irrelevant degrees of freedom. A closed expression for the relevant variables can be deduced by first integrating the second equation in time leading to:

$$D_{\mathcal{Q}}(t) \;=\; \mathcal{G}_{+}^{Q}(t,0)D_{\mathcal{Q}}(0) + \int_0^t ds \mathcal{G}_{+}^{Q}(t,s)\mathcal{L}(s)\mathcal{P}D_{\mathcal{P}}(s) \tag{23}$$

which is then reported into Eq. (21). The density R_E is often chosen in such a way that odd-moments of V_I cancel out, i.e. $Tr_E\left(V_I(t_1)\cdots V_I(t_{2n+1})R_B\right) = 0$ which is equivalent to have $\mathcal{P}\mathcal{L}(t_1)\cdots\mathcal{L}(t_{2n+1})\mathcal{P}D(s) = 0$. Altogether, the evolution of the relevant degrees of freedom reduces to the exact NZ equation:

$$\partial_t D_{\mathcal{P}}(t) \;=\; \mathcal{I}^{NZ}(t,0)D_{\mathcal{Q}}(0) + \int_0^t \mathcal{K}^{NZ}(t,s)D_{\mathcal{P}}(s)ds \qquad (\text{Nakajima} - \text{Zwanzig}) \tag{24}$$

where

$$\mathcal{K}^{NZ}(t,s) \;=\; \mathcal{P}\mathcal{L}(t)\mathcal{G}_{+}^{Q}(t,s)\mathcal{Q}\mathcal{L}(s)\mathcal{P}, \quad \text{and} \quad \mathcal{I}^{NZ}(t,0) \;= \mathcal{P}\mathcal{L}(t)\mathcal{G}_{+}^{Q}(t,0). \tag{25}$$

The first term in the NZ equation, corresponds to the propagation of the initial state of the environment. If the initial density is already separable, this term does not contribute due to the fact that $D(0) = \mathcal{P}D(0)$ (i.e. $\mathcal{Q}D(0) = 0$). An alternative treatment of this term, as proposed in (Mori, 1965), is to use a stochastic description with a random ensemble of initial conditions. The second term in Eq. (24) is the generalization of Eq. (7) and includes all non-Markovian effects.

The NZ equation is highly non-local in time. An alternative exact reformulation which closely follows the Redfield equation spirit, is provided by the TCL method where the dynamical evolution only depends on the density at time t. In TCL, the density at time s entering in the NZ equation is re-expressed in terms of the density at time t by backward propagation, i.e.

$$D(s) \;=\; \mathcal{G}_{-}(s,t)D(t) = \mathcal{G}_{-}(s,t)(\mathcal{P}+\mathcal{Q})D(t) \tag{26}$$

Reporting in the evolution of $D_{\mathcal{Q}}(t)$, we deduce

$$D_{\mathcal{Q}}(t) \;=\; \frac{1}{(1-\mathcal{E}(t))}\Big\{\mathcal{E}(t)\mathcal{P}D_{\mathcal{P}}(t) + \mathcal{G}_{+}^{Q}(t,0)D_{\mathcal{Q}}(0)\Big\} \tag{27}$$

where

$$\mathcal{E}(t) = \int_0^t \mathcal{Q}\mathcal{L}(t)\mathcal{G}_+^{\mathcal{Q}}(t,s)\mathcal{L}(s)\mathcal{P}\mathcal{G}_-(s,t) \tag{28}$$

Combining with Eq. (24), an exact time-local master equation for the system density is derived

$$\partial_t D_{\mathcal{P}}(t) \;=\; \mathcal{I}^{TCL}(t,0)D_{\mathcal{Q}}(0) + \mathcal{K}^{TCL}(t)D_{\mathcal{P}}(t) \qquad (\text{Time} - \text{Convolution} - \text{Less}) \tag{29}$$

with

$$\mathcal{I}^{TCL}(t,0) \;=\; \mathcal{P}\mathcal{L}(t)\frac{1}{(1-\mathcal{E}(t))}\mathcal{G}_+^{\mathcal{Q}}(t,0), \qquad \mathcal{K}^{TCL}(t) = \mathcal{P}\mathcal{L}(t)\frac{1}{(1-\mathcal{E}(t))}\mathcal{E}(t). \tag{30}$$

Again, expression (29) is the strict generalization of the Redfield equation (11).

3. Perturbative expansion

Both methods are exact and incorporate fully non-Markovian effects. However, they differ significantly in their numerical implementation as well as in their predicting power. In practice, exact formalisms can rarely be integrated and a perturbation expansion in term of the coupling strength is used. Such an expansion is obtained by using the transformation $\mathcal{L}(t) \to \alpha\mathcal{L}(t)$ where α gives a measure of the coupling strength between the two sub-systems. Then, a development of the propagator of the form $\mathcal{K} = \sum_n \alpha^n \mathcal{K}_n$ is obtained. We only give here the result up to fourth order, technical details can be found in ref. (Breuer and Petruccione, 2002). In the NZ case, the projected density evolution is given by

$$\begin{aligned}\partial_t D_{\mathcal{P}}(t) \;=\; & \int_0^t \underbrace{\mathcal{P}\mathcal{L}_t\mathcal{L}_{s_1}\mathcal{P}}_{\mathcal{K}_2^{NZ}(t,s_1)} D_{\mathcal{P}}(s_1)ds_1 \\ & + \int_0^t ds_1 \int_{s_1}^t ds_2 \int_{s_1}^{s_2} ds_3 \underbrace{\mathcal{P}\Big\{\mathcal{L}_t\mathcal{L}_2\mathcal{L}_3\mathcal{L}_1 - \mathcal{L}_t\mathcal{L}_2\mathcal{P}\mathcal{L}_3\mathcal{L}_1\Big\}\mathcal{P}}_{\mathcal{K}_4^{NZ}(t,s_1)} D_{\mathcal{P}}(s_1) + \cdots \,,\end{aligned} \tag{31}$$

while for the TCL case:

$$\begin{aligned}\partial_t D_{\mathcal{P}}(t) \;=\; & \Big\{ \int_0^t ds_1 \underbrace{\mathcal{P}\mathcal{L}_t\mathcal{L}_{s_1}\mathcal{P}}_{\mathcal{K}_2^{TCL}(t)} \\ & + \int_0^t ds_1 \int_0^{s_1} ds_2 \int_0^{s_2} ds_3 \underbrace{\mathcal{P}\Big[\mathcal{L}_t\mathcal{L}_1\mathcal{L}_2\mathcal{L}_3 - \mathcal{L}_t\mathcal{L}_1\mathcal{P}\mathcal{L}_2\mathcal{L}_3 - \mathcal{L}_t\mathcal{L}_2\mathcal{P}\mathcal{L}_1\mathcal{L}_3 - \mathcal{L}_t\mathcal{L}_3\mathcal{P}\mathcal{L}_1\mathcal{L}_2\Big]\mathcal{P}}_{\mathcal{K}_4^{TCL}(t)} + \cdots \Big\} D_{\mathcal{P}}(0)\end{aligned} \tag{32}$$

Last expression is nothing but the result of the cumulant expansion developed by van Kampen (Van Kampen, 2007).

Second order contributions corresponding to $\mathcal{K}_2^{NZ}$ and $\mathcal{K}_2^{TCL}$ give exactly Eqs. (7) and (11) resp. which have been introduced empirically in section II.B.1. Therefore, more physics is a priori incorporated at the NZ2 level than at the TCL2 one. However, due to the appearance of projected densities in the time integrals, even at a given order, higher orders of perturbation may mixed up. This is a major drawback of the NZ method compared to the TCL case where orders of perturbation can be clearly identified. As a consequence, TCL turns out to be rather effective numerically and converges towards the exact solution as the order of perturbation increases (see figure (2)). On opposite, NZ differs more from the exact case at fourth order than at second order.

4. "Separable" ansatz, Mean-Field and Beyond Mean-Field for Open Quantum Systems

Up to know, rather "standard" methods to incorporate non-Markovian effects have been introduced. In the following, less conventional approximations are discussed. A simplification in open

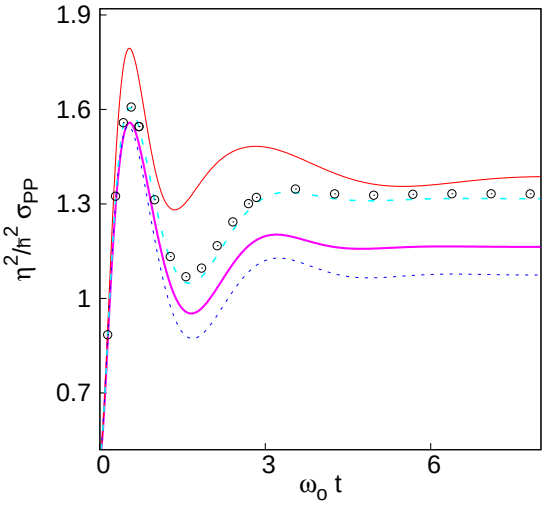

FIG. 2: *Comparison between the exact (open circles), TCL2 (thin dashed line), TCL4 (thick dashed line), NZ2 (thin solid line) and NZ4 (thick solid line) evolution of* $\sigma_{PP} = \langle P^2 \rangle - \langle P \rangle^2$. *While the TCL4 significantly improves the dynamics compared to TCL2, the discrepancy between the exact and approximate evolution is higher in the NZ4 than in the NZ2 case. The simulation is performed assuming a temperature* $T = 1\hbar\omega_0$ $\eta = 0.5\hbar\omega_0$ *and a cut-off* $\Delta_c = 20\hbar\omega_0$ *[see ref. (Lacroix and Hupin, 2008) for precise definition of these parameters].*

quantum system is to assume that the total density remains separable during the time evolution, $D(t) \simeq \rho_S(t) \otimes \rho_E(t)$. In analogy with the many-body problem where densities are written as a (anti-)symmetric product of one-body densities in the independent particle case, this approximation will be called mean-field in the following. The method has been recently used in the context of open quantum system in ref. (Lacroix, 2005b, 2008). Using the separable form of the density in Eq. (2) and taking the partial trace with respect to each subspace leads to coupled mean-field equations between the system and environment densities:

$$\begin{cases} i\hbar\partial_t \rho_S(t) &= [H_S + \langle B(t) \rangle_E Q, \rho_S(t)] \\ i\hbar\partial_t \rho_E(t) &= [H_E + \langle Q(t) \rangle_S B, \rho_E(t)] \end{cases} . \tag{33}$$

These equations have some interesting features. Indeed, introducing the propagator associated to H_E, the evolution of $\rho_E(t)$ can be integrated

$$\rho_E(t) \;=\; U_E(t,0)\rho_E(0)U_E^\dagger(t,0) + \int_0^t \frac{ds}{i\hbar} \langle Q(s) \rangle_S \;\; U_E(t,s)[B, \rho_E(s)]U_E^\dagger(t,s) \tag{34}$$

to give $\langle B(t) \rangle_E = -\frac{1}{\hbar}\int_0^t ds D(t,s)\langle Q(s) \rangle_S$, where the contribution of the first term is neglected and where $D(t,s)$ is the correlation function given by Eq. (9). Reporting in the system evolution, a closed expression for ρ_S is found:

$$i\hbar\frac{d}{dt}\rho_S(t) = [H_S, \rho_S] - \frac{1}{\hbar}\left\{\int_0^t ds D(t,s)\langle Q(s) \rangle_S\right\}[Q, \rho_S(t)] \qquad \text{(Mean - Field)} \tag{35}$$

The mean-field equation is particularly suited to provide accurate estimates of observables mean values. Indeed, considering the Caldeira-Leggett model, the equation of $\langle P \rangle$ and $\langle Q \rangle$ deduced from the mean-field evolution identify with the Born approximation (Eq. (15)) and is exact in that case. Therefore, mean-field theory can be regarded as the optimum path for mean values of collective variables assuming separable densities. Note finally that a mean-field with random initial conditions can also be introduced to account for the absence of knowledge of the environment initial state.

Mean-field transport equations can be easily solved numerically for any system potential using standard numerical methods developed in the Many-Body context. However we do not expect that it properly account for fluctuations of observables. This is indeed expected at least due to the absence of the second correlation function D_1 in the evolution of ρ_S (Eq. (35)). More generally, since this approximation leads to a unitary transformation of the system density, it will be unable to describe the transfer of energy from the system to the bath and more generally the onset of dissipation and/or decoherence. Beyond mean-field theories which improve the description of observables can be obtained by adapting projection methods described in section II.C.

At any time, the total Hamiltonian can be decomposed into a mean-field and residual coupling hamiltonian as :

$$H = \underbrace{H_S + \langle Q(t)\rangle 1_S \otimes B + \langle B(t)\rangle Q \otimes 1_E + \langle Q(t)\rangle\langle B(t)\rangle}_{H_{MF}(t)} + \underbrace{(Q - \langle Q(t)\rangle) \otimes (B - \langle B(t)\rangle)}_{V_{\rm res}(t)} \quad (36)$$

Starting from this decomposition, both the Nakajima-Zwanzig and Time-ConvolutionLess method can be reformulated using the interaction picture of the mean-field Hamiltonian. In that case, the mean-field propagator reads

$$U_{MF}(t,0) = T_+\left\{e^{-\frac{i}{\hbar}\int_0^t H_{MF}(s)ds}\right\}, \quad U_{MF}^{-1}(t,0) = T_-\left\{e^{+\frac{i}{\hbar}\int_0^t H_{MF}(s)ds}\right\} \quad (37)$$

There are several advantages in the introduction of mean-field:

- First, part of the effect of the environment is incorporated into the mean-field term. Accordingly, we do expect that the remaining residual part $V_{\rm res}$ to be treated in perturbation theory is sensibly lower in intensity compared to the full original coupling H_I.
- In standard projection methods, the choice of a reference density R_E has the advantage to greatly simplify the projection technique but appear rather artificial. In addition, this approximation is not expected to hold if the environment is itself significantly affected by the coupling. Mean-field theory offers the possibility to incorporate partially this effect. For instance, a projector at time t can be defined through

$$\mathcal{P}(t)D \equiv \rho_S(t) \otimes \rho_E^{MF}(t) \quad (38)$$

  where $\rho_S(t) = Tr_E D(t)$ while $\rho_E^{MF}(t) = U_{MF}(t,0)\rho_E(0)U_{MF}^\dagger(t,0)$ denotes the initial environment density propagated through the mean-field Hamiltonian.

Let us illustrate theories beyond mean-field incorporating the effect of the coupling up to second order. The total density evolution reads:

$$i\hbar\frac{dD(t)}{dt} = [H_{MF}(t), D(t)] + [V_{\rm res}(t), D(t)]. \quad (39)$$

Following closely the different steps of section II.B, the system density evolution can be written in the Schrödinger picture as:

$$\frac{d\rho_S(t)}{dt} = [H_{MF}(t), \rho_S(t)] - \frac{1}{\hbar^2}\int_0^t {\rm Tr}_E[V_{\rm res}(t), U_{MF}(t,s)[V_{\rm res}(s), D(s)]U_{MF}^\dagger(t,s)]ds. \quad (40)$$

Assuming that the density is separable at time s, which implies to replace the exact density by its mean-field equivalent, a closed expression very similar to expression (10) is deduced except that the operator Q and B are replaced by centered observables, i.e. $O \to O'(t) \equiv (O - \langle O(t)\rangle_S)$ and $B \to B'(t) \equiv (B - \langle B(t)\rangle_E)$ and where the propagator of H_S is replaced by the the mean-field propagator with for instance $Q'(t-s) = U_{MF}(t,s)Q'(s)U_{MF}^\dagger(t,s)$. Accordingly, two new memory functions defined by

$$D(t,s) \to D'(t,s) \equiv i\langle[B'(t), B'(t-s)]\rangle_E, \text{ and } D_1(t,s) \to D_1'(t,s) \equiv \langle\{B'(t), B'(t-s)\}_+\rangle_E \quad (41)$$

replace the D and D_1 functions in Eq. (10). The introduction of mean-field prior to a perturbative expansion in powers of the coupling leads to alternative equations compared to the original perturbation theory.

D. Unraveling quantum master equation with Stochastic Schroedinger Equations

For the Caldeira-Leggett model, starting from equation (10) in the Born-Markov approximation, the system density evolution can be transformed into a master equation of the form (Breuer and Petruccione, 2002):

$$\frac{d}{dt}\rho_S \;=\; \frac{1}{i\hbar}[H_S,\rho_S(t)] - \frac{1}{2\hbar^2}\sum_k \gamma_k \left(2A_k\rho_S(t)A_k - A_kA_k\rho_S(t) - \rho_S(t)A_kA_k\right) \tag{42}$$

where the A_k are linear combinations of the P and Q operators. Above equation of motion is known as a Lindblad master equations. In the Markovian limit, master equations discussed previously can be simulated by a stochastic process in the Hilbert space of wave-functions (Breuer and Petruccione, 2002; Carmichael, 1993; Castin and Mölmer, 1996; Dalibard *et al.*, 1992; Dum *et al.*, 1992; Gardiner and Zoller, 2000; Gisin and Percival, 1992; Plenio and Knight, 1998; Rigo and Gisin, 1996). Indeed, let us consider a density written as:

$$\rho_S(t) = |\Phi(t)\rangle\langle\Phi(t)|, \tag{43}$$

where the wave-functions evolves according to the Stochastic Schrödinger Equation (SSE):

$$d|\Phi(t)\rangle \;=\; \Big(\frac{dt}{i\hbar}H_S - \frac{dt}{2\hbar^2}\sum_k \gamma_k A_kA_k\Big)|\Phi(t)\rangle + \sum_k dx_k A_k|\Phi(t)\rangle. \tag{44}$$

Here, where the $\{dx_k\}$ are independent Gaussian random numbers with mean zero (written with the Ito convention for stochastic calculus). The average evolution of $\rho_S(t)$ can be evaluated through

$$d\overline{\rho_S}(t) \;=\; \overline{|d\Phi(t)\rangle}\langle\Phi(t)| + |\Phi(t)\overline{\langle d\Phi(t)|} + \overline{|d\Phi(t)\rangle\langle d\Phi(t)|} \tag{45}$$

where

$$\begin{aligned}
\overline{|d\Phi(t)\rangle} \;&=\; dt\Big(\frac{1}{i\hbar}H_S - \frac{1}{2\hbar^2}\sum_k \gamma_k A_kA_k\Big)|\Phi(t)\rangle,\\
\overline{\langle d\Phi(t)|} \;&=\; dt\langle\Phi(t)|\Big(-\frac{1}{i\hbar}H_S - \frac{1}{2\hbar^2}\sum_k \gamma_k A_kA_k\Big)\\
\overline{|d\Phi(t)\rangle\langle d\Phi(t)|} \;&=\; \sum_k \overline{dx_k^2}A_k|\Phi(t)\rangle\langle\Phi(t)|A_k
\end{aligned}$$

Under the condition that $dx_k^2 = dt\gamma_k/\hbar^2$, the average evolution identifies with the dissipative equation (42). Therefore, in the Markovian limit, the evolution of an OQS can be replaced by the average over densities of pure states, where each state evolves according to a stochastic process in the Hilbert space. Note that equation (44) do not preserves the normalization of the state $|\Phi(t)\rangle$ along the path but additional terms could be added to insure proper normalization. The concept of SSE has a clear practical advantage. Assume that the size of the Hilbert space is N. The evolution of a wave function requires to know its N components while for the density N^2 terms should be followed in time. For several years, application of SSE were restricted to master equation in the Markovian limit. Large theoretical efforts are actually devoted to the inclusion of non-Markovian effects. Among the most recent approaches, one could mention Quantum State Diffusion (QSD) (Diósi and Strunz, 1996; Diósi *et al.*, 1998; Strunz *et al.*, 1999; Strunz, 2005) or Quantum Monte-Carlo methods (Piilo *et al.*, 2008) where non-Markovian effects are accounted for through non-local memory kernels and state vectors evolve according to integro-differential stochastic equations.

E. Exact Quantum Monte-Carlo methods

During the past decade, important advances have been made in the approximate and exact description of system embedded in an environment using stochastic methods. Recently the description of open quantum systems by Stochastic Schroedinger Equation (SSE) has received much attention (Breuer and Petruccione, 2002; Plenio and Knight, 1998; Shao, 2004; Stockburger and Grabert, 2002). Indeed, alternative exact formulation (Breuer, 2004b; Lacroix, 2005b, 2008) have been developed to treat the system+environment problem that avoid evaluation of non-local memory kernels although non-Markovian effects are accounted for exactly (see also (Breuer and Petruccione, 2007; Breuer *et al.*, 2004; Breuer, 2004a,b; Lacroix, 2005b; Zhou *et al.*, 2005)).

For the sake of simplicity, we assume an initial separable density $D(t_0) = \rho_S(t_0) \otimes \rho_B(t_0)$. This assumption could be eventually relaxed. Several works using either Stochastic Schrödinger Equation concepts or path integral have shown that the exact density of the total system $D(t)$ could be obtained as an average over simple separable densities, i.e. $D(t) = \overline{\rho_S(t) \otimes \rho_B(t)}$. In its simplest version, the stochastic process takes the form (Lacroix, 2005b)

$$\begin{cases} d\rho_S &= \frac{dt}{i\hbar}[H_S, \rho_S] + d\xi_S Q\rho_S + d\lambda_S \rho_S Q \\ d\rho_E &= \frac{dt}{i\hbar}[H_E, \rho_E] + d\xi_E B\rho_E + d\lambda_E \rho_E B \end{cases} \tag{46}$$

where the Ito convention for stochastic calculations is used(Gardiner, 1985). $d\xi_{S/E}$ and $d\lambda_{S/E}$ denote Markovian Gaussian stochastic variables with zero means and variances

$$\overline{d\xi_S d\xi_E} = \frac{dt}{i\hbar}, \quad \overline{d\lambda_S d\lambda_E} = -\frac{dt}{i\hbar}, \quad \overline{d\xi_S d\lambda_E} = \overline{d\lambda_S d\xi_E} = 0. \tag{47}$$

The average over stochastic paths described by Eqs. (46) matches the exact evolution. Indeed, assuming that at a time t the total density writes $D(t) = \rho_S(t) \otimes \rho_B(t)$, the average evolution over a small time step dt is given by

$$\overline{dD} = \overline{d\rho_S \otimes \rho_E} + \overline{\rho_S \otimes d\rho_E} + \overline{d\rho_S \otimes d\rho_E}. \tag{48}$$

Using statistical properties of stochastic variables (Eqs. (47)), we obtain

$$\overline{d\rho_S \otimes \rho_E} + \overline{\rho_S \otimes d\rho_E} = \frac{dt}{i\hbar}[H_S + H_E, \rho_S \otimes \rho_E], \tag{49}$$

$$\overline{d\rho_S \otimes d\rho_E} = \frac{dt}{i\hbar}[Q \otimes B, \rho_S \otimes \rho_E]. \tag{50}$$

Therefore, the last term simulates the interaction Hamiltonian exactly and the average evolution of the total density over a time step dt reads

$$\overline{dD} = \frac{dt}{i\hbar}[H, D], \tag{51}$$

which is nothing but the exact evolution. Here, the exactness of the method is proved assuming that the density $D(t)$ is a single separable density. In practice, the total density at time t is already an average over separable densities obtained along each stochastic path, i.e. $\overline{D(t)} = \overline{\rho_S(t) \otimes \rho_E(t)}$. Since Eq. (51) is valid for any density written as $\rho_S(t) \otimes \rho_E(t)$, by summing individual contributions, we deduce that the evolution of the total density obtained by averaging over different paths is given by $i\hbar d\overline{D} = dt[H, \overline{D(t)}]$ which is valid at any time and corresponds to the exact system+environment dynamics.

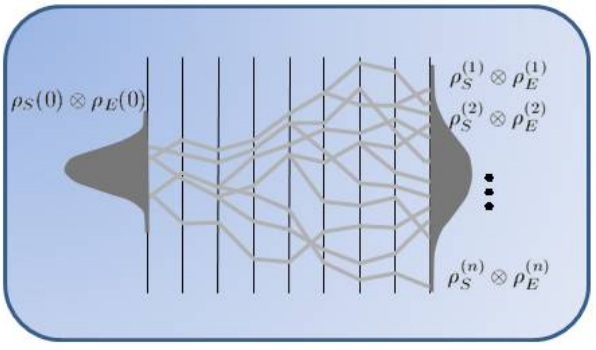

FIG. 3: *Illustration of Exact Monte-Carlo method introduced to treat Open-Quantum Systems. In this approach, the exact deterministic evolution of the total system+environment density is replaced by an ensemble of stochastic evolutions where the density remains simpler along each trajectories. In the open quantum system case, the word "simpler" means separable, i.e.* $D(t) = \rho_S(t) \otimes \rho_E(t)$.

2. Flexibility of stochastic methods and Exact Stochastic mean-field dynamics

The stochastic process is far from being unique. One can use this flexibility to impose some specific constraints along the trajectories or reduce the number of trajectories necessary to accurately describe the evolution (Lacroix, 2005b). Let us introduce a first kind of modification of (46) that could be made without breaking the exactness of the theory. Denoting by $\Delta_S(t)$ and $\Delta_E(t)$ time-dependent c-numbers, the following modified stochastic evolution is considered:

$$\left\{\begin{array}{lcl} d\rho_S &=& \frac{dt}{i\hbar}[H_S + Q\Delta_E, \rho_S] + d\xi_S(Q-\Delta_S)\rho_S + d\lambda_S\rho_S(Q-\Delta_S) \\ d\rho_E &=& \frac{dt}{i\hbar}[H_E + B\Delta_S, \rho_E] + d\xi_E(B-\Delta_E)\rho_E + d\lambda_E\rho_E(B-\Delta_E) \end{array}\right. . \tag{52}$$

These stochastic equation provides an exact reformulation of the initial system+environment. Indeed, we now have

$$\begin{aligned} \overline{d\rho_S \otimes \rho_E} + \overline{\rho_S \otimes d\rho_E} &= \frac{dt}{i\hbar}[H_S + Q\Delta_E, \rho_S \otimes \rho_E] + \frac{dt}{i\hbar}[H_E + B\Delta_S, \rho_S \otimes \rho_E], \\ \overline{d\rho_S \otimes d\rho_E} &= \frac{dt}{i\hbar}[(Q-\Delta_S)\otimes(B-\Delta_E), \rho_S \otimes \rho_E]. \end{aligned}$$

Therefore, the additional terms appearing in the deterministic part are exactly compensated by equivalent terms coming from the average over the noise. Up to now, this flexibility has been used essentially by introducing mean-field prior to the stochastic process. In that case, we have

$$\Delta_E(t) = \langle B(t)\rangle_E, \quad \Delta_S(t) = \langle Q(t)\rangle_S. \tag{53}$$

The stochastic mean-field theory has several advantages compared to the original equations given in (46). First, the traces of densities are constant and remain equal to their initial values, i.e. $d\mathrm{Tr}(\rho_{S/E}) = 0$. This greatly simplify expectation values of system and/or environment observables. Indeed, denoting by X a system operator, along the trajectory, we have

$$\langle X\rangle = \mathrm{Tr}(XD(t)) = \mathrm{Tr}(\rho_E(t))\mathrm{Tr}(X\rho_S(t)). \tag{54}$$

For stochastic processes with varying trace of densities (like the original one given by Eqs. (46)), the observable evolution will contain terms coming from $d\mathrm{Tr}(\rho_{S/E})$ and cross terms coming from $d\mathrm{Tr}(\rho_{S/E})d\mathrm{Tr}(X\rho_S(t))$. In the mean-field case, we simply have

$$d\langle X\rangle = \mathrm{Tr}(\rho_E(t))d\mathrm{Tr}(X\rho_S(t)). \tag{55}$$

A second expected improvement is the reduction of statistical errors or said differently of the number of trajectories needed to simulate various physical situations. Since mean-field account for part of the coupling in the deterministic evolution, the amount of coupling to be treated by the noise should be significantly reduced. One could indeed show analytically that mean-field induces a reduction of the standard deviation around the mean trajectory (Lacroix, 2005b).

Mean-field is not the only way to modify the stochastic process and eventually improve its accuracy. An extra flexibility has been used in ref. (Lacroix, 2005b) to improve further quantum Monte-Carlo methods, for instance the simultaneous transformation $d\lambda_S \to x d\lambda_S$ and $d\lambda_E \to d\lambda_E/x$ leaves the average evolution invariant. An illustration of the efficiency of (i) the scaling transformation and (ii) mean-field is given in figure 4. The use of scaling optimized at each time step already greatly reduces the standard deviation. The most efficient Quantum Monte-Carlo (QMC) method is obtained when both mean-field and scaling is made.

3. Reduced system density evolution and connection with Path integrals

The stochastic formulation suffers a priori from the same difficulty as the total dynamics: the environment is in general rather complex and has a large number of degrees of freedom which can hardly be followed in time. In Eq. (52), the influence of the environment on the system only enters through $\langle B(t)\rangle_E$. Therefore, instead of following the full environment density evolution, one

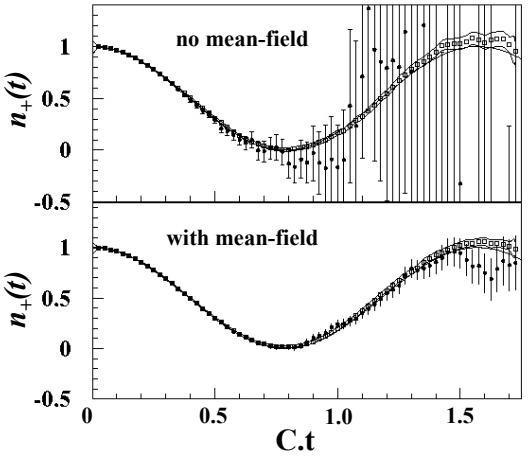

FIG. 4: *Exact Monte-Carlo method applied to interacting spin systems. The system consist of a two level system coupled to a bath of two level systems. The occupation probability of the upper level, denoted n_+ obtained by using average over stochastic trajectories is shown as a function of time and compared to the exact dynamics (solid line) with 10^4 trajectories. Top: Results obtained using the Stochastic Schrödinger Equation (SSE) with (open squares) and without (filled circles) optimization. Bottom, results obtained using quantum Monte-Carlo method with (open squares) and without (filled circles) optimization. The error-bars represents in each case the standard deviation calculated with the generated trajectories (adapted from (Lacroix, 2005b)).*

can concentrate on this observable only. As shown in ref. (Lacroix, 2008), the second stochastic equation in Eqs. (52) can be integrated in time to give:

$$\begin{aligned}\langle B(t)\rangle_E &= \mathrm{Tr}(B^I(t-t_0)\rho_E(t_0)) \\ &\quad -\frac{1}{\hbar}\int_0^t D(t,s)\,\langle Q(s)\rangle_S\,ds - \int_0^t D(t,s)du_E(s) + \int_0^t D_1(t,s)dv_E(s),\end{aligned} \tag{56}$$

where D and D_1 are the memory functions given by Eq. (41). A new set of stochastic variables $dv_{S/E}$ and $du_{S/E}$ have been introduced through $d\xi_{S/E} = dv_{S/E} - idu_{S/E}$ and $d\lambda_{S/E} = dv_{S/E} + idu_{S/E}$ and verify

$$\overline{du_S du_E} = \overline{dv_S dv_E} = \frac{dt}{2\hbar}, \quad \overline{du_S dv_E} = \overline{dv_S du_E} = 0. \tag{57}$$

Reporting the evolution of $\langle B(t)\rangle_E$ into the evolution of ρ_S, we end up with a closed stochastic equation of motion for the system density (Lacroix, 2008):

$$\begin{aligned}d\rho_S &= \frac{dt}{i\hbar}\left[\mathcal{H}_S,\rho_S\right] + dt[Q,\rho_S]\int_0^t dsD(t-s)\,\langle Q(s)\rangle_S \\ &\quad + d\xi(t)[Q,\rho_S] + d\eta(t)\{Q-\langle Q\rangle,\rho_S\} \quad \text{(exact QMC)}\end{aligned} \tag{58}$$

with

$$d\xi(t) = dt\int_0^t D_1(t-s)dv_E(s) - dt\int_0^t D(t-s)du_E(s) - idv_S(t), \quad d\eta(t) = du_S(t). \tag{59}$$

The first two terms in expression (58) are nothing but the mean-field contribution already discussed in section II.C.4. By integrating out the evolution of the environment, a new stochastic term is found that depends not only on the noise at time t but also on its full history through the time integrals. Using standard Ito rules for stochastic calculus, we deduce:

$$\begin{aligned}\overline{d\eta(t)d\eta(t')} &= 0, \\ \overline{d\xi(t)d\eta(t')} &= -\frac{dt}{2\hbar}\Theta(t-t')D(t-t') \quad \text{and} \quad \overline{d\xi(t)d\xi(t')} = -\frac{idt}{2\hbar}D_1(|t-t'|),\end{aligned} \tag{60}$$

where $\Theta(t-t') = 1$ for $t > t'$ and zero if $t < t'$. Surprisingly enough, the exact QMC equations given by (58) identifies with the stochastic master equation obtained in ref. (Stockburger and Grabert, 2002) using a completely different method based on the Feynman-Vernon influence functional theory (Feynman and Vernon, 1963).

4. Equivalent stochastic process in Hilbert space

Thanks to the last stochastic rule in Eq. (47), the exact stochastic master equation has also its Stochastic Schroedinger Equation counterpart. System density evolution along each path can be replaced by $\rho_S(t) = |\phi_1(t)\rangle \langle\phi_2(t)|$, where wave functions evolve according to

$$\left\{ \begin{array}{rcl} d|\phi_1\rangle & = & \left\{ \frac{dt}{i\hbar}(H_S + \langle B(t)\rangle Q) + d\xi_S(Q - \langle Q(t)\rangle_S) \right\} |\phi_1\rangle \\ d\langle\phi_2| & = & \langle\phi_2| \left\{ -\frac{dt}{i\hbar}(H_S + \langle B(t)\rangle Q) + d\lambda_S(Q - \langle Q(t)\rangle_S) \right\} \end{array} \right. . \tag{61}$$

As explained above, the introduction of SSE instead of master equations can lead to a further reduction of the numerical complexity.

Despite the apparent complexity of Eq. (58), the stochastic mean-field approach has been recently applied with success to the spin-boson model coupled to a heat bath of oscillators (Lacroix, 2008). In particular, the introduction of mean-field seems to cure difficulties that have been encountered in this model (Zhou *et al.*, 2005). An alternative illustration on the Caldeira-Leggett model is given in the insert below. As seen in the insert, hermitian observables makes large excursion in the complex plane. This stems from the specific noise used to design the exact formulation that leads to non-Hermitian densities along paths. Part of the conceptual difficulties in understanding the physical meaning of observable evolutions can be overcome by noting that if $\rho_S(t) = |\phi_1(t)\rangle \langle\phi_2(t)|$ belongs to the set of trajectories, by symmetry $\rho'_S(t) = |\phi_2(t)\rangle \langle\phi_1(t)|$ also belongs to the set. By grouping these two trajectories to estimate observables, real quantities are deduced.

Application of Stochastic Mean-Field to the Caldeira-Leggett model

In the Caldeira-Leggett model, starting from an initial Gaussian density, the exact stochastic evolution of the system density reduces to the first and second moments evolution of P and Q given by:

$$\begin{cases} d\langle Q\rangle &= \frac{\langle P\rangle}{M}dt + 2du_S\sigma_{QQ} \\ d\langle P\rangle &= -M\omega_0^2\langle Q\rangle dt - dt\langle B\rangle + 2du_S\sigma_{PQ} - \hbar dv_S \\ d\sigma_{QQ} &= 2\frac{dt}{M}\sigma_{PQ} \\ d\sigma_{PP} &= -2M\omega_0^2 dt\sigma_{PQ} \\ d\sigma_{PQ} &= \frac{dt}{M}\sigma_{PP} - M\omega_0^2\sigma_{QQ}dt \end{cases} \quad (6$$

These equations illustrate the differences between the new exact reformulation and standard methods to treat dissipation. Generally, the noise enters into the evolution of P only and affects directly the second moment. Here, we see that seconds moments identifies with the unperturbed ones while the random forces enters in both Q and P. In addition, the noise is complex, which implies that observables make excursion in the complex plane. The exact evolution is obtained by averaging over different trajectories. For second moments, this leads to $\Sigma_{QQ} \equiv \overline{\langle Q^2\rangle} - \overline{\langle Q\rangle}^2 = \sigma_{QQ} + \overline{\langle Q\rangle^2} - \overline{\langle Q\rangle}^2$. In the particular Caldeira-Leggett case, total fluctuations are recovered by simply adding up quantum and statistical fluctuations.

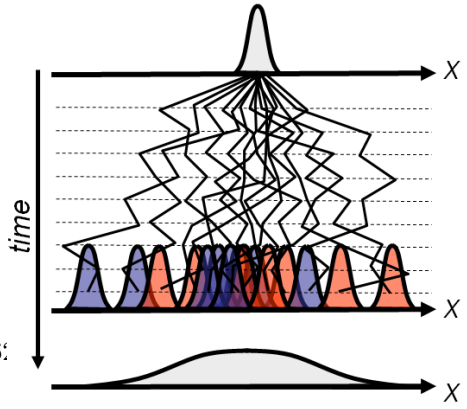

Schematic illustration of the SMF process in the Caldeira-Leggett model where the exact evolution is replaced by a set of Gaussian density evolutions. Total fluctuations are calculated by adding the quantum and statistical widthes.

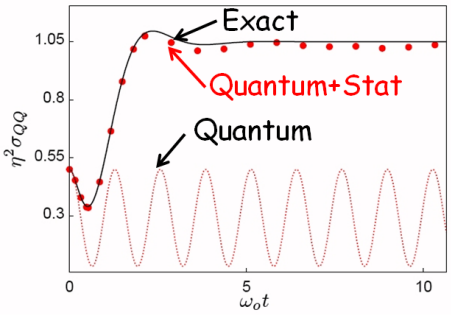

Example of second moment evolution. The exact result (filled circles) is compared to the quantum only (dashed line) and quantum+statistical (solid line) average.

Recent prospective studies have shown that exact QMC methods can be highly efficient in some cases, however the application to non harmonic potential leads in general to the appearance of numerical instabilities associated to divergent trajectories. For the moment, no clear solution to this problem has been proposed so far and the application to exact quantum Monte-Carlo theory remains a challenging problem.

F. Summary and discussion

Here, a summary of different approaches used to treat open quantum system has been given. These approaches have been dissociated into conventional one (NZ and TCL) and less conventional (Mean-Field, Stochastic Schrödinger Equation, exact QMC) to insist on recent developments. The possibility to treat non-Markovian effect using new exact QMC methods offers new perspectives for system coupled to a complex surrounding under the condition that numerical problems observed quite systematically can be solved.

Most of the theories introduced in this section have their counterpart in the theory of interacting particle systems. Indeed, to simplify the many-body problem, few relevant degrees of freedom are selected forming the system under interest. Other degrees of freedom then serves as an environment. In the following, the separation of degrees of freedom is first introduced in III while transport theories guided by OQS theories are discussed in section IV.

III. VARIATION ON A THEME OF MEAN-FIELD IN MANY-BODY SYSTEMS

We consider here an ensemble of N particles interacting through the following Hamiltonian

$$H = \sum_{ij} t_{ij}\, a_i^\dagger\, a_j + \frac{1}{4}\sum_{ijkl} \tilde{v}^{(2)}_{ijkl}\, a_i^\dagger\, a_j^\dagger\, a_l\, a_k + \frac{1}{36}\sum_{ijklmn} \tilde{v}^{(3)}_{ijklmn}\, a_i^\dagger a_j^\dagger a_k^\dagger a_n a_m a_l + \cdots, \tag{63}$$

where $\{a_i^\dagger, a_i\}$ are creation/annihilation operators associated to a complete single-particle basis. t denotes matrix elements of the kinetic energy term while $\tilde{v}^{(2)}$ and $\tilde{v}^{(3)}$, ... correspond to fully anti-symmetric two-, three-, ... N-body interaction matrix elements respectively.

The quantum description of such a system requires a priori the knowledge of its N-Body wave function $\Psi^*(\{\mathbf{r}_i\}, t)$ or more generally its N-body density matrix denoted by $D(\{\mathbf{r}_i\}, t)$. $\{\mathbf{r}_i\}$ is a short-hand notation for the particles coordinates $(\mathbf{r}_1, \cdots, \mathbf{r}_N)$. The complexity of the Many-body problem comes from the number of degrees of freedom to consider. Except for very small number of particles, the total number of degrees of freedom to treat becomes prohibitory to get the exact ground state or the evolution of such a complex system. Therefore, we are forced to seek simplifications where much less relevant degrees of freedom are considered. The most common strategy is to assume a hierarchy between those degrees of freedom depending on their complexity. The starting point of the hierarchy consists in focusing on one-body degrees of freedom only. At the second level, one- and two-body degrees of freedom are incorporated simultaneously and so on and so forth up to the exact description.

The aim of the present section is to consider the first level. Such an approach is motivated first by the fact that most of the observations generally made on an interacting system are related to one-body quantities: deformation, collective motion... Since any one-body operator writes $O^{(1)} = \sum_{ij} \langle i|O|j\rangle\, a_i^\dagger a_j$, all the information on one-body properties is contained in the one-body density matrix defined as

$$\rho^{(1)}_{ji}(t) \;=\; Tr(a_i^\dagger a_j D(t)) \equiv \langle a_i^\dagger a_j \rangle. \tag{64}$$

Some properties of the one-body density as well as its connection with higher order densities are discussed in appendix A. Large effort is devoted to provide the best approximation on the one-body density only without solving the full problem. The main difficulty comes from the fact that the one-body density could not be fully isolated from other more complex degrees of freedom. Therefore by reducing the information on a closed system into a small set of variables, we are left with an open quantum system problem (discussed in section II) where this subset is coupled to the surrounding sets of irrelevant degrees of freedom.

In this chapter, variational principles are used as a starting point to discuss the reduction of information in many-body systems. Concepts like relevant/irrelevant observables, effective Hamiltonian dynamics, projections are first introduced from a rather general point of view. These concepts are then illustrated in the specific case of interacting particles.

A. Variational principles in closed systems

Variational principles are powerful tools to provide approximate solutions for static or dynamical properties of a system when few degrees of freedom are expected to contain the major part of the information (Blaizot and Ripka, 1986; Drozdz *et al.*, 1986; Feldmeier and Schnack, 2000; Kerman and Koonin, 1976). Here, general aspects related to variational principle are presented. Then, the specific N-body problem is discussed. For time dependent problem, the Rayleigh-Ritz variational principle generalizes as

$$S = \int_{t_0}^{t_1} ds\, \langle \Psi(t)|\, i\hbar\partial_t - H\, |\Psi(t)\rangle\,, \tag{65}$$

where S denotes the action. The action should be minimized, i.e. $\delta S = 0$ under fixed boundary conditions $|\delta\Psi(t_0)\rangle = 0$ and $\langle\delta\Psi(t_1)| = 0$. The variation has to be made on all components of the

wave-function. Denoting by Ψ_i these components in a specific basis, S becomes[3]

$$S = \int_{t_0}^{t_1} ds \sum_i \Big\{ i\hbar \Psi_i^*(t) \partial_t \Psi_i(t) - \sum_j \Psi_i^*(t) H_{ij} \Psi_j(t) \Big\} \tag{67}$$

$$\equiv \int_{t_0}^{t_1} ds \Big\{ i\hbar \Psi^* \partial_t \Psi - \mathcal{H}\left[\Psi, \Psi^*\right] \Big\} = \int_{t_0}^{t_1} ds \mathcal{L}[\Psi^*, \Psi, \dot{\Psi}], \tag{68}$$

where $\mathcal{H}[\Psi^*, \Psi]$ and $\mathcal{L}[\Psi^*, \Psi]$ stands for the time-dependent Hamiltonian and Lagrangian respectively written in a functional form. In expression (68) a discrete basis is used, the generalization to continuous basis is straightforward. If the states $\{i\}$ do form a complete basis of the full Hilbert space relevant for the considered problem, then the minimization procedure leads to

$$\begin{cases} i\hbar \partial_t |\Psi(t)\rangle &= H|\Psi(t)\rangle, \\ -i\hbar \partial_t \langle \Psi(t)| &= \langle \Psi(t)|H, \end{cases} \tag{69}$$

which is nothing but the standard Schrödinger equation and its adjoint. Note that the second equation has been obtained by making variations with respect to the components Ψ_i after integrating by parts and underlines the crucial role of boundary conditions. The connection to classical equation of motion can be made using the functional form and introducing the field Φ and momenta Π coordinate such that $\Psi = (\Phi + i\Pi)/\sqrt{2}$, leading to (Kerman and Koonin, 1976)

$$\frac{\partial \Phi}{\partial t} = \frac{\partial \mathcal{H}}{\partial \Pi}, \quad \frac{\partial \Pi}{\partial t} = -\frac{\partial \mathcal{H}}{\partial \Phi}, \tag{70}$$

which are nothing but Hamilton's equations for the conjugate variables (Φ, Π).

1. Selection of specific degrees of freedom and Ehrenfest theorem

The interest of variational principle is obviously not to recover the Schrödinger equation but stems from the possibility to restrict the variation to a smaller sub-space of the full Hilbert space and/or to a specific class of wave-functions. Then, the dynamics is not exact anymore but will be the best approximation within the selected space or trial states class.

We will consider here the important case where specific local transformations exist between any of the trial state $|\Psi\rangle$ and surrounding states. Explicitly, we consider the case:

$$|\Psi + \delta\Psi\rangle = e^{\sum_\alpha \delta q_\alpha A_\alpha} |\Psi\rangle, \tag{71}$$

where $\{\delta q_\alpha\}$ and A_α denotes respectively a set of parameters and operators. In most cases, the set of trial states is written as (Chomaz, 1996)

$$|\Psi(\mathbf{Q})\rangle = R(\mathbf{Q})|\Psi(0)\rangle = e^{\mathbf{Q}.\mathbf{A}}|\Psi(0)\rangle \tag{72}$$

$R(\mathbf{Q})$ is an element of the Lie Group constructed from a parameters set $\mathbf{Q} \equiv \{q_\alpha\}$ and from its generators $\mathbf{A} \equiv \{A_\alpha\}$. Most often $|\Psi(0)\rangle$, is a state of the irreducible representation of the group. The most common examples are coherent states, independent particle states or quasi-particles vacuum (the two latter cases will be illustrated below). States written as in eq. (72) are implicit functionals of $\mathbf{Q}$, in the following, the simple notation $|\mathbf{Q}\rangle \equiv |\Psi(\mathbf{Q})\rangle$ is used. Variations with respect to the wave-function are now replaced by variations with respect to the parameters $\mathbf{Q}$ with:

$$|\delta\mathbf{Q}\rangle = \sum_\alpha \delta q_\alpha \left(\frac{\partial}{\partial q_\alpha} |\mathbf{Q}\rangle \right) \qquad \text{and} \qquad \langle \delta\mathbf{Q}| = \sum_\alpha \delta q_\alpha^*(t) \left(\frac{\partial}{\partial q_\alpha^*} \langle \mathbf{Q}| \right), \tag{73}$$

---

[3] Note that, last expression can very easily be transformed into a more symmetric and natural form:

$$S = \int_{t_0}^{t_1} dt \mathcal{L}[\Psi^*, \Psi, \dot{\Psi}, \dot{\Psi}^*]. \tag{66}$$

or using the transformation (72) between trial states:

$$|\delta\mathbf{Q}\rangle \;=\; \sum_\alpha \delta q_\alpha A_\alpha |\mathbf{Q}\rangle \qquad \text{and} \qquad \langle\delta\mathbf{Q}| = \langle\mathbf{Q}| \sum_\alpha \delta q^*_\alpha(t) A_\alpha. \tag{74}$$

Using expressions (73) in the minimization, leads to the classical Euler-Lagrange equation of motion for the parameters (Feldmeier and Schnack, 2000):

$$\frac{d}{dt}\frac{\partial\mathcal{L}}{\partial\dot{q}_\alpha} = \frac{\partial\mathcal{L}}{\partial q_\alpha}, \qquad \frac{d}{dt}\frac{\partial\mathcal{L}}{\partial\dot{q}^*_\alpha} = \frac{\partial\mathcal{L}}{\partial q^*_\alpha} \tag{75}$$

If instead, expressions (74) are used, the following two equations of motion, corresponding respectively to the variations δq^*_α and δq_α, are obtained:

$$\begin{cases} i\hbar\langle\mathbf{Q}|A_\alpha|\dot{\mathbf{Q}}\rangle \;=\; \langle\mathbf{Q}|A_\alpha H|\mathbf{Q}\rangle, \\ i\hbar\langle\dot{\mathbf{Q}}|A_\alpha|\mathbf{Q}\rangle \;=\; -\langle\mathbf{Q}|HA_\alpha|\mathbf{Q}\rangle, \end{cases} \tag{76}$$

which combined together gives the evolution

$$i\hbar\frac{d\langle A_\alpha\rangle}{dt} = \langle[A_\alpha, H]\rangle. \tag{77}$$

We recognize here nothing but the Ehrenfest theorem, giving the evolution of any operator $\{A_\alpha\}$ with the Hamiltonian H. Therefore, starting from a density $D(t_0) = |Q\rangle\langle Q|$, for one time step the $\{\langle A_\alpha\rangle\}$ evolutions identify to the exact evolution although the state is constrained to remains in a sub-class of trial states. Thus, we do expect that the mean-field approximation is particularly suited to focus on a specific class of degrees of freedom $\langle A_\alpha\rangle$ for short time evolution. For degrees of freedom that do not belong to the $\{A_\alpha\}$, mean-field expectation will generally differ from their exact dynamics. For them, it is often said that "mean-field dynamic corresponds to the projected evolution onto a sub-space of the total observable manifold". In the following, we show how projector can explicitly be introduced. Such a projector formulation gives a better insight into the mean-field approximation.

2. Correlations between observables and Projection techniques

To properly introduce the projection onto a subspace of observables, the notion of independence and correlation between observables should be first discussed. The strategy followed here is essentially the same as in the Principal Component Analysis (PCA) used in statistical analysis. Let us consider a set of operators $\{A_\alpha\}$ and a density D describing the properties of a system at a given time which is interpreted as a probability. The $\{A_\alpha\}$ form a subset of the total space of observables. In the following, It is shown how any other observables can be projected out on this subset. Part of the method presented here has been used to introduce stochastic mean-field approaches in closed system in ref. (Lacroix, 2007). Readers that are not interest in technical details may skip this part and directly jump to section III.A.3

a. **Creation of an independent set of operators in the $\{A_\alpha\}$ subspace:** Observables $\{A_\alpha\}$ are not necessarily statistically independent from each others with respect to the state D. In the following, we will just say that they are D-correlated or D-independent in the opposite case. To measure correlation between observables, we introduce the variance-covariance matrix defined as [4]:

$$C_{\alpha\beta} = \langle A_\alpha A_\beta\rangle - \langle A_\alpha\rangle\langle A_\beta\rangle, \tag{79}$$

---

[4] It is worth mentioning that the strict equivalent of statistical mechanics would be the symmetric quantity:

$$C'_{\alpha\beta} = \frac{1}{2}\langle A_\alpha A_\beta + A_\beta A_\alpha\rangle - \langle A_\alpha\rangle\langle A_\beta\rangle. \tag{78}$$

Strictly speaking, only the above quantity can be regarded as a scalar product. However, as it will become clear in the following, it is more convenient to define the non-symmetric $C_{\alpha\beta}$.

has non zero off-diagonal matrix elements. We assume here that the $\{A_\alpha\}$ are hermitian operators implying that C is also hermitian. Below, the different notations:

$$C_{\alpha\beta} \;=\; C(A_\alpha, A_\beta) = \langle\langle A_\alpha | A_\beta \rangle\rangle \tag{80}$$

will be used. In the following, it is assumed that C is not singular. Note that, if it is the case, it does only mean that their is redundant information and that the subset of observables can be further reduced. C could be diagonalized by a unitary transformation U and has only positive eigenvalues denoted by λ_α[5]. It is then convenient to introduce a new set of operators $\{e^\dagger_\alpha\}$, defined from the relationship

$$e_\alpha = \frac{1}{\sqrt{\lambda_\alpha}} \sum_\beta U^{-1}_{\alpha\beta}(A_\beta - \langle A_\beta \rangle) \tag{81}$$

It is worth to mention that these operators are explicitly dependent on the density D. Using this definition, we have $< e_\alpha >=< e^\dagger_\beta >= 0$ while

$$\langle\langle e^\dagger_\alpha | e_\beta \rangle\rangle = \frac{1}{\sqrt{\lambda_\alpha \lambda_\beta}} \left(U^{-1} C U\right)_{\alpha\beta} = \delta_{\alpha\beta} \tag{82}$$

Therefore, couples of operators $(e^\dagger_\alpha, e_\beta)$ are D-independent. We also have the inverse relation

$$A_\alpha - \langle A_\alpha \rangle \;=\; \sum_\beta \sqrt{\lambda_\beta} U_{\alpha\beta} e_\beta = \sum_\beta \sqrt{\lambda_\beta} e^\dagger_\beta U^{-1}_{\beta\alpha}; \tag{83}$$

provided that the $\{A_\alpha\}$ are hermitian operators.

b. **Projection of observables:** With the aid of eq. (80) and new operators (eq. 81), any observable, denoted by B could be projected onto the subspace of the $\{A_\alpha\}$. Let us now consider a new operator B and assume that it is eventually partially correlated to A_α, the new operator

$$B^\perp = B - \sum_\alpha e_\alpha \langle\langle e^\dagger_\alpha | B \rangle\rangle \tag{84}$$

is statistically independent of the $\{A_\alpha\}$ with respect to D (D-independent). First, $B^\perp$ verifies $\langle B^\perp \rangle = \langle B \rangle$, while for any operator $e^\dagger_\beta$, we have

$$\langle\langle B^\perp | e^\dagger_\beta \rangle\rangle \;=\; \langle\langle B | e^\dagger_\beta \rangle\rangle - \sum_\alpha \langle\langle B | e^\dagger_\alpha \rangle\rangle \langle\langle e^\dagger_\beta | e_\alpha \rangle\rangle = 0 \tag{85}$$

due to $\langle\langle e^\dagger_\beta | e_\alpha \rangle\rangle = \delta_{\alpha\beta}$. Since, the A_α are linear combination of the $e^\dagger_\beta$, $\langle\langle B^\perp | A_\alpha \rangle\rangle = 0$ for any α. The new operator can also directly be expressed in terms of the operator A_α, we finally obtain

$$B^\perp = B - \sum_{\alpha\beta} (A_\alpha - \langle A_\alpha \rangle) C^{-1}_{\alpha\beta} \langle\langle A_\beta | B \rangle\rangle, \tag{86}$$

or written differently

$$B \;=\; B^\parallel + B^\perp \qquad \text{with} \qquad B^\parallel = \sum_{\alpha\beta} (A_\alpha - \langle A_\alpha \rangle) C^{-1}_{\alpha\beta} \langle\langle A_\beta | B \rangle\rangle. \tag{87}$$

Therefore, using the same technique as the Principal Component Analysis, any operators can be decomposed into two operators, the second one is statistically independent from the observables $\{A_\alpha\}$, while the first one could be written as a linear combination of the $\{A_\alpha\}$ and contains all

---

[5] Note that the λ_i measure the information content with respect to D of the new operators e_α.

the information on the correlation between B and the latter observables. Properties of the two operators $B^{\|}$ and $B^{\perp}$ are:

$$\begin{aligned} \langle B^{\|}\rangle &= 0, \qquad \text{and} \qquad \langle\langle B^{\|}|A_\alpha\rangle\rangle = \langle\langle B|A_\alpha\rangle\rangle \quad , \qquad (88)\\ \langle B^{\perp}\rangle &= \langle B\rangle, \qquad \text{and} \qquad \langle\langle B^{\perp}|A_\alpha\rangle\rangle = 0, \qquad (89)\end{aligned}$$

valid for any α. In the limit where B is fully described in the subspace of the $\{A_\alpha\}$, then $B^{\perp}$ simply identifies with a number $\langle B\rangle$. If on opposite case, B is statistically independent from these observables, $B^{\|} = 0$.

c. **Projection operators:** Using the notation $|B\rangle\rangle$, two projectors denoted respectively by $\mathbb{P}_A$ and $\mathbb{Q}_A$, can be introduced with

$$\begin{aligned} |B^{\|}\rangle\rangle &= \mathbb{P}_A|B\rangle\rangle, \\ |B^{\perp}\rangle\rangle &= \mathbb{Q}_A|B\rangle\rangle = (1-\mathbb{P}_A)|B\rangle\rangle, \end{aligned} \qquad (90)$$

with the convention

$$\mathbb{P}_A \equiv \sum_\alpha |e^\dagger_\alpha\rangle\rangle\langle\langle e^\dagger_\alpha| = \sum_{\alpha\beta} |A_\alpha\rangle\rangle C^{-1}_{\alpha\beta}\langle\langle A_\beta|. \qquad (91)$$

It could be easily checked that $\mathbb{P}_A^2 = \mathbb{P}_A$ and $\mathbb{Q}_A^2 = \mathbb{Q}_A$ and therefore verify standard properties of projectors. The projection onto the subspace of $\{|A\rangle\rangle\}$ is illustrated in figure 5.

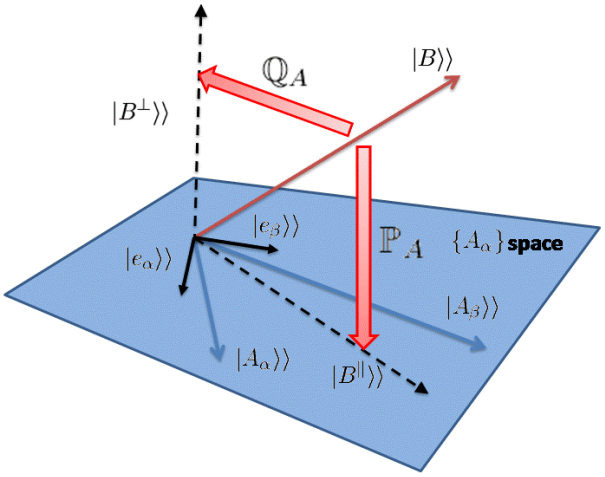

FIG. 5: *Schematic representation of the projection technique assuming only two observables (A_α, A_β). Different entities introduced in the text are shown.*

3. Variational Principle, Projected dynamics and effective Hamiltonian

Coming back to the variational principle, from section III.A.1, we already known that variational principle used in combination with variational states given by (71) leads to the exact evolution of the $\{A_\alpha\}$ over short time. It is shown here that mean-field evolution corresponds to a projected dynamic onto the subspace of variables $\{A_\alpha\}$ where the projection is nothing but the statistical projection introduced previously.

Trial states given by eq. (71) are not a priori normalized along the path. To enforce normalization, an additional parameter is generally added (Feldmeier and Schnack, 2000). Equivalently, one could sightly modify equation (71) as

$$|\mathbf{Q}+\delta\mathbf{Q}\rangle = e^{\sum_\alpha \delta q_\alpha (A_\alpha - \langle A_\alpha\rangle)}|\mathbf{Q}\rangle. \qquad (92)$$

This automatically insures a constant normalization of the state along the path. Accordingly equation (76) now becomes:

$$i\hbar\langle\mathbf{Q}|(A_\alpha - \langle A_\alpha\rangle)|\dot{\mathbf{Q}}\rangle \;=\; \langle\mathbf{Q}|(A_\alpha - \langle A_\alpha\rangle)H|\mathbf{Q}\rangle, \tag{93}$$

where $|\dot{\mathbf{Q}}\rangle$ could be written in terms of the $\{q_\alpha\}$ evolutions as

$$|\dot{\mathbf{Q}}\rangle \;=\; \sum_\alpha \dot{q}_\alpha (A_\alpha - \langle A_\alpha\rangle)|\mathbf{Q}\rangle. \tag{94}$$

The evolution of $\mathbf{Q}$ given above is nothing but an approximate evolution with an effective Hamiltonian written in terms of a linear combination of the $\{A_\alpha\}$ operators. Combining these equations leads to

$$i\hbar \sum_\beta \dot{q}_\beta C_{\alpha\beta} \;=\; \langle\mathbf{Q}|(A_\alpha - \langle A_\alpha\rangle)H|\mathbf{Q}\rangle, \tag{95}$$

where C denotes the correlation matrix whose components are defined in eq. (79). Inverting the equation to obtain $\dot{q}_\alpha$ explicitly finally gives:

$$\begin{aligned} i\hbar|\dot{\mathbf{Q}}\rangle \;&=\; \Big\{ \sum_{\alpha\beta} (A_\alpha - \langle A_\alpha\rangle)|\mathbf{Q}\rangle \; C^{-1}_{\alpha\beta} \; \langle\mathbf{Q}|(A_\beta - \langle A_\beta\rangle)\Big\} H|\mathbf{Q}\rangle \\ &=\; \Big\{ \sum_{\alpha\beta} (A_\alpha - \langle A_\alpha\rangle) C^{-1}_{\alpha\beta} \langle\langle A_\beta|H\rangle\rangle \Big\}|\mathbf{Q}\rangle = H^{\parallel}(t)|\mathbf{Q}\rangle. \end{aligned} \tag{96}$$

Therefore, the mean-field evolution is indeed equivalent to a projected dynamics onto a sub-space containing the relevant information on selected observables. More generally, for any observable that are eventually out of the relevant subspace, mean-field will provide the best approximation retaining only the optimal path for the $\{\langle A_\alpha\rangle\}$ observables. The projected dynamic corresponds to an effective mean-field Hamiltonian, denoted hereafter simply by $H_{\rm MF}(t)$. This Hamiltonian writes as a linear combination of the $\{A_\alpha\}$ operators and identifies with the projected part of H onto the relevant space. Note that same conclusion can be drawn using a slightly different approach based on Liouville representation (Balian, 1999).

In a pure density case, i.e. $D = |\mathbf{Q}\rangle\langle\mathbf{Q}|$, one can further precise the approximation made by introducing a projector $\mathcal{P}_A$ directly acting in Hilbert space

$$\mathcal{P}_A(t) \;=\; \sum_{\alpha\beta} (A_\alpha - \langle A_\alpha\rangle)|\mathbf{Q}\rangle \; C^{-1}_{\alpha\beta} \; \langle\mathbf{Q}|(A_\beta - \langle A_\beta\rangle). \tag{97}$$

According to eq. (96), we simply have $H_{\rm MF}(t) = \mathcal{P}_A(t)H$.

4. Validity of the mean-field approximation

The validity of the mean-field approximation strongly depends on the information carried out by the observables $\{A_\alpha\}$ and on the effects of the residual part of the Hamiltonian, denoted by $V_{\rm res}(t)$, which is neglected. Using the projection operator defined above, the exact Hamiltonian splits into

$$H \;=\; \underbrace{\mathcal{P}_A(t)H}_{H_{\rm MF}(t)} + \underbrace{(1-\mathcal{P}_A(t))H}_{V_{\rm res}(t)}.$$

Assume that at a given time, the exact wave-function $|\Psi(t)\rangle$ is properly described by the trial wave-function, i.e. $|\Psi(t)\rangle = |\mathbf{Q}(t)\rangle$. At latter time, due to the residual interaction, the exact wave-function $|\Psi(t+\Delta t)\rangle$ will deviate from the mean-field approximation $|\mathbf{Q}(t+\Delta t)\rangle$. In Hilbert space, the accuracy of mean-field depends on the difference between the two wave-packets (Feldmeier and Schnack, 2000) that, for small time-step $\Delta t = dt$, reads:

$$|\Delta(t+dt)\rangle \;=\; |\Psi(t+dt)\rangle - |\mathbf{Q}(t+dt)\rangle = \frac{dt}{i\hbar}\left(H - i\hbar\frac{d}{dt}\right)|\mathbf{Q}(t)\rangle \tag{98}$$

$$\;=\; \frac{dt}{i\hbar}(1-\mathcal{P}_A(t))H\,|\mathbf{Q}(t)\rangle\,. \tag{99}$$

The use of a variational principle insures that the optimal path is obtained within the class of trial state. This is indeed automatically the case due to:

$$\left(\frac{\partial}{\partial q^*_\alpha}\langle \mathbf{Q}(t)|\right)|\Delta(t+dt)\rangle \;=\; \frac{\partial}{\partial q^*_\alpha}\langle \mathbf{Q}(t)|H - i\hbar\frac{d}{dt}|\mathbf{Q}(t)\rangle = 0, \tag{100}$$

where we recognize nothing but the variation of the action (65) with respect to δq^*_α. Therefore, by construction, any alternative choice than mean-field at time $t+dt$ within the class of trial state one would have given a larger deviation. A global measure of the deviation from mean-field could be estimated using $\langle\Delta(t+dt)|\Delta(t+dt)\rangle$ (for further discussion see (Feldmeier and Schnack, 2000)).

In many situations, for instance when the number of degrees of freedom is much larger than the one described by the $\{A_\alpha\}$, we do expect that mean-field wave-packet can deviate significantly from the exact one even for rather short time. Nevertheless, for some observables, mean-field can still be a good approximation. Indeed, requiring to have specific degrees of freedom correct is much less demanding than having the correct wave-function. Let us consider an observable B and assume that its initial value identifies with the exact one, we now define the quantity

$$\Delta_B(t+\Delta t) = \langle B(t+\Delta t)\rangle_\Psi - \langle B(t+\Delta t)\rangle_{\mathbf{Q}} \tag{101}$$

where $\langle B(t+\Delta t)\rangle_\Psi$ and $\langle B(t+\Delta t)\rangle_{\mathbf{Q}}$ denote respectively the exact and mean-field expectation value of B at time $t+\Delta t$. Since at the mean-field level the Hamiltonian is approximated by the projected one, we obtain for small time interval dt:

$$\Delta_B(t+dt) \;=\; \frac{dt}{i\hbar}\langle \mathbf{Q}(t)|[B, V_{\rm res}(t)]\,|\mathbf{Q}(t)\rangle = \frac{dt}{i\hbar}\langle \mathbf{Q}(t)|[B^\perp, H]\,|\mathbf{Q}(t)\rangle$$

Therefore, the mean-field approximation will provide a good approximation for all observables if $V_{\rm res}(t)$ is small. Even if the neglected part of the Hamiltonian might not be negligible, variables with small $B^\perp$, i.e. if the information on B is mainly contained in the sub-space of the $\{A_\alpha\}$, will be accurately described at the mean-field level. Obviously, this is the case for the operators $\{A_\alpha\}$ for which $A^\perp_\alpha = \langle A_\alpha\rangle$ and $\Delta_{A_\alpha}(t+dt) = 0$ as shown in section III.A.1.

B. Application to the Many-Body problem

Notions introduced in previous section are illustrated here for the problem of N interacting particles. Our starting point is the variational principle written in this case as

$$S \;=\; \int_{t_0}^{t_1} ds \int_{\{\mathbf{r}_i\}} \left[\prod_i d^3\mathbf{r}_i\right] \Psi^*(\{\mathbf{r}_i\},t)\Big(i\hbar\partial_t - H(\{\mathbf{r}_i\})\Big)\Psi^*(\{\mathbf{r}_i\},t) \tag{102}$$

where Ψ denotes a N-body wave-packets functional of the particles positions $\{\mathbf{r}_i\} \equiv (\mathbf{r}_1, \cdots, \mathbf{r}_N)$. H corresponds to a Many-Body Hamiltonian given by (63). For the sake of simplicity, we will consider here two-body Hamiltonian only.

In the following, the so-called "independent particle" or "mean-field" approximation is first presented for fermions. As illustrated previously, different strategies can be employed to introduce mean-field, namely variational principle, Ehrenfest theorem, or projection leading to effective Hamiltonian. Although, strong connections exist between them, important features might be completely missed by using only one of them. For instance, the reduction of information is best seen using variational principle while missing pieces appears more clearly using the Ehrenfest theorem and/or a direct separation of the Hamiltonian into a mean-field and residual part as done in section II.C.4. For this reason, different approaches are discussed below.

1. The independent particle approach for fermionic systems

If the two-body interaction is neglected in the Hamiltonian, then, the exact many-body wave-function is exactly known and reduces to an anti-symmetric product (Slater determinant) of single-particle orthogonal states, denoted by $\{\varphi_\alpha\}$

$$\Psi(\{\mathbf{r}_i\}) \;=\; \mathcal{A}\left(\varphi_1(\mathbf{r}_1)\cdots\varphi_N(\mathbf{r}_N)\right) \tag{103}$$

where $\mathcal{A}(.)$ denotes the anti-symmetrization operator. The associated one-body density matrix ρ reads $\rho = \sum_{\alpha=1,N} |\varphi_\alpha\rangle\langle\varphi_\alpha|$. It can be easily checked that $Tr(\rho) = N$ and $\rho^2 = \rho$ underlining that it has exactly N occupation numbers equal to one while the others equal to zero. In the following, we will use the α for occupied (hole) states. For independent particle states, correlations matrices vanish at any order and all the information on the system is contained in the one-body density matrix. This is illustrated by the fact that, for any order k, the k-body density matrix is given by an anti-symmetric product of the one-body density matrix (see appendix A):

$$\begin{aligned} \rho_{12} &= \rho_1\rho_2\,(1 - P_{12})\,, \\ \rho_{123} &= \rho_1\rho_2\rho_3\,(1 - P_{12})\,(1 - P_{13} - P_{23})\,, \\ &\dots \end{aligned}$$

Here, notations of refs. (Lacroix *et al.*, 2004a; Simenel *et al.*, 2008)) are used, where the indices refer to the particle on which the operator is applied.

a. **Direct application of the variational principle** When the two- (and more) body interaction is plugged in, the wave-function cannot be written in the simple form (103). However, one could still find an approximate solution by restricting the trial wave-function to a Slater determinant, this is the so-called Hartree-Fock or Time-Dependent Hartree-Fock approximation first proposed in refs. (Fock, 1930; Hartree, 1928) and (Dirac, 1930). In that case, the action reduces to (Kerman and Koonin, 1976)

$$S = \int_{t_0}^{t_1} dt \sum_\alpha \int_{\mathbf{r}} d^3\mathbf{r} \Big\{ i\hbar\varphi_\alpha^*(\mathbf{r},t)\dot{\varphi}_\alpha^*(\mathbf{r},t) - \mathcal{H}[\{\varphi_\alpha\},\{\varphi_\alpha^*\}] \Big\}, \tag{104}$$

where $\mathcal{H}[\{\varphi_\alpha\},\{\varphi_\alpha^*]\}]$ is given by

$$\mathcal{H}[\{\varphi_\alpha\},\{\varphi_\alpha^*\}] = \sum_\alpha \langle\varphi_\alpha|T|\varphi_\alpha\rangle + \frac{1}{4}\sum_{\alpha,\beta}\langle\varphi_\alpha\varphi_\beta|\tilde{v}_{12}|\varphi_\alpha\varphi_\beta\rangle, \tag{105}$$

where $\tilde{v}_{12}$ is anti-symmetric. Such a state can grasp part of the two-body effects through the introduction of a self-consistent mean-field. Variation of the action (104) have to be made with respect to the components of the single-particle basis $\{\varphi_\alpha^*(\mathbf{r})\}$ or its complex conjugate $\{\varphi_\alpha(\mathbf{r})\}$ leading to

$$i\hbar\frac{\partial}{\partial t}\varphi_\alpha(\mathbf{r}) = \frac{\delta\mathcal{H}}{\delta\varphi_\alpha^*(\mathbf{r})} \qquad \text{and} \qquad i\hbar\frac{\partial}{\partial t}\varphi_\alpha^*(\mathbf{r}) = -\frac{\delta\mathcal{H}}{\delta\varphi_\alpha(\mathbf{r})}. \tag{106}$$

Above equations of motion are generally written in terms of the mean-field Hamiltonian defined through [6]

$$\frac{\delta\mathcal{H}}{\delta\varphi_\alpha^*} \equiv h[\rho]\varphi_\alpha\,, \qquad \text{with} \qquad h[\rho] = t + \mathrm{Tr}_2\tilde{v}_{12}\rho_2. \tag{107}$$

Here, t denotes matrix elements of the kinetic part while the second term corresponds to the average potential created by the N particles. In equation (107), $\mathrm{Tr}_2(.)$ is the partial trace on the second particle (for instance $\langle i|\mathrm{Tr}_2\tilde{v}_{12}\rho_2|j\rangle = \sum_{kl}\langle ik|\tilde{v}_{12}|jl\rangle\,\langle l|\rho|k\rangle$).

b. **One-body density evolution:** From the single-particle state evolution (106), we deduce that (using the short-hand notation $|\varphi_\alpha\rangle = |\alpha\rangle$)

$$i\hbar\partial_t\rho = (i\hbar\partial_t|\alpha\rangle)\langle\alpha| + i\hbar\partial_t|\alpha\rangle(i\hbar\partial_t\langle\alpha|) = [h[\rho],\rho]. \tag{108}$$

---

[6] For the sake of simplicity, when no ambiguity exist, we simply write $\rho^{(1)} = \rho$

This equation of motion, called mean-field approximation or Time-Dependent Hartree-Fock approximation (TDHF), represents the optimal path in the space of one-body observables for short time evolutions. Slater determinants correspond to a specific class of trial states discussed in section III.A.1. Indeed, according to the Thouless theorem (Thouless, 1960), any local transformation of a Slater determinant $|\Psi\rangle$ into another Slater determinant writes

$$|\Psi + \delta\Psi\rangle = e^{\sum_{ij} \delta Z_{ij} a_i^\dagger a_j} |\Psi\rangle. \tag{109}$$

Said differently, the set of one-body operators $\{a_i^\dagger a_j\}$ are generators of the transformation between Slater determinants. Accordingly, the variational principle automatically ensures that

$$i\hbar \frac{d}{dt}\langle a_i^\dagger a_j\rangle \;=\; \langle [a_i^\dagger a_j, H]\rangle \tag{110}$$

along the path. It could indeed be checked that the evolution of one-body observables estimated through the Ehrenfest theorem using a Slater determinant gives the mean-field evolution (108).

2. Mean-field dynamics from Thouless Theorem

Mean-field evolution corresponds to a projected dynamic onto the space of relevant one-body degrees of freedom where the coupling to irrelevant degrees of freedom (correlation) is neglected. A projected Hamiltonian could be explicitly constructed using the projection technique introduced in section III.A.3. Here, a more direct method is used first to directly separate the Hamiltonian into a mean-field part and residual part and second to illustrate that mean-field could be obtained even without the variational principle.

To precise the missing part, we write the Slater determinant in second quantization form $|\Psi\rangle = \Pi_\alpha a_\alpha^\dagger|-\rangle$ and complete the occupied states by a set (possibly infinite) of unoccupied single-particle states (also called particle states) labeled by $\bar{\alpha}$ and associated to the creation/annihilation $a_{\bar{\alpha}}^\dagger$ and $a_{\bar{\alpha}}$. The completed basis verifies

$$\sum_\alpha |\alpha\rangle\langle\alpha| + \sum_{\bar{\alpha}} |\bar{\alpha}\rangle\langle\bar{\alpha}| \equiv \rho + (1-\rho) = 1. \tag{111}$$

From this closure relation, any creation operator associated to a single-particle states $|i\rangle$ decomposes as

$$a_i^\dagger \;=\; \sum_\alpha a_\alpha^\dagger \langle\alpha \,|\, i\rangle + \sum_{\bar{\alpha}} a_{\bar{\alpha}}^\dagger \langle\bar{\alpha} \,|\, i\rangle\,. \tag{112}$$

For instance, restarting from the general expression of H and expressing the different single-particle states (i,j,k,l) in the particle-hole basis gives:

$$\begin{aligned} H\,|\Psi\rangle \;=\; \Big\{ & -\tfrac{1}{2} Tr(\tilde{v}_{12}\rho_1\rho_2) && \Longleftrightarrow \quad E_0[\rho] \\ & + \textstyle\sum_{\alpha,\beta} \langle\beta\,|\rho h[\rho]|\,\alpha\rangle\, a_\beta^\dagger a_\alpha + \sum_{\bar{\alpha}\alpha} \langle\bar{\alpha}\,|h[\rho]|\,\alpha\rangle\, a_{\bar{\alpha}}^\dagger a_\alpha && \Longleftrightarrow \quad H_{MF}[\rho] \\ & + \tfrac{1}{4} \textstyle\sum_{\bar{\alpha}\bar{\beta}\alpha\beta} \langle\bar{\alpha}\bar{\beta}\,|\tilde{v}|\,\alpha\beta\rangle\, a_{\bar{\alpha}}^\dagger a_{\bar{\beta}}^\dagger a_\beta a_\alpha && \Longleftrightarrow \quad V_{res}[\rho] \\ & \Big\}\,|\Psi\rangle \end{aligned} \tag{113}$$

where commutations have been performed in such a way that all creation operators are on the left and where $a_\alpha^\dagger|\Psi\rangle = a_{\bar{\alpha}}|\Psi\rangle = 0$ has been used.

This expression is helpful to understand the approximation made at the mean-field level. In previous section, we have shown that mean-field provides the best approximation for one-body degrees of freedom using the Ehrenfest theorem. Here, we will show that the mean-field evolution is equivalent to an effective Hamiltonian dynamics where V_{res} is neglected.

Assuming that only $E_0[\rho]$ and $H_{MF}[\rho]$ contribute to the evolution. Then, over an infinitesimal time step dt, the new state is approximated by

$$|\Psi(t+dt)\rangle \simeq \exp\left(\frac{dt}{i\hbar} E_0[\rho]\right) \exp\left(\frac{dt}{i\hbar} H_{MF}[\rho]\right) |\Phi\rangle\,. \tag{114}$$

The first exponential is simply a global phase factor and will not contribute to observable evolution. The second contribution corresponds to an exponential of a one-body operator, which according to the Thouless Theorem (Thouless, 1960) transforms a Slater Determinant into another Slater determinant.

Indeed, using fermionic commutation rules, gives [7]

$$\exp\left(\frac{dt}{i\hbar}H_{MF}(\rho)\right)|\Phi\rangle \;=\; \Pi_\alpha a^\dagger_{\alpha+d\alpha}\,|-\rangle \tag{117}$$

where the states $|\alpha+d\alpha\rangle$ are the new single-particle states deduced from the $|\alpha\rangle$ through the standard mean-field evolution. Besides the fact that we the mean-field is directly recovered, another interest of the present approach is to provide an effective Hamiltonian that is directly separated into a relevant and irrelevant part. As shown in next chapter, an explicit expression of $\hat{V}_{res}$ is useful to discuss the departure from a mean-field dynamics.

3. Mean-field with pairing correlations

Mean-field theory is sometime restricted to the approximation were the many-body wave-function is replaced by a Slater determinant state. Here, mean-field will be more generally referred to the approximation where the trial state is a quasi-particle vacuum. Slater determinants is a sub-class of quasi-particle states with occupation 1 and 0. Applying the same technique as above, leads to the Time-Dependent Hartree-Fock Bogolyubov (TDHFB) where pairing correlations can be included. In that case, the generator of transformations between quasi-particle vaccua are the set of operators $\{\; a^\dagger_i a_j \;,\; a^\dagger_i a^\dagger_j \;,\; a_i a_j \;\}$.

a. **Quasi-particle vacuum:** We now consider a quasi-particle vacuum written as

$$|\Psi\rangle \sim \prod_\alpha \beta_\alpha |-\rangle, \tag{118}$$

where the β_α denotes a complete set of quasi-particle annihilation operators. This form automatically insures $\beta_\alpha|\Psi\rangle = 0$ for any α. The new quasi-particle states are defined through a specific linear combination (Bogolyubov transformation) of single-particle creation/annihilation operators $\{\; a^\dagger_i, a_i \;\}$ (Ring and Schuck, 1980)

$$\left\{\begin{array}{l} \beta_\alpha = \;\sum_i U^*_{i\alpha} a_i + V^*_{i\alpha} a^\dagger_i \\ \beta^\dagger_\alpha = \;\sum_i U_{i\alpha} a^\dagger_i + V_{i\alpha} a_i. \end{array}\right. \tag{119}$$

---

[7] **Proof:** Using the fact that $e^{-\frac{dt}{i\hbar}H_{MF}} e^{\frac{dt}{i\hbar}H_{MF}} = 1$ and $e^{\frac{dt}{i\hbar}H_{MF}}|-\rangle = |-\rangle$

$$\begin{aligned} e^{\frac{dt}{i\hbar}H_{MF}}|\Psi\rangle \;&=\; e^{\frac{dt}{i\hbar}H_{MF}}\Pi_\alpha a^\dagger_\alpha|-\rangle \\ &=\; e^{\frac{dt}{i\hbar}H_{MF}} a^\dagger_{\alpha_1} e^{-\frac{dt}{i\hbar}H_{MF}} e^{\frac{dt}{i\hbar}H_{MF}} a^\dagger_{\alpha_2} e^{\frac{dt}{i\hbar}H_{MF}} \cdots e^{-\frac{dt}{i\hbar}H_{MF}} a^\dagger_{\alpha_N} e^{-\frac{dt}{i\hbar}H_{MF}} e^{+\frac{dt}{i\hbar}H_{MF}}|-\rangle\,. \end{aligned}$$

Considering the transformation of each creation operator separately, we have

$$\begin{aligned} e^{\frac{dt}{i\hbar}H_{MF}} a^\dagger_\alpha e^{-\frac{dt}{i\hbar}H_{MF}} \;&=\; a^\dagger_\alpha + \frac{dt}{i\hbar}[H_{MF}, a^\dagger_\alpha] + O(dt) \\ &=\; a^\dagger_\alpha + \frac{dt}{i\hbar}\sum_i a^\dagger_i \langle i\,|h[\rho]|\,\alpha\rangle + O(dt) \equiv a^\dagger_{\alpha+d\alpha} + O(dt), \end{aligned} \tag{115}$$

where the expression of the mean-field operator defined in eq. (113) has been used and where "i" refers to the complete original basis. From the above identity, we see that, the propagated many-body state writes $|\Psi(t+dt)\rangle \propto \Pi_\alpha a^\dagger_{\alpha+d\alpha}|-\rangle$ where, using $\sum_i |i\rangle\langle i| = 1$, the single-particle states evolves according to

$$i\hbar\frac{d\,|\alpha\rangle}{dt} = h[\rho]\,|\alpha\rangle\,, \tag{116}$$

which is nothing but the standard mean-field evolution.

where matrices U et V have specific properties to insure that new operators $\{\beta_\alpha, \beta_\alpha^\dagger\}$ verify fermionic anti-commutation rules.

The information on the system is not anymore contained only in the normal density. Indeed, one should introduce the anomalous density whose matrix elements are defined by $\kappa_{ij} = \langle a_j a_i \rangle$ (which also implies $\kappa_{ij}^* = \langle a_i^\dagger a_j^\dagger \rangle$). Latter contractions cancel out for independent particle systems. The Bogolyubov transformation (Eq. (119))can be inverted to express the $a^\dagger$ and a operators in terms of quasi-particles operators :

$$\left\{ \begin{array}{l} a_i = \sum_\alpha U_{i\alpha}\beta_\alpha + V_{i\alpha}^*\beta_\alpha^\dagger \\ a_i^\dagger = \sum_\alpha V_{i\alpha}\beta_\alpha + U_{i\alpha}^*\beta_\alpha^\dagger. \end{array} \right. \tag{120}$$

Using these expressions in ρ et κ, we deduce

$$\rho_{ij} = \sum_\alpha V_{j\alpha}V_{i\alpha}^* = \left(V^* V^T\right)_{ij}, \qquad \kappa_{ij} = \left(V^* U^T\right)_{ij} \ . \tag{121}$$

These contractions are generally presented as a generalized density matrix defined as

$$\mathcal{R} = \left(\begin{array}{cc} \left(\langle a_j^\dagger a_i \rangle\right) & \left(\langle a_j a_i \rangle\right) \\ \left(\langle a_j^\dagger a_i^\dagger \rangle\right) & \left(\langle a_j a_i^\dagger \rangle\right) \end{array} \right) = \left(\begin{array}{cc} \rho & \kappa \\ -\kappa^* & 1-\rho^* \end{array} \right). \tag{122}$$

The new contractions enable to treat a certain class of correlations that were neglected previously. Using the Wick theorem (Blaizot and Ripka, 1986; Ring and Schuck, 1980), components of the associated two-body correlation matrix now read

$$\begin{array}{rcl} \rho_{ijkl}^{(2)} = \langle ij|\rho_{12}|kl\rangle = \langle a_k^\dagger a_l^\dagger a_j a_i \rangle &=& \overline{a_k^\dagger a_i}\ \overline{a_l^\dagger a_j} - \overline{a_k^\dagger a_j}\ \overline{a_l^\dagger a_i} + \overline{a_k^\dagger a_l^\dagger}\ \overline{a_j a_i} \\ &=& \rho_{ik}\rho_{jl} - \rho_{il}\rho_{jk} + \kappa_{ij}\kappa_{kl}^*. \end{array} \tag{123}$$

On opposite to Slater determinant, the correlation matrix denoted by C_{12} does not a priori vanish anymore. We further see that the HFB theory leads to separable form of the two body correlation matrix elements:

$$C_{ijkl} = \kappa_{ij}\kappa_{kl}^*. \tag{124}$$

In turn, the HFB is more complex than the HF one. For instance, the state is not anymore an eigenstate of the particle number operator. We say that the particle number symmetry is explicitly broken. Fluctuations associated to the particle number $N = \sum_\alpha a_\alpha^\dagger a_\alpha$ now write

$$\langle N^2 \rangle - \langle N \rangle^2 = 2\,\mathrm{Tr}\ (\kappa\kappa^\dagger) = 2\,\mathrm{Tr}\ (\rho - \rho^2). \tag{125}$$

In general, this quantity is non-zero for a quasi-particle vacuum. This implies for instance that at least the particle number should be constrained in average in nuclear structure studies (this is generally done by adding a specific Lagrange multiplier to the variational principle). It is also worth to mention that in dynamical TDHFB evolution, the expectation value $\langle N \rangle$ is a constant of motion. Therefore, no specific care of particle number is necessary in the dynamical case.

b. **TDHFB Equations:** Since the generators of transformation between quasi-particle states now include the $\{a_i a_j\}$ and their hermitian conjugate, minimization of the action is now equivalent to optimize associated equations of motion given by the Ehrenfest theorem :

$$i\hbar\frac{d}{dt}\rho_{ji} = i\hbar\frac{d}{dt}\langle a_i^\dagger a_j \rangle = \langle [a_i^\dagger a_j, \hat{H}] \rangle, \tag{126}$$

$$i\hbar\frac{d}{dt}\kappa_{ji} = i\hbar\frac{d}{dt}\langle a_i a_j \rangle = \langle [a_i a_j, \hat{H}] \rangle. \tag{127}$$

Using the Wick theorem, one directly obtained the set of coupled equations (Simenel *et al.*, 2008):

$$i\hbar\frac{d}{dt}\rho = [h, \rho] + \kappa\Delta^* - \Delta\kappa^*, \tag{128}$$

and

$$i\hbar\frac{d}{dt}\kappa = h\kappa + \kappa h^* - \rho\Delta - \Delta\rho^* + \Delta, \tag{129}$$

where Δ denotes the pairing field:

$$\Delta_{ij} = \frac{1}{2}\sum_{kl}\tilde{v}_{ijkl}\kappa_{kl}. \tag{130}$$

Finally, using the generalized density matrix $\mathcal{R}$ and generalized HFB Hamiltonian $\mathcal{H}$, defined as

$$\mathcal{H} \equiv \begin{pmatrix} h & \Delta \\ -\Delta^* & -h^* \end{pmatrix}, \tag{131}$$

equations on ρ and κ can be written, in a more convenient form, as

$$i\hbar\frac{d\mathcal{R}}{dt} = [\mathcal{H}, \mathcal{R}]\,. \tag{132}$$

The TDHFB equation generalizes the TDHF case (Eq. (108)) by accounting for pairing effects in the dynamical evolution. Note finally that, similarly to the TDHF case, one can also directly obtain the mean-field equation with pairing by splitting the Hamiltonian into a HFB part and a residual interaction part (not shown here).

C. Summary and discussion

In this section, basic ingredients of mean-field theory have been presented starting from a variational principle. Variational principles are very helpful to understand to what extend mean-field approximation provides an optimal description of selected degrees of freedom and could be understood as a projection of the exact dynamics on a subspace of observables.

The independent particle approximation has the great advantage to replace the exact many-body problem by a much simpler one-body problem that could most often be treated numerically. However, it is rarely used in the form presented here, i.e. starting from an Hamiltonian and performing the Hartree-Fock or the Hartree-Fock Bogolyubov approximation. The first reason is that correlations called "beyond mean-field" play an important role: direct two-body effects, pairing, quantum zero point motion in collective space. TDHFB, presented above, corresponds to one of the possible extension of mean-field able to account for pairing effects. In the next section, a description of recent advances in quantum transport theory beyond mean-field is made.

A second and more subtle difficulty is that Hartree-Fock approximation starting from the bare interaction, for instance in condensed matter or in nuclear physics, does not provide a sufficiently good approximation to serve as a starting point for the nuclear many-body problem. To overcome this difficulty, the independent particle picture is still used but in a functional spirit within the Density Functional Theory (condensed matter) or Energy Density Functional (nuclear physics) framework. The concept of functional theory is discussed in section V.

IV. DYNAMICAL THEORIES BEYOND MEAN-FIELD

In previous sections, the independent particle approximation to the N-body problem has been introduced. This approximation has played and continues to play a major role for our understanding of interacting systems. While the gross features of most nuclei are properly accounted for by replacing the complex many-body wave-function by a Slater determinant and an effective Hamiltonian (EDF), most often, physical processes reveal correlations beyond mean-field (Bender *et al.*, 2003). The complexity of nuclei reveals the many facets of correlations (see Figure 6). For instance short and long range correlations in static nuclei could only be accounted for by a proper treatment of pairing effects and configuration mixing. Conjointly, as collision energies between two nuclei increase, the Pauli principle becomes less effective to block direct nucleon-nucleon collisions. Then, two-body correlations should explicitly be accounted for. During the past decades, several approaches have been introduced to treat correlations beyond mean-field in a quantum theory. The development of such a theory has been strongly influenced by concepts developed in section II for open quantum systems. In that case, one-body degrees of freedom are the relevant observables and play the role of a system coupled to the surrounding environment of more complex observables. Recent advances in theories treating correlations beyond mean-field are presented in this section. A comprehensive list of theories introduced in this section is given in table I, in each case the associated acronym and key observables are given.

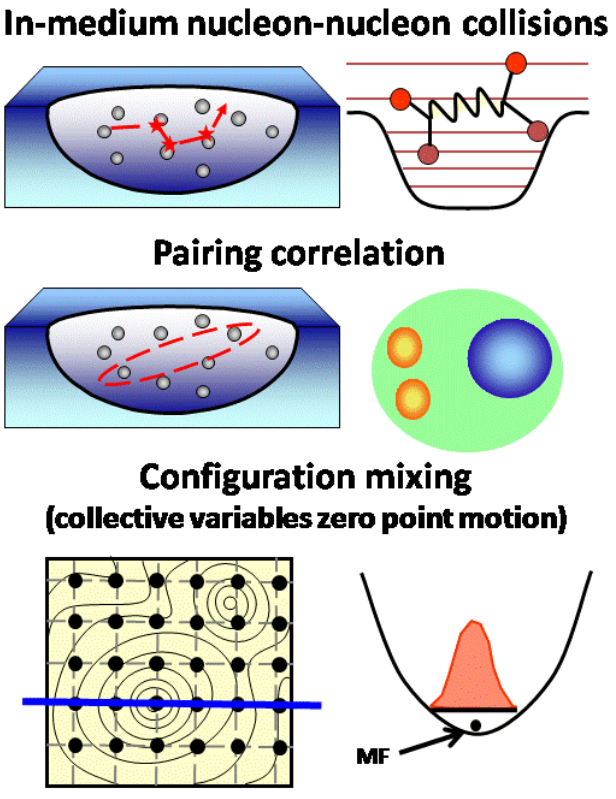

FIG. 6: *Schematic illustration of the different types of correlation beyond mean-field. From top to bottom, direct in-medium nucleon-nucleon collisions, pairing and correlations associated to configuration mixing are respectively shown. Assuming that a system is properly described by a Slater determinant, direct nucleon-nucleon collisions is the first source of departure from the independent particle picture and is the physical process at the origin of thermalization. However, at low internal excitation energies, this effect is strongly hindered due to Pauli effect induced by surrounding nucleons and other correlations dominate. Pairing affects nuclear structure properties like masses, collective motion, pair transfer, ... Configuration mixing, generally incorporated through the Generator Coordinate method, tell us that nuclei could not a priori be simply described by a single Slater determinant. While the latter misses fluctuations collective space, configuration mixing incorporates it properly.*

A. Limitation of the mean-field theory and departure from the single-particle (or quasi-particle) picture

In expression (113), a clear separation is made between what is properly treated at the mean-field level ($E_0[\rho]$ and $H_{MF}[\rho]$) and what is neglected, i.e. $V_{res}[\rho]$. At this point several comments are in order:

- The validity of the mean-field approximation depends on the intensity of the residual inter-

Name	approximation	Quantities evolved	associated observables
TDHF	mean-field (m.-f.)	$\rho = \sum_\alpha \|\varphi_\alpha\rangle\langle\varphi_\alpha\|$	one-body
TDHF-Bogoliubov (TDHFB)	m.-f. + pairing	ρ, κ	generalized one-body
Extended-TDHF (ETDHF)	m.-f. + NN collision (dissipation)	$\rho = \sum_\alpha \|\varphi_\alpha\rangle n_\alpha \langle\varphi_\alpha\|$	one-body
Stochastic-TDHF (STDHF)	m.-f. + NN collision (dissipation+fluctuations)	$D = \overline{\|\Psi\rangle\langle\Psi\|}$ Quant. Jump between SD	one-body
Stochastic mean-field (SMF)	m.-f. + initial fluctuation	$D = \overline{\|\Psi\rangle\langle\Psi\|}$ Random Initial Value	conf. mixing
Time Dept. Density Mat. (TDDM)	m.f. + two-body correlations	ρ, C_{12}	one- and two-body
TDDM^P	m.f. + two-body correlations (approximation of TDDM focused on pairing)	ρ, C_{12}	one- and two-body
Quantum Monte-Carlo (QMC)	Exact (within stat. errors) Quantum Jump	$D = \overline{\|\Psi_1\rangle\langle\Psi_2\|}$	all

TABLE I: Summary of microscopic approaches presented in this document.

action which itself depends on the SD state $|\Phi\rangle$ and therefore will significantly depend on the physical situation. Using simple arguments (Lichtner and Griffin, 1976), the time τ_{SD} over which the Slater determinant picture breaks down could be expressed as:

$$\tau_{SD} \;=\; \frac{\hbar}{2}\Big(\frac{1}{N}\sum_{\bar\alpha\bar\beta\alpha\beta} |\left\langle \bar\alpha\bar\beta\left|\tilde v\right|\alpha\beta\right\rangle|^2\Big)^{-1/2}. \tag{133}$$

In nuclear physics, typical values of the residual interaction leads to $\tau_{SD} \simeq 100 - 200$ fm/c. Therefore, even if the starting point is given by an independent particle wave-packet, the exact evolution will deviate rather fast from the mean-field dynamics. This gives strong arguments in favor of theories beyond TDHF.

- An alternative expression of the residual interaction which is valid in any basis, is

$$V_{res}[\rho] \;=\; \frac{1}{4}\sum_{ijkl}\langle ij\,|(1-\rho_1)(1-\rho_2)\tilde v_{12}\rho_1\rho_2|\,kl\rangle\, a_i^\dagger a_j^\dagger a_l a_k. \tag{134}$$

This expression illustrates that the residual interaction associated to a Slater determinants could be seen as a "dressed" interaction which properly account for Pauli principle. Physically, the residual interaction corresponds to direct nucleon-nucleon collisions between occupied states (2 holes) which could only scatter toward unoccupied states (2 particles) due to Pauli blocking. We say sometimes that the residual interaction has a 2 particles-2 holes (2p-2h) nature.

Due to the residual interaction, the exact many-body state will become a more and more complex superposition of Slater determinants during the time evolution. As stressed in the introduction, due to the complexity of the nuclear many-body problem, the exact dynamics is rarely accessible. In the following section, methods to include correlations beyond mean-field, like direct nucleon-nucleon collisions or pairing, are discussed.

B. General correlated dynamics: the BBGKY hierarchy

The use of the Ehrenfest theorem (section III.A.1), underlines that the mean-field theory is particularly suited to describe one-body degrees of freedom. A natural extension of mean-field consists in following explicitly two-body degrees of freedom. Considering now the Ehrenfest theorem for the one and two-body degrees of freedom leads to two coupled equations for the one and two-body density matrix components $\rho^{(1)}_{ij} = \langle a^\dagger_j a_i \rangle$ and $\rho^{(2)}_{ij,kl} = \langle a^\dagger_k a^\dagger_l a_j a_i \rangle$

$$\left\{ \begin{array}{ll} i\hbar\frac{\partial}{\partial t}\rho_1 = & [t_1, \rho_1] + \frac{1}{2}\mathrm{Tr}_2\left[\tilde{v}_{12}, \rho_{12}\right] \\ & \\ i\hbar\frac{\partial}{\partial t}\rho_{12} = & [t_1 + t_2 + \frac{1}{2}\tilde{v}_{12}, \rho_{12}] + \frac{1}{2}Tr_3\left[\tilde{v}_{13} + \tilde{v}_{23}, \rho_{123}\right] \end{array} \right. . \tag{135}$$

Above equations are the first two equations of a hierarchy equations, known as the Bogolyubov-Born-Green-Kirkwood-Yvon (BBGKY) hierarchy(Bogolyubov, 1946; Born and Green, 1946; Kirkwood, 1946) where the three-body density evolution is also coupled to the four body density and so on and so forth. Here, we will restrict to the equations on ρ_1 and ρ_{12} which have often served as the starting point to develop transport theories beyond mean-field (Abe *et al.*, 1996; Cassing and Mosel, 1990; Lacroix *et al.*, 2004a; Reinhard and Toepffer, 1994).

C. The Time-Dependent Density-Matrix Theory

Mean-field approximation neglects two-body and higher correlations ($C_{12} = 0$). In that case, the equations on ρ_1 reduces to TDHF. A natural extension corresponds to neglecting three-body and higher order correlations ($C_{123} = 0$) [8]. The resulting theory where coupled equations between the one-body density ρ_1 and the two-body correlation C_{12} are followed in time are generally called Time-Dependent Density-Matrix (TDDM) theory (see for instance (Cassing and Mosel, 1990)):

$$\left\{ \begin{array}{lll} i\hbar\frac{\partial}{\partial t}\rho_1 = & [h_1[\rho], \rho_1] + \frac{1}{2}\mathrm{Tr}_2\left[\tilde{v}_{12}, C_{12}\right] & \\ & & \\ i\hbar\frac{\partial}{\partial t}C_{12} = & [h_1[\rho] + h_2[\rho], C_{12}] & \\ & + \frac{1}{2}\Big\{(1-\rho_1)(1-\rho_2)\tilde{v}_{12}\rho_1\rho_2 - \rho_1\rho_2\tilde{v}_{12}(1-\rho_1)(1-\rho_2)\Big\} & \Longleftrightarrow B_{12} \\ & + \frac{1}{2}\Big\{\left(1-\rho_1-\rho_2\right)v_{12}C_{12} - C_{12}v_{12}\left(1-\rho_1-\rho_2\right)\Big\} & \Longleftrightarrow P_{12} \\ & +\mathrm{Tr}_3\left[v_{13}, \left(1-P_{13}\right)\rho_1 C_{23}\left(1-P_{12}\right)\right] & \\ & +\mathrm{Tr}_3\left[v_{23}, \left(1-P_{23}\right)\rho_1 C_{23}\left(1-P_{12}\right)\right], & \Longleftrightarrow H_{12} \end{array} \right. \tag{138}$$

where we have dissociated explicitly three terms which will be responsible for the build up of correlations with time. The first term B_{12}, called the Born term, contains the physics of direct in-medium nucleon-nucleon collisions. Comparing B_{12} and expression (134), we see that it is directly

---

[8] Introducing the permutation operator P_{12} between two particles, defined as $P_{12}\left|ij\right\rangle = \left|ji\right\rangle$. The two-body correlation matrix is given by:

$$C_{12} = \rho_{12} - \rho_1\rho_2(1 - P_{12}) \tag{136}$$

while the three-body correlations C_{123} reads

$$\begin{array}{ll} C_{123} = & \rho_{123} - \rho_1 C_{23}\left(1 - P_{12} - P_{13}\right) - \rho_2 C_{13}\left(1 - P_{21} - P_{23}\right) \\ & -\rho_3 C_{12}\left(1 - P_{31} - P_{32}\right) - \rho_1\rho_2\rho_3\left(1 - P_{13}\right)\left(1 - P_{12} - P_{23}\right). \end{array} \tag{137}$$

proportional to the residual interaction. Indeed, starting from a Slater determinant ($C_{12}(t_0) = 0$), this is the only term that does not cancel out in the evolution of C_{12} over short time. In particular, it will be responsible for the departure from an independent particle picture. The physical interpretation of the term P_{12} and H_{12} is less straightforward. For instance, it has been shown that P_{12} could be connected to pairing correlations (Tohyama and Takahara, 2004) (see discussion below) while H_{12} contains higher order p-p and h-h correlations. It is finally worth mentioning that the last term could eventually be modified to better account for conservation laws (see discussion in (Peter *et al.*, 1994)).

Applications of the TDDM theory faces two major difficulties. First, since two-body degrees of freedom are explicitly considered, huge matrices have to be treated numerically and appropriate truncation schemes should be performed. In addition, to make numerical applications applicable to realistic problems suggest the use of contact interactions (Skyrme like). These interactions, which are zero range in r-space are thus of infinite range in momentum space. This unphysical behavior of the interaction is critical in practice, since during nucleon-nucleon collisions, particles will scatter to too high momentum. No clear solution to this problem exists so far in the TDDM theory (Lacroix *et al.*, 2004a). Due to these difficulties, only a few applications have been carried out so far for collective vibrations (De Blasio *et al.*, 1992; Luo *et al.*, 1999; Tohyama and Umar, 2001, 2002b), and very recently for nuclear collisions (Tohyama and Umar, 2002a).

D. Link between TDDM and TDHFB

The connection between the TDDM framework and TDHFB has been clarified in ref. (Tohyama and Takahara, 2004). Assuming a separable correlation in the p-p and h-h channel given by equation (124) leads to:

$$\begin{aligned}\frac{1}{2}\left\langle\lambda\left|Tr_2\left[\tilde{v}_{12},C_{12}\right]\right|\lambda'\right\rangle &= \frac{1}{2}\sum_{kmn}\left\langle\lambda k\left|\tilde{v}_{12}\right|mn\right\rangle\left\langle mn\left|C_{12}\right|\lambda' k\right\rangle-\frac{1}{2}\left\langle\lambda k\left|C_{12}\right|mn\right\rangle\left\langle mn\left|v_{12}\right|\lambda' k\right\rangle,\\ &= \Delta_{\lambda k}\kappa^*_{\lambda' k}-\kappa_{\lambda k}\Delta^*_{\lambda' k}=(\kappa\Delta^*-\Delta\kappa^*)_{\lambda\lambda'},\end{aligned}\tag{139}$$

where Δ is nothing but the pairing field introduced in previous section. Then, the one-body density evolution reduces to

$$i\hbar\frac{d}{dt}\rho=[h[\rho],\rho]+\kappa\Delta^*-\Delta\kappa^*.\tag{140}$$

In ref. (Tohyama and Takahara, 2004), it has been shown that neglecting term B and H in the second equation of (138) leads to a TDHF like equation. Keeping only P and assuming (124) leads to

$$i\hbar\frac{d}{dt}C_{ijkl} = i\hbar\Big\{\frac{d\kappa_{ij}}{dt}\kappa^*_{kl}+\kappa_{ij}\frac{d\kappa^*_{kl}}{dt}\Big\}\tag{141}$$

where the evolution of κ (or κ^*) are given by Eq. (129). The above equation does not insure that the correlation matrix remains separable during the time-evolution. However, assuming that $C_{ijkl}(t)\simeq\kappa_{ij}(t)\kappa^*_{kl}(t)$ is valid for all time, equations of motion identify with the TDHFB equation. It is worth mentioning that the above discussion gives an alternative derivation of the TDHFB equation starting from TDDM illustrating the physical content of P.

E. Direct in-medium two-body collisions and Extended TDHF

Pairing correlations become less important when the internal excitation of the system increases. Conjointly, Pauli principle is less effective to block direct nucleon-nucleon collisions. Two-body collisions are included in the Born term B in eq. (138). In the following, we neglect the term P and H in the evolution of C_{12}(Ayik, 1980; Botermans and Malfliet, 1990; Danielewicz, 1984; Wong and Tang, 1978, 1979) leading to

$$i\hbar\frac{\partial}{\partial t}C_{12}-[h_1[\rho]+h_2[\rho],C_{12}]=B_{12}.\tag{142}$$

The standard strategy to include collisions is closely related to the theory of open quantum systems developed in section II. Then two-body correlations are interpreted as an environment for one-body degrees of freedom. To account for two-body effects without dealing directly with two-body matrices, a projection technique "a la Nakajima-Zwanzig" (see section II.C) is used. First, the correlation equation of motion is integrated from the initial time to t_0 to time t as

$$C_{12}(t) = -\frac{i}{\hbar} ds \int_{t_0}^{t} U_{12}\left(t,s\right) B_{12}\left(s\right) U_{12}^{\dagger}\left(t,s\right) + \delta C_{12}(t), \tag{143}$$

where $U_{12}(t,s)$ represents the independent particle propagation of two particles, $U_{12} = U_1 \otimes U_2$ with $U(t,s) = \exp\left(-\frac{i}{\hbar}\int_s^t h[\rho(t')]dt'\right)$. In expression (143), the first term represents correlations due to the residual interaction during the time interval. The second term describes propagation of the initial correlations $C_{12}(t_0)$ from t_0 to t, i.e. $\delta C_{12}(t) = U_{12}(t,t_0)C_{12}(t_0)U_{12}^{\dagger}(t,t_0)$. Reporting this expression in the evolution of ρ_1, a generalization of TDHF theory is obtained (where we omit the indice "1" in ρ_1)

$$i\hbar\frac{\partial}{\partial t}\rho = [h[\rho],\rho] + K[\rho] + \delta K(t), \tag{144}$$

which is a closed equation for the one-body density. $K[\rho]$, called collision term, reads

$$K[\rho] \;=\; -\frac{i}{\hbar}\int_{t_0}^{t} ds \mathrm{Tr}_2[v_{12}, U_{12}(t,s)B_{12}(s)U_{12}^{\dagger}(t,s)], \tag{145}$$

while $\delta K(t)$ is given by:

$$\delta K(t) = \; Tr_2[v_{12}, \delta C_{12}(t)]. \tag{146}$$

and account for initial correlation effect.

1. Irreversible process and Extended TDHF

Let us first illustrate the advantages of the introduction of collision term on top of the mean-field dynamics and neglect initial correlations, i.e. $\delta K[\rho] = 0$. The resulting theory is called Extended TDHF with a non-Markovian collision term (or with "memory effects"). The terminology "non-Markovian" (in opposition to "Markovian") comes from the fact that the system at time t depends not only on the density at time t but also on its full history due to the presence of a time integral in Eq. (145).

Extended TDHF has rarely been directly applied because of the numerical effort required. In order to illustrate these difficulties, let us introduce the single-particle basis $|\alpha\left(t\right)\rangle$ that diagonalizes the one body density $\rho_1(t)$ at a given time:

$$\rho(t) = \sum |\alpha(t)\rangle \;\; n_\alpha(t) \;\; \langle\alpha(t)| \, . \tag{147}$$

This basis explicitly depends on time and will be called "natural" basis or "canonical" basis hereafter. As we do expect from nucleon-nucleon collisions, the collision term induces a mixing of single-particle degrees of freedom during time evolution. Indeed, if we consider a time $t' \geq t$, the propagated basis $|\overline{\alpha}(t')\rangle = U(t',t)\,|\alpha(t)\rangle$ can be introduced. It should be noticed that $|\overline{\alpha}(t')\rangle \neq |\alpha(t')\rangle$ since the mean-field propagation of $|\alpha\rangle$ is not the extended TDHF propagation of the natural basis. Using these notations, matrix elements of the incoherent collision terms express as

$$\begin{aligned}\langle\alpha\,|K(t)|\,\alpha'\rangle = -\frac{1}{2\hbar^2} \;\; \Big\{ \int_{t_0}^{t} ds \sum \left\langle\overline{\alpha\delta}|\tilde{v}_{12}|\overline{\lambda\beta}\right\rangle_A\Big|_t \;\; \left\langle\overline{\lambda\beta}|\tilde{v}_{12}|\overline{\alpha'\delta}\right\rangle_A\Big|_s \\ \left(n_{\alpha'}n_\delta\left(1-n_\lambda\right)\left(1-n_\beta\right) - n_\lambda n_\beta\left(1-n_\alpha\right)\left(1-n_\delta\right)\right)\big|_s + h.c.\Big\},\end{aligned} \tag{148}$$

where the sum runs over all indices but α and α' and where we have introduced the notation $\langle . \rangle|_{t'}$ to express the fact that the matrix elements are taken at time t'.

Using the weak coupling approximation in combination with the first order perturbation theory, the ETDHF equation can be transformed into a generalized master equation for occupation numbers which account for the Pauli principle :

$$\frac{d}{dt}n_\alpha(t) = \int_{t_0}^{t} ds \left\{ \left(1 - n_\alpha\left(s\right)\right) \mathcal{W}_\alpha^+\left(t,s\right) - n_\alpha\left(s\right) \mathcal{W}_\alpha^-\left(t,s\right) \right\}. \tag{149}$$

Here, the explicit form of the gain $\mathcal{W}_\lambda^+$ and loss $\mathcal{W}_\lambda^-$ kernels could be found in ref. (Lacroix *et al.*, 1999a). Therefore, in contrast to TDHF where occupation numbers are constant during the time evolution, in ETDHF the n_α evolve and could eventually relax toward equilibrium. Such a relaxation is the only way to properly account for thermalization process in nuclei. In ref. (Lacroix *et al.*, 1999a), the inclusion of correlation effect with Extended TDHF has been tested in the simple case of two interacting nucleons in one dimension. In that case, the exact dynamics could be solved numerically. In Fig. 7, starting from an initially uncorrelated state, the exact evolution of single-particle occupation numbers is compared to the Extended TDHF prediction. Fig. 7, shows

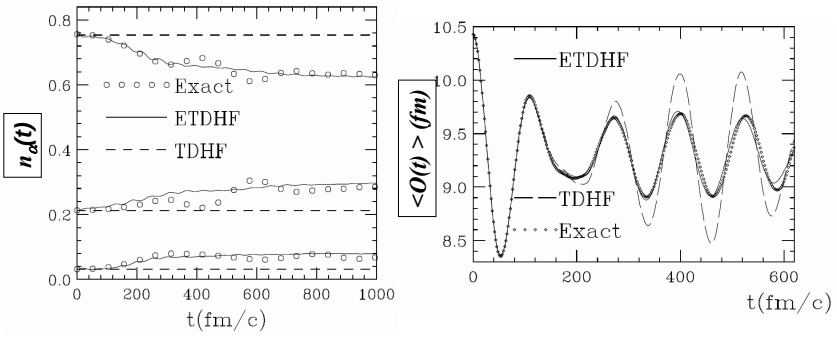

FIG. 7: *Exact (circles), TDHF (dashed line) and Extended TDHF (solid line) evolutions of a two nucleon correlated system in one dimension interacting through gaussian two-body interaction. The system is initially compressed by an external field. At $t > 0$, the constraint is relaxed. Left: Occupation numbers, right: one-body centroid as a function of time (adapted from (Lacroix* et al., *1999a).*

that the Extended TDHF is able to reproduce fairly well the evolution of one-body occupation numbers and one-body observables over long time. This result is very promising and indicates that Extended TDHF seems to be an appropriate theory for the description of dissipation when the residual interaction is weak. This application has also demonstrated the importance of memory effects to properly describe interacting systems although it significantly increases numerical efforts.

2. Time-scales and Markovian approximation

The two major difficulties in the application of ETDHF are the integral in time and the summation over many indices in eq. (148). The collision term essentially involves two different characteristic times. The first one is the correlation time τ_{cor}, If we note $V_{12}\left(t\right) = \left\langle \overline{\alpha\beta} | v_{12} | \overline{\lambda\delta} \right\rangle_A |_t$, the correlation time is defined as

$$\overline{V_{12}\left(t\right) V_{12}\left(s\right)} \propto e^{-|t-s|/\tau_{cor}}, \tag{150}$$

where the average denotes an average over all single-particle states combinations. This time, characteristic of the residual interaction, is directly related to the mean energy Δ exchanged during nucleon-nucleon collisions through the relation $\tau_{cor} = \hbar/\Delta$ (Weidenmüller, 1980). The second

characteristic time, called relaxation time τ_{rel}, corresponds to the time-scale associated to the reorganization of occupation numbers.

These two time-scales correspond in the semi-classical limit respectively to the average duration time of binary collisions and to the mean time between two collisions. Here, we consider the weak coupling regime specified by $\tau_{cor} << \tau_{rel}$, which is valid for a sufficiently dilute system when the binary collisions are well separated in time (Weidenmüller, 1980). In this case, the decay time of the collision kernel is determined by the correlation time, and the memory effect associated with the evolution of occupation numbers might be neglected. Using $U(t,s)\rho_1(s)U^\dagger(t,s) \approx \rho_1(t)$, we can make the following substitution in the collision term,

$$U_{12}(t,s)F_{12}(s)U_{12}^\dagger(t,s) = (1-\rho_1)(1-\rho_2)\tilde{v}_{12}(t,s)\rho_1\rho_2 - \rho_1\rho_2\tilde{v}_{12}(t,s)(1-\rho_1)(1-\rho_2), \quad (151)$$

where $\tilde{v}_{12}(t,s) = U_{12}(t,s)\tilde{v}_{12}U_{12}^\dagger(t,s)$, and all density matrices are evaluated at time t. In this limit, a Markovian master equation is deduced for the one-body density. The Extended TDHF enables to treat the onset of two-body dissipation in a many-body system. This theory is intimately connected to the theory of open quantum system. We have seen in section II that dissipative processes in the Markovian limit are associated to Lindblad equation which can eventually be treated as a stochastic process. In the following, the connection between the extended TDHF and stochastic process in the Hilbert space of Slater determinants is made explicitly.

F. Stochastic process in Slater Determinant space

1. General discussion

Before describing the specific case of ETDHF, let us understand in a simple manner how a stochastic process can be introduced. Starting from a simple Slater determinant state $|\Psi(t=0)\rangle = |\Phi(t_0)\rangle$, correlations will develop in time and we do expect that the exact Many-Body state writes:

$$|\Psi(t)\rangle = \sum_k c_k(t)\,|\Phi_k(t)\rangle\,, \quad (152)$$

where $|\Phi_k\rangle$ denotes a complete (eventually time-dependent) basis of Slater-Determinant states. Accordingly, the many-body density writes

$$D(t) \;=\; \sum_{k,k'} c_k(t)c_{k'}(t)\,|\Phi_k(t)\rangle\,\langle\Phi_{k'}(t)|\,. \quad (153)$$

The extended and stochastic version of TDHF that will be presented below, implicitly assume that the many-body density can be properly approximated by its diagonal components (Lacroix, 2006b; Reinhard and Suraud, 1992b)

$$D(t) \;\simeq\; \sum_k P_k\,|\Phi_k(t)\rangle\,\langle\Phi_k(t)|\,, \quad (154)$$

where $P_k = |c_k(t)|^2$. The probability P_k obeys a master equation that eventually could be simulated using quantum jumps. The resulting density is obtained through the average over different stochastic paths, i.e.

$$D(t) \;\simeq\; \overline{|\Phi_k(t)\rangle\,\langle\Phi_k(t)|} \quad (155)$$

Physically, this could be understood as follows. The irrelevant degrees of freedom (complex internal degrees of freedom) interacts with the relevant degrees of freedom (single-particle degrees of freedom) and induce a fast decay towards zero of the off-diagonal matrix elements. This phenomenon is know as a decoherence process (Joos *et al.*, 2003; Kuebler and Zeh, 1973).

2. Stochastic TDHF

The Extended TDHF can eventually be interpreted as an average over quantum jumps between Slater determinants, a theory generally called Stochastic TDHF (STDHF) (Balian and Vénéroni,

1981; Lacroix, 2006b; Reinhard and Suraud, 1992a,b). Let us first introduce ETDHF using a different technique than the truncation of the BBGKY hierarchy. This theory is expected to be valid in the weak coupling limit, i.e. when the residual interaction introduced in section III.B.2 is small. Such a theory can indeed be obtained using time-dependent perturbation theory. Starting from an initial density $D(t_0)$, the evolution is given at second order in perturbation theory by

$$i\hbar\frac{dD(t)}{dt} = [H_{\rm MF}(t),D(t)] - \frac{1}{2\hbar^2}{\rm T}\left(\iint [V_{\rm res}(s'),[V_{\rm res}(s),D(s)]]\,ds'ds\right), \quad (156)$$

where T(.) denotes the time-ordering operator and where $V_{\rm res}(s)$ denotes the residual interaction written in the interaction picture using the mean-field propagator. Here, we consider the limit $\tau_{cor} << \tau_{rel}$ and use

$$\overline{V_{\rm res}(s')V_{\rm res}(s)} \propto V_{\rm res}^2(t)F\left(\frac{|s'-s|}{\tau_{\rm cor}}\right). \quad (157)$$

where F is a function that tends to zero over a time-scale $\tau_{\rm cor}$ much smaller than the typical time associated to the reorganization of one-body degrees of freedom. In that limit, the density in the integral can be approximated by $D(s) \simeq D(t)$ leading finally to

$$\begin{aligned} i\hbar\frac{dD(t)}{dt} &= [H_{\rm MF}(t),D(t)] \\ &- \frac{g}{2}\Big\{V_{\rm res}(t)V_{\rm res}(t)D(t) + D(t)V_{\rm res}(t)V_{\rm res}(t) - 2V_{\rm res}(t)D(t)V_{\rm res}(t)\Big\} \end{aligned} \quad (158)$$

where the constant

$$g \equiv \frac{1}{\hbar^2}\iint F(|s-s'|/\tau_{\rm cor})dsds' \quad (159)$$

is introduced. This equation is nothing but a Lindblad equation introduced in section II.D. Therefore, starting from second-order perturbation theory and assuming the short memory approximation leads naturally to an Open Quantum System equation of motion. Eq. (158) is however rather complicated and involves complex many-body operators. Here, we are mainly interested in one-body degrees of freedom. Starting from Eq. (158), the one-body density matrix evolution reads (Lacroix, 2006b):

$$\frac{d\rho}{dt} = \frac{1}{i\hbar}\left[h_{MF}(\rho),\rho\right] - \frac{g}{2}\mathcal{D}(\rho). \quad (160)$$

$\mathcal{D}(\rho)$, called "dissipator" hereafter, corresponds to the average effect of the residual interaction and reads

$$\langle j\,|\mathcal{D}|\,i\rangle = {\rm Tr}\left(D\left[\left[a_i^+a_j,V_{\rm res}\right],V_{\rm res}\right]\right). \quad (161)$$

Assuming that the system is initially in a pure state described by a Slater determinant $|\Phi(t_0)\rangle$ formed of N orthonormal single particle states denoted by $|\alpha\rangle$, the associated initial one-body density matrix reads $\rho = \sum_\alpha |\alpha\rangle\langle\alpha|$. Using the residual interaction expression, Eq. (113), $\mathcal{D}(\rho)$ can finally be recast as:

$$\mathcal{D}(\rho) = Tr_2\left[\tilde{v}_{12},B_{12}\right], \quad (162)$$

where B_{12} is nothing but the Born term appearing in the Extended TDHF theory. Indeed, a similar expression could have been directly obtained starting from the ETDHF theory in the Markovian limit. Equation (160) is a master equation for the one-body density. It could also be put into a Lindblad form using the fact that the residual interaction can always be decomposed as (see for instance (Juillet and Chomaz, 2002; Koonin *et al.*, 1997))

$$V_{\rm res} = -\frac{1}{4}\sum_n \lambda_n\mathcal{O}_n^2, \quad (163)$$

where λ_n are real and where the $\mathcal{O}_n$ correspond to a set of commuting Hermitian one-body operators written as $\mathcal{O}_n = \sum_{\bar{\alpha}\alpha} \langle \bar{\alpha} | O_n | \alpha \rangle a^\dagger_{\bar{\alpha}} a_\alpha$. Reporting in eq. (162), $\mathcal{D}(\rho)$ can be recast as

$$\mathcal{D}(\rho) = \sum_{mn} \Gamma_{mn} \left[O_n O_m \ \rho + \rho \ O_n O_m - 2 O_m \ \rho \ O_n \right]. \tag{164}$$

The coefficient Γ_{mn} are given by

$$\Gamma_{mn} = \frac{1}{2} \lambda_m \lambda_n Tr(O_m (1-\rho) O_n \rho). \tag{165}$$

We recognize in this expression, the quantum covariance between the operator $\mathcal{O}_n$ and $\mathcal{O}_m$, i.e. $Tr(O_m(1-\rho)O_n\rho) = \langle \mathcal{O}_m \mathcal{O}_n \rangle - \langle \mathcal{O}_m \rangle \langle \mathcal{O}_n \rangle$. Expression (164) has the form of the dissipator appearing usually in the Lindblad equation(Breuer and Petruccione, 2002). Therefore, the evolution of one-body degrees of freedom associated to equation (158) identifies with a Markovian quantum master equation generally obtained in quantum open systems. A large amount of work is devoted to the simulation of such master equation by quantum jump methods (see for instance (Breuer and Petruccione, 2002; Carmichael, 1993; Disi, 1986; Plenio and Knight, 1998; Rigo and Gisin, 1996)) and one can take advantage of the most recent advances in this field. This aspect has however rarely been discussed in the context of self-interacting system.

a. **Explicit form of the stochastic process:** Following ref. (Breuer and Petruccione, 2002), we introduce the Hermitian matrix Γ with components Γ_{mn}. An economical method to introduce quantum jumps is to use the unitary transformation u that diagonalizes Γ, i.e. $\Gamma = u^{-1} \gamma u$, where γ is the diagonal matrix of the eigenvalues of Γ. New operators A_k can be defined by the transformation $A_k = \sum_n u^{-1}_{kn} O_n$. The dissipator is then recast as

$$\mathcal{D}(\rho) = \sum_k \gamma_k \left[A_k^2 \rho + \rho A_k^2 - 2 A_k \rho A_k \right]. \tag{166}$$

Last expression can be simulated using the average over the stochastic mean-field dynamics:

$$d\rho \ = \ \frac{dt}{i\hbar} \left[h_{MF}(\rho), \rho \right] - g \frac{dt}{2} \mathcal{D}(\rho) + dB_{sto}, \tag{167}$$

where dB_{sto} is a stochastic one-body operator which, using Ito rules (Gardiner, 1985), reads

$$dB_{sto} \ = \ \sum_k \left\{ dW_k (1-\rho) A_k \rho + dW_k^* \rho A_k (1-\rho) \right\}. \tag{168}$$

Here dW_k denotes stochastic variables given by $dW_k = -i d\xi_k \sqrt{g\gamma_k}$, where $\{d\xi_k\}$ correspond to a set of real gaussian stochastic variables with mean zero and $\overline{d\xi_k d\xi_{k'}} = \delta_{kk'} dt$.

b. **Nature of the stochastic process in Hilbert space:** It is worth noticing that the proposed dissipative equation and its stochastic counterpart are only well defined if the density is initially prepared as a pure Slater-determinant state. We now turn to the essential properties of equation (167). First, it preserves the number of particles $Tr(d\rho) = 0$. In addition, if initially $\rho^2 = \rho$, then

$$d\rho d\rho - g \frac{dt}{2} \left[\rho \mathcal{D}(\rho) + \mathcal{D}(\rho) \rho \right] = -g \frac{dt}{2} \mathcal{D}(\rho) \tag{169}$$

which is obtained using Ito stochastic rules and retaining only terms linear in dt. Last expression demonstrates that $(\rho + d\rho)^2 = \rho + d\rho$. Thus, ρ remains a projector along the stochastic path. As a consequence, the pure state nature of the many-body density matrix is preserved along the stochastic path, i.e. $D = |\Phi(t)\rangle \langle \Phi(t)|$ where $|\Phi\rangle$ is a normalized Slater determinant at all time. The associated stochastic Schroedinger equation for single-particle states reads

$$d|\alpha\rangle = \left\{ \frac{dt}{i\hbar} h_{MF}(\rho) + \sum_k dW_k (1-\rho) A_k - g \frac{dt}{2} \sum_k \gamma_k \left[A_k^2 \rho + \rho A_k \rho A_k - 2 A_k \rho A_k \right] \right\} |\alpha\rangle. \tag{170}$$

This last expression can be directly used for practical applications.

In this section, we have shown that the effect of residual interaction at second order in perturbation and projected on one-body degrees of freedom gives the Extended TDHF approximation in the short-memory time (Markovian) approximation. In such a limit, starting from a pure Slater Determinant state, the dissipative dynamics can be replaced by a quantum jump process where the N-body state remains a SD along each stochastic trajectory. The possibility to account for the effect of correlation on top of a mean-field dynamics has been discussed extensively in the early 80's. For instance, it has been for instance proposed to treat each direct nucleon-nucleon collisions as a random process (Balian and Vénéroni, 1981; Grange *et al.*, 1981). Alternatively, following a similar strategy as the one presented in this section and starting from perturbation theory (Reinhard and Suraud, 1992a,b), the Fermi golden rule has been used to introduce a Stochastic TDHF theory. The main difficulty is to avoid the explosion of the number of stochastic trajectories and therefore find physical criteria to only follow relevant trajectories. The approach presented here makes more transparent the connection of a many-body system where specific degrees of freedom are of interest and the theory of Open Quantum Systems. In addition, the stochastic evolution of single-particle states are directly the equations that should be implemented in practice. It should however be noted that the possible explosion of trajectories is not the only reason that may limit the application of Stochastic TDHF. Indeed, such a theory is well defined if we start from a Hamiltonian. As we will see in section V, the building block of the independent particle approximation in nuclei is a functional theory and does not start from a Hamiltonian.

3. Initial correlations with a Stochastic Mean-Field approach

TDHF or Extended TDHF provides a deterministic evolution of the single-particle density matrix, starting from a well-defined initial state and leading to a well-defined final state. These approaches are appropriate to describe mean values of one-body observables but generally misses fluctuations in collective space. In order to incorporate fluctuation mechanisms in the dynamics, one should give up the description in terms of single Slater determinants, and consider a superposition of SD.

To treat the quantum zero point motion in collective space, one could for instance account for configuration mixing through the so-called Time-Dependent Generator Coordinate Method (TDGCM) (Goeke and Reinhard, 1980; Goeke *et al.*, 1981; Reinhard and Goeke, 1987; Ring and Schuck, 1980). Such an approach is however rather involved numerically (Goutte *et al.*, 2005) and is nowadays restricted to system close to the adiabatic limit and at rather small internal excitation.

To treat approximately both quantal zero-point fluctuations and possible thermal statistical fluctuations, a stochastic scheme, called hereafter Stochastic Mean-Field (SMF) theory, has been proposed in ref. (Ayik, 2008). In SMF, the initial density fluctuations are simulated by representing the initial system in terms of a suitable ensemble of Slater determinants, denoted by $\{\Psi^\lambda\}$, where λ denotes a member of the ensemble. Accordingly, a one-body density

$$\rho^\lambda(t) = \sum_{ij} \Phi_i^*(t;\lambda)\rho_{ij}^\lambda \Phi_j(t;\lambda). \tag{171}$$

is associated to each state. Here $\Phi_j(t;\lambda)$ is a complete set of single particle basis. Matrix elements ρ_{ij}^λ are time-independent and equal to 1 or 0. The initial values of ρ_{ij}^λ associated to each event are chosen randomly such that the average over different initial conditions fulfill $\overline{\rho_{ij}^\lambda}(\sigma\tau) = \delta_{ij} n_j^{\sigma\tau}$ and

$$\overline{\rho_{ij}^\lambda \rho_{j'i'}^\lambda} \;=\; \frac{1}{2}\delta_{jj'}\delta_{ii'}\left[n_i(1-n_j) + n_j(1-n_i)\right], \tag{172}$$

where n_j denotes the average occupation factor. Once the initial set of SD is generated, each SD is evolved independently from the others according to its self-consistent mean-field,

$$i\hbar\frac{\partial}{\partial t}\Phi_j(t;\lambda) = h(\rho^\lambda)\Phi_j(t;\lambda), \tag{173}$$

where $h(\rho^\lambda)$ is the self-consistent mean-field Hamiltonian in that event.

The SMF theory has important aspects that make this theory very attractive. On the theoretical side (Ayik, 2008), for small amplitude fluctuations, this model gives a result for dispersion of a one-body observable that is identical to the result obtained using the Balian-Véneroni variational approach (Balian and Véneroni, 1985). It is also shown that, when the SMF is projected on a collective variable, it gives rise to a generalized Langevin equation (Mori, 1965) that incorporates one-body dissipation and one-body fluctuation mechanisms in accordance with quantal dissipation-fluctuation relation. These connections give a strong support that the SMF approach provides a consistent microscopic description for dynamics of density fluctuations in low energy nuclear reactions.

From the practical point of view, this approach is much simpler than the TDGCM one. Indeed, by neglecting the interferences between trajectories, each evolution can be made independently from the others. In addition, on contrary to the Stochastic TDHF case, randomness appear only at the initial time and should not a priori face the difficulty of a statistical explosion of the trajectory number. SMF framework has been recently applied to fusion (Ayik *et al.*, 2009) and transfer reactions (Washiyama *et al.*, 2009a). The latter study has in particular pointed out that fluctuations of one-body observables are largely increased compared to TDHF and seems consistent with experimental observations. This issue is a long standing problem that was unsolved until now in a fully microscopic approach .

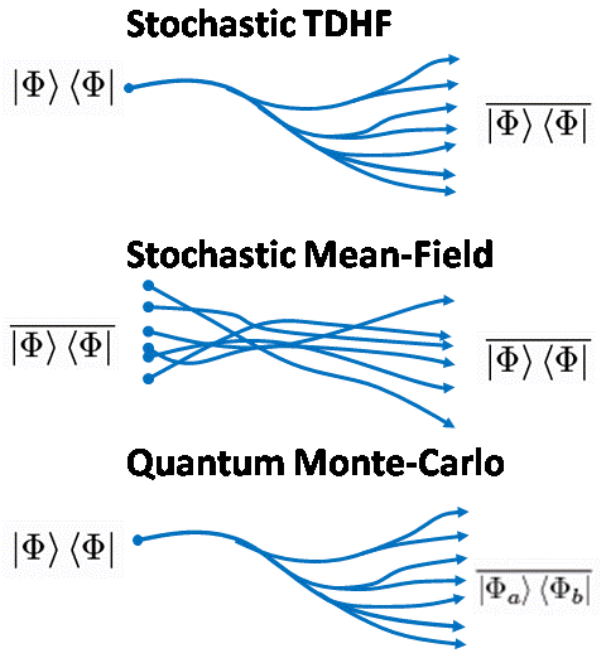

FIG. 8: *Illustration of the different types of stochastic theories introduced in this section. Top: In the Stochastic TDHF theory, a random noise is introduced at each time step. This noise induces quantum jumps between densities of pure Slater determinants states. By averaging over different trajectories, the effect of two-body collisions on one-body density evolution is incorporated similarly to the Extended TDHF theory. Middle: The Stochastic Mean-Field theory is introduced to account for the effect of possible initial correlation. In that case, a statistical ensemble of initial SD densities is chosen and each SD evolves independently from the others. Bottom: In the Quantum Monte-Carlo approach, all two-body correlations are a priori treated. In that case, starting from an initial independent particle state, the evolution is replaced by an ensemble of stochastic density evolution each being written as a dyadic of Slater determinants $D = |\Phi_a\rangle\langle\Phi_b|$. The exact evolution is expected to be recovered by averaging over the dyadic.*

G. Exact Quantum Monte-Carlo from functional integrals method

Approximations to the N-body problem such as ETDHF, STDHF or SMF focus on one-body degrees of freedom. In each framework some many-body effects such as interferences between different channels are lost. In particular, we do expect that most of the extensions of TDHF presented above will not be able to describe two-body or more complex degrees of freedom. Mean-field theories by projecting out the evolution onto a specific class of degrees of freedom can then be regarded as a system open to the surrounding more complex observables (see for instance discussion

in IV.F.2). From the Open Quantum System point of view, the introduction of Extended TDHF and then Stochastic TDHF can be considered as a rather standard way to introduce dissipation using first the Nakajima-Zwanzig approach, second the Markovian approximation and then the stochastic unraveling (see section II). At the end of section II, it was shown that less conventional approaches based on quantum Monte-Carlo can be used to treat exactly the dynamics of a system coupled to an environment. A similar exact reformulation also exists in the case of interacting particle using the functional integral method.

Functional integrals techniques have often been used to replace the exact Many-Body problem by an average over different "effective" one-body problem (Levit *et al.*, 1980; Levit, 1980; Negele and Orland, 1988). In ref. (Koonin *et al.*, 1997), the general strategy to obtain ground state properties of a many-body system using Monte-Carlo methods, the so called Shell-Model Monte-Carlo, is described. Recently, this technique has been combined with mean-field theory to obtain Stochastic TDHF equations which in average lead to the exact evolution (Carusotto *et al.*, 2001; Juillet and Chomaz, 2002). The goal of the present section is to demonstrate that one could always treat exactly the problem of interacting particle with density given by Eq. (153) by an appropriate stochastic process between Slater determinants. The exact density will then be obtained by an average

$$D(t) \;\simeq\; \overline{|\Phi_k(t)\rangle \langle\Phi'_k(t)|} \tag{174}$$

where states in the left differ from states on the right.

a. **Functional integrals for schematic residual interaction:** We again consider that, at a given time, the Many-Body state is a Slater Determinant $|\Psi(t)\rangle = |\Phi\rangle$. For short time step Δt, we have

$$|\Psi(t+\Delta t)\rangle \;=\; \exp\left(\frac{\Delta t}{i\hbar}H\right)|\Phi(t)\rangle \simeq \left(1+\frac{\Delta t}{i\hbar}H+0(\Delta t)\right)|\Phi(t)\rangle\,. \tag{175}$$

Due to the presence of a two-body interaction in H, the state $|\Psi(t+\Delta t)\rangle$ differs from a Slater Determinant. However, it is proved here that it could be replaced exactly by an average over quantum jumps between SD states.

At any time, the Hamiltonian can be decomposed as a mean-field and a residual part. For simplicity, it is first assumed that

$$V_{\rm res} = O^2, \tag{176}$$

O being a one-body operators. A Gaussian probability $G(x)$ with mean zero and variance 1 is introduced and the complex number $\Delta\omega \equiv \sqrt{\frac{2\Delta t}{i\hbar}}$ is defined as well as the one-body operator $S(\Delta t, x)$ with

$$S(\Delta t, x) \equiv \frac{\Delta t}{i\hbar}H_{\rm MF} + x\Delta\omega O. \tag{177}$$

Considering the average value of $S(\Delta t, x)$ and keeping only terms up to Δt, we obtain:

$$\begin{aligned}\int_{-\infty}^{+\infty} e^{S(\Delta t,x)}G(x)dx \;&=\; 1+\frac{\Delta t}{i\hbar}H_{\rm MF}+\overline{x}\;\Delta\omega O+\overline{x^2}\;(\Delta\omega)^2O^2+0(\Delta t)\\ &=\; 1+\frac{\Delta t}{i\hbar}H+0(\Delta t)\end{aligned} \tag{178}$$

By averaging over the different realization of x, we recover the exact propagator over short time step. Note that more general relations could be found using the Hubbard-Stratonovish transformation (see for instance (Koonin *et al.*, 1997)). Using the above relation, we see that

$$\exp\left(\frac{\Delta t}{i\hbar}H\right)|\Phi\rangle = \int_{-\infty}^{+\infty} dxG(x)e^{S(\Delta t,x)}\,|\Phi(t)\rangle \equiv \int_{-\infty}^{+\infty} dxG(x)\,|\Phi_x(t+\Delta t)\rangle \tag{179}$$

Due to the one-body nature of S, each $|\Phi_x(t+\Delta t)\rangle$ is a Slater determinant. Therefore, we have demonstrated that the evolution of the exact state could be replaced by an ensemble of Slater determinants. The technique could be iterated for each $|\Phi_x(t+\Delta t)\rangle$ to obtain the exact long time dynamics as an average over Slater determinant states. Several comments are in order:

- Since $S(\Delta t, x)$ is not a priori Hermitian, the dynamics does not preserves the orthogonality of the single-particle wave-function. Such a non-orthogonality should properly be treated during the time evolution (Juillet *et al.*, 2001; Lacroix, 2005b).
- Starting from a Many-Body density written as $D(t) = |\Phi\rangle\langle\Phi|$, at an intermediate time, the average density writes

$$D(t) = \overline{|\Phi_1(t)\rangle\langle\Phi_2(t)|} \tag{180}$$

where $|\Phi_1\rangle$ evolves according to Eq. (181) while $\langle\Phi_2|$ evolves according to

$$\langle\Phi_2(t+\Delta t)| \;=\; \langle\Phi_2(t)|\exp\left\{-\frac{\Delta t}{i\hbar}H_{\rm MF} + y\Delta\omega^* O\right\}. \tag{181}$$

y is a noise independent of x, with mean zero and $\overline{yy} = 1$. Since the evolution is exact, any one-, two- or k-body observable A estimated through $\langle A\rangle \equiv Tr(D(t)A)$ will follow the exact dynamics (Lacroix, 2005b).

b. **General Many-Body Hamiltonian:** The functional integral method has been introduced above using a schematic separable residual interaction. For a general two-body Hamiltonian, one can take advantage of the decomposition of the residual interaction according to Eq.(163. Therefore, for realistic interactions one should introduce as many stochastic Gaussian independent variables as the number of operators entering in the sum. In practice, this number defines the numerical effort which in general is very large. For this reasons only few applications to the dynamics of rather simple systems exists so far. Last, the extension of above stochastic theories to HFB state has been given in ref. (Lacroix, 2006a).

H. Quantum Monte-Carlo method for closed systems from optimal observables evolution

Using the functional integral method, it has been shown above that the exact evolution of particles interacting through a two-body Hamiltonian can be replaced by a set of stochastic evolutions of densities written as $D = |\Phi_a\rangle\langle\Phi_b|$ where both $|\Phi_a\rangle$ and $|\Phi_b\rangle$ are independent particle states. More generally, several studies (Breuer *et al.*, 2004; Breuer, 2004a; Carusotto *et al.*, 2001; Juillet and Chomaz, 2002; Juillet *et al.*, 2004; Lacroix, 2005a) have shown that the exact dynamics of a many-body system can be replaced by the average over "densities" of the form

$$D(t) = |Q_a\rangle\langle Q_b|\,, \tag{182}$$

where $|Q_a\rangle$ and $|Q_b\rangle$ belong to a specific class of trial states introduced in section III.A.1. One of the disadvantage of the functional integral approach is that the link with observable evolution is highly non-trivial. Here, a different strategy proposed in ref. (Lacroix, 2007) is introduced to design the quantum Monte-Carlo process. The method is not specifically dedicated to the N-body problem. Therefore, it is presented starting from any class of trial states. The basic idea is to use observables evolution at the first place to deduce the stochastic contribution. In section III.A.1, it is shown that mean-field approximation can be regarded as the optimal path for the expectation values of the observables $\{\langle A_\alpha\rangle\}$ that generate transformations between trial states. Accordingly, mean-field dynamics insures that the exact Ehrenfest evolution is obtained for these observables over short time. Here, we consider evolution within the class of trial states given by

$$|Q_a + \delta Q_a\rangle \;=\; e^{\sum_\alpha \delta q_\alpha^{[a]} A_\alpha}|Q_a\rangle\,, \tag{183}$$

$$|Q_b + \delta Q_b\rangle \;=\; e^{\sum_\alpha \delta q_\alpha^{[b]} A_\alpha}|Q_b\rangle\,, \tag{184}$$

where now $\delta q_\alpha^{[a]}$ and $\delta q_\alpha^{[b]}$ may also contain a stochastic part.

The aim of the present section is to show that, given a class of trial states, a hierarchy of Monte-Carlo formulations can be systematically obtained, written as

$$\left\{\begin{array}{c} \delta q_\alpha^{[a]} = \delta q_\alpha^a + \delta\xi_\alpha^{[2]} + \delta\xi_\alpha^{[3]} + \cdots \\ \delta q_\alpha^{[b]\,*} = \delta q_\alpha^{b\,*} + \delta\eta_\alpha^{[2]} + \delta\eta_\alpha^{[3]} + \cdots \end{array}\right. \tag{185}$$

where the second, third... terms represent stochastic variables added on top of the deterministic contribution. Those are optimized to not only insure that the average evolution of $\langle A_\alpha \rangle$ matches the exact evolution at each time step but also that the average evolutions of higher moments $\langle A_\alpha A_\beta \rangle$, $\langle A_\alpha A_\beta A_\gamma \rangle$,... follow the exact Ehrenfest dynamics.

1. Link between stochastic process and observables evolution

a. **Step 1: deterministic evolution** Assuming first that stochastic contributions $\xi_\alpha^{[i]}$ and $\eta_\alpha^{[i]}$ are neglected in eq. (185), we show how variational principles described previously can be used for mixed densities given by eq. (182). It is worth noticing that variational principles have also been proposed to estimate transition amplitudes (Blaizot and Ripka, 1986) (see also discussion in (Balian and Vénéroni, 1985)). In that case, different states are used in the left and right hand side of the action. This situation is similar to the case we are considering. We are interested here in the short time evolution of the system, therefore we disregard the time integral in equation (65) and consider directly the action

$$S = \mathrm{Tr}\left(\{i\hbar\partial_t^{\triangleright} - i\hbar\partial_t^{\triangleleft} - H\}\, D\right). \tag{186}$$

Starting from the above action, different aspects discussed in section III.A can be generalized to the case of densities formed of trial states couples. For instance, the minimization with respect to the variations $\langle \delta Q_b|$ and $|\delta Q_a\rangle$ leads to the two conditions

$$\begin{cases} i\hbar \langle Q_b | A_\alpha | \, dQ_a \rangle = \langle Q_b | A_\alpha H | \, Q_a \rangle \,, \\ \\ i\hbar \langle dQ_b | A_\alpha | \, Q_a \rangle = \langle Q_b | H A_\alpha | \, Q_a \rangle \,, \end{cases} \tag{187}$$

from which we deduce that

$$i\hbar \frac{d}{dt} \langle A_\alpha \rangle = \langle [A_\alpha, H] \rangle \,, \tag{188}$$

where $\langle A_\alpha \rangle = \langle Q_b | A_\alpha | \, Q_a \rangle$. Therefore, the minimization of the action again insures that the exact Ehrenfest evolution is followed by the A_α observable over one time step. Similarly, the evolution of both $|Q_a\rangle$ and $|Q_b\rangle$ are given by [9]

$$\begin{cases} |dQ_a\rangle &= \sum_\alpha dq_\alpha^a A_\alpha |Q_a\rangle = \frac{dt}{i\hbar} \mathcal{P}_1 H |Q_a\rangle \\ \\ \langle dQ_b| &= \langle Q_b| \sum_\alpha dq_\alpha^{b\,*} A_\alpha = -\frac{dt}{i\hbar} \langle Q_b| H \mathcal{P}_1 \end{cases}$$

where $\mathcal{P}_1$ now reads

$$\mathcal{P}_1 = \sum_{\alpha\beta} A_\alpha |Q_a\rangle \, C^{-1}_{\alpha\beta} \langle Q_b| \, A_\beta. \tag{189}$$

In opposite to previous section, $\mathcal{P}_1$ cannot be interpreted as a projector onto the space of observable. Indeed, $C_{\alpha\beta} = \langle Q_b | A_\alpha A_\beta | \, Q_a \rangle$ is not anymore a metric for that space. However, the total Hamiltonian can still be split into two parts

$$H \;=\; \mathcal{P}_1 H + (1 - \mathcal{P}_1) H = H\mathcal{P}_1 + H(1 - \mathcal{P}_1) \tag{190}$$

the first part being responsible for the mean-field deterministic evolution.

---

[9] For simplicity, we consider here non-necessarily normalized states.

b. **Step 2 : Introduction of Gaussian stochastic processes:** In this section, it is shown that the description of the dynamics can be further improved by introducing diffusion in the Hilbert space of trial states. We consider that the evolutions of $q_\alpha^{[a]}$ and $q_\alpha^{[b]}$ now read

$$\begin{aligned} dq_\alpha^{[a]} &= dq_\alpha^a + d\xi_\alpha^{[2]}, \\ dq_\alpha^{[b]\,*} &= dq_\alpha^{b\,*} + d\eta_\alpha^{[2]}, \end{aligned}$$

where $d\xi_\alpha^{[2]}$ and $d\eta_\alpha^{[2]}$ correspond to two sets of stochastic gaussian variables with mean values equal to zero and variances verifying

$$d\xi_\alpha^{[2]} d\xi_\beta^{[2]} = d\omega_{\alpha\beta}, \quad d\eta_\alpha^{[2]} d\eta_\beta^{[2]} = d\sigma_{\alpha\beta}, \quad d\xi_\alpha^{[2]} d\eta_\beta^{[2]} = 0 \tag{191}$$

We assume that $d\omega_{\alpha\beta}$ and $d\sigma_{\alpha\beta}$ are proportional to dt. The advantage of introducing the Monte-Carlo method can be seen in the average evolutions of the states. Keeping only linear terms in dt in eq. (184) gives for instance

$$\overline{|dQ_a\rangle} = \left\{ \sum_\alpha dq_\alpha^a A_\alpha + \sum_{\alpha<\beta} d\omega_{\alpha\beta} \left(A_\alpha A_\beta + A_\beta A_\alpha \right) \right\} |Q_a\rangle \,. \tag{192}$$

Mean field approximation leads to an approximate treatment of the dynamics associated to effective Hamiltonian which can only be written as a linear superposition of the A_α (see Eq. (93)). Last expression underlines that, while the states remain in a simple class of trial states, the average evolution can now simulate the evolution with an effective Hamiltonian containing not only linear but also quadratic terms in A_α.

The goal is now to take advantage of this generalization and reduce further the distance between the average evolution and the exact one. The most natural generalization of mean-field is to minimize the average action

$$S = \overline{\mathrm{Tr}\left(\{ i\hbar \partial_t^{\triangleright} - i\hbar \partial_t^{\triangleleft} - H \} \, D \right)}, \tag{193}$$

with respect to the variations of different parameters, i.e. δq_α^a, $\delta q_\alpha^{b\,*}$, $\delta\omega_{\alpha\beta}$ and $\delta\sigma_{\alpha\beta}$. In the following, a formal solution of the minimization procedure is obtained. The variational principle applied to stochastic process generalizes the deterministic case by imposing that not only that expectation values $\langle A_\alpha \rangle$ but also the second moments $\langle A_\alpha A_\beta \rangle$, follow the Ehrenfest theorem prescription.

c. **Effective Hamiltonian dynamics deduced from the minimization:** The variations with respect to $\delta q_\alpha^{b\,*}$ and $\delta\sigma_{\alpha\beta}$ give two sets of coupled equations between dq_α^a and $d\omega_{\alpha\beta}$. The formal solution of the minimization can however be obtained by making an appropriate change on the variational parameters prior to the minimization. In the following, the notation $B_\nu = A_\alpha A_\beta + A_\beta A_\alpha$ is introduced where ν denotes (α, β) with $\alpha < \beta$. Starting from the general form of the effective evolution (192), we dissociate the part which contributes to the evolution of the $\langle A_\alpha \rangle$ from the rest. This could be done by introducing the projection operator $\mathcal{P}_1$. Equation (192) then reads

$$\overline{|dQ_a\rangle} = \left\{ \sum_\alpha dz_\alpha^a A_\alpha + \sum_\nu d\omega_\nu (1 - \mathcal{P}_1) B_\nu \right\} |Q_a\rangle \,, \tag{194}$$

where the new set of parameters dz_α^a are given by

$$dz_\alpha^a = dq_\alpha^a + \sum_{\beta\nu} d\omega_\nu C_{\alpha\beta}^{-1} \langle Q_b | A_\beta B_\nu | Q_a \rangle \,. \tag{195}$$

Similarly, the average evolution $\langle dQ_b|$ transforms into

$$\overline{\langle dQ_b|} = \langle Q_b | \left\{ \sum_\alpha dz_\alpha^{b\,*} A_\alpha + \sum_\nu d\sigma_\nu B_\nu (1 - \mathcal{P}_1) \right\}, \tag{196}$$

where dz_α^b is given by

$$dz_\alpha^{b\,*} = dq_\alpha^{b\,*} + \sum_{\beta\nu} d\sigma_\nu \langle Q_b | B_\nu A_\beta | Q_a \rangle C^{-1}_{\beta\alpha}. \tag{197}$$

In the following, we write $B'_\nu = (1-\mathcal{P}_1)B_\nu$ and $B''_\nu = B_\nu(1-\mathcal{P}_1)$. The great interest of this transformation is to have $\langle A_\alpha B'_\nu \rangle = 0$ and $\langle B''_\nu A_\alpha \rangle = 0$ for all α and ν. Accordingly, the variations with respect to $\delta z_\alpha^{b\,*}$ and δz_α^a lead to

$$\begin{cases} i\hbar\overline{\langle Q_b | A_\alpha | dQ_a \rangle} = \langle Q_b | A_\alpha H | Q_a \rangle \\ \\ i\hbar\overline{\langle dQ_b | A_\alpha | Q_a \rangle} = \langle Q_b | H A_\alpha | Q_a \rangle \,, \end{cases} \tag{198}$$

leading to closed equations for the variations dz_α^a and $dz_\alpha^{b\,*}$ that are decoupled from the evolution of $d\omega_\nu$ and $d\sigma_\nu$. These equations are identical to the ones derived in step 1 and can be again inverted as

$$\sum_\alpha dz_\alpha^a A_\alpha |Q_a\rangle = \frac{dt}{i\hbar}\mathcal{P}_1 H |Q_a\rangle \,, \tag{199}$$

$$\langle Q_b| \sum_\alpha dz_\alpha^{b\,*} A_\alpha = -\frac{dt}{i\hbar} \langle Q_b| H\mathcal{P}_1. \tag{200}$$

On the other hand, the variations with respect to $\delta\sigma_\nu$ and $\delta\omega_\nu$ lead to

$$\begin{cases} i\hbar\overline{\langle Q_b | B''_\nu | dQ_a \rangle} = \langle Q_b | B''_\nu H | Q_a \rangle \,, \\ \\ i\hbar\overline{\langle dQ_b | B'_\nu | Q_a \rangle} = \langle Q_b | H B'_\nu | Q_a \rangle \,, \end{cases} \tag{201}$$

which again gives closed equations for $d\omega_\nu$ and $d\sigma_\nu$. These equations can be formally integrated by introducing the two projectors $\mathcal{P}_2$ and $\mathcal{P}'_2$ associated respectively to the subspaces of operators $B_\nu(1-\mathcal{P}_1)$ and $(1-\mathcal{P}_1)B_\nu$. $\mathcal{P}_2$ differs from $\mathcal{P}'_2$ due to the fact that B_ν operators and A_α operators do not a priori commute. Then, the effective evolution given by eq. (192) becomes

$$\begin{aligned} \overline{|dQ_a\rangle} &= \frac{dt}{i\hbar}\left(\sum_\alpha dz_\alpha^a A_\alpha + (1-\mathcal{P}_1)\sum_\nu d\omega_\nu B_\nu\right)|Q_a\rangle \\ &= \frac{dt}{i\hbar}\left(\mathcal{P}_1+\mathcal{P}_2\right) H\,|Q_a\rangle \,, \end{aligned} \tag{202}$$

while

$$\overline{\langle dQ_b|} = -\frac{dt}{i\hbar}\langle Q_b| H\left(\mathcal{P}_1+\mathcal{P}'_2\right). \tag{203}$$

In both cases, the first part corresponds to the projection of the exact dynamics on the space of observable $\langle A_\alpha \rangle$. The second term corresponds to the projection on the subspace of the observable $\langle A_\alpha A_\beta \rangle$ "orthogonal" to the space of the $\langle A_\alpha \rangle$.

d. **Interpretation in terms of observable evolution:** The variation with respect to an enlarged set of parameters does a priori completely determine the deterministic and stochastic evolution of the two trial state vectors. The associated average Schroedinger evolution corresponds to a projected dynamics. The interpretation of the solution obtained by variational principle is rather clear in terms of observable evolution. Indeed, from the two variational conditions, we can easily deduce that

$$\begin{aligned} \overline{d\langle A_\alpha\rangle} &= \langle [A_\alpha, H]\rangle \,, \\ \overline{d\langle B_\nu\rangle} &= \frac{dt}{i\hbar}\langle [B_\nu, H]\rangle \,. \end{aligned}$$

In summary, using the additional parameters associated with the stochastic contribution as variational parameters for the average action given by eq. (193), one can further reduce the distance between the simulated evolution and the exact solution. When gaussian noises are used, this is equivalent to impose that the evolution of the correlations between operators A_α obtained by averaging over different stochastic trajectories also matches the exact evolution.

e. **Step 3: Generalization** If the Hamiltonian H applied to the trial state can be written as a quadratic Hamiltonian in terms of A_α and if the trial states form an over-complete basis of the total Hilbert space, then the above procedure provides an exact stochastic reformulation of the problem. If it is not the case, the above methods can be generalized by introducing higher order stochastic variables. Considering now the more general form

$$\left\{ \begin{array}{c} \delta q_\alpha^{[a]} = \delta q_\alpha^a + \delta \xi_\alpha^{[2]} + \delta \xi_\alpha^{[3]} + \cdots \\ \delta q_\alpha^{[b]^*} = \delta q_\alpha^{b^*} + \delta \eta_\alpha^{[2]} + \delta \eta_\alpha^{[3]} + \cdots \end{array} \right.$$

we suppose now that the only non vanishing moments for $d\xi_\alpha^{[k]}$ and $d\eta_\alpha^{[k]}$ are the moments of order k (which are then assumed to be proportional to dt). For instance, we assume that $d\xi_\alpha^{[3]}$ verifies

$$\overline{d\xi_\alpha^{[3]}} = \overline{d\xi_\alpha^{[3]} d\xi_\beta^{[3]}} = 0, \tag{204}$$

$$\overline{d\xi_\alpha^{[3]} d\xi_\beta^{[3]} d\xi_\gamma^{[3]}} \neq 0. \tag{205}$$

Then without going into details, the method presented in step 2 can be generalized. The average evolutions of the trial states will be given by

$$\begin{aligned} \overline{|dQ_a\rangle} &= \frac{dt}{i\hbar} \left\{ \mathcal{P}_1 + \mathcal{P}_2 + \mathcal{P}_3 + \cdots \right\} H |Q_a\rangle \\ \overline{\langle dQ_b|} &= -\frac{dt}{i\hbar} \langle Q_b| H \left\{ \mathcal{P}_1 + \mathcal{P}_2' + \mathcal{P}_3' + \cdots \right\} \end{aligned}$$

where the first terms contain all the information on the evolution of the $\langle A_\alpha \rangle$, the second terms contain all the information on the evolution of the $\langle A_\alpha A_\beta \rangle$ which is not accounted for by the first term, the third terms contain all the information on the evolution of the $\langle A_\alpha A_\beta A_\gamma \rangle$ which is not contained in the first two terms, ... The procedure described here gives an exact Monte-Carlo formulation of a given problem if the Hamiltonian H applied on $|Q_a\rangle$ or $\langle Q_b|$ can be written as a polynomial of A_α. If the polynomial is of order k, then the sum stops at $\mathcal{P}_k$.

2. Summary and discussion on applications

Considering a restricted class of trial state vectors associated to a set of observable A_α, a hierarchy of stochastic approximations can be obtained. The method discussed here insures that at the level k of the hierarchy, all moments of order k or below of the observable A_α evolve according to the exact Ehrenfest equation over short time. The Monte-Carlo formulation might becomes exact if the Hamiltonian applied to the trial state writes as a polynomial of the A_α operators.

Aside of the use of variational techniques, we end up with the following important conclusion: *Given an initial density $D = |Q_a\rangle \langle Q_b|$ where both states belongs to a given class of trial states associated to a set of operators A_α, we can always find a Monte-Carlo process which preserves the specific form of D and insures that expectations values of all moments of the A_α up to a certain order k evolve in average according to the Ehrenfest theorem associated to the exact Hamiltonian at each time step and along each trajectory.*

This statement is referred to as the "existence theorem" in ref. (Lacroix, 2007). Such a general statement is very useful in practice to obtain stochastic processes. Indeed, the use of variational techniques might become rather complicated due to the large number of degrees of freedom involved. An alternative method is to take advantage of the natural link made between the average effective evolution deduced from the stochastic evolution and the phase-space dynamics. Indeed, according to the existence theorem, we know that at a given level k of approximation, the dynamics of each

trial state can be simulated by an average effective Hamiltonian insuring that all moments of order k or below matches the exact evolution. In practice, it is easier to express the exact evolution of the moments and then "guess" the associated stochastic process. Many examples taken from general quantum mechanics, atomic physics, interacting bosons or fermions have been given in ref. (Lacroix, 2007).

As an illustration, let us come back to the problem of interacting fermions with a two-body Hamiltonian. Assuming that at a given time step, the exact density can be recovered by averaging over an ensemble of densities

$$D = |\Phi_a\rangle \langle \Phi_b| \,, \tag{206}$$

where both states correspond to SD states. If we denote by $\{|\beta_i\rangle\}_{i=1,N}$ and $\{|\alpha_i\rangle\}_{i=1,N}$ the set of N single-particle states, we assume in addition that for each couples of SD, associated singles-particle wave-functions verify $\langle \beta_j \,|\, \alpha_i \rangle = \delta_{ij}$. Accordingly, the one-body density matrix associated to a given D reads (Lacroix, 2005b, 2006b; Löwdin, 1955)

$$\rho_1 = \sum_i |\alpha_i\rangle \langle \beta_i| \,. \tag{207}$$

It can be easily verified that $\rho_1^2 = \rho_1$ and $Tr(D) = 1$. For each D given by eq. (206), the two-body density writes as $\rho_{12} = (1 - P_{12})\rho_1\rho_2$. The evolution of ρ_1 and ρ_{12} over one time step are given by the two first equations of the BBGKY hierarchy which reads in that case

$$\begin{aligned} i\hbar \frac{d}{dt}\rho_1 &= [h_{MF}, \rho_1] \,, & (208) \\ i\hbar \frac{d}{dt}\rho_{12} &= [h_{MF}(1) + h_{MF}(2), \rho_{12}] \\ &+ (1-\rho_1)(1-\rho_2)v_{12}\rho_1\rho_2 - \rho_1\rho_2 v_{12}(1-\rho_1)(1-\rho_2). & (209) \end{aligned}$$

Again, decomposing the interaction as a sum over separable terms built from a complete set of hermitian operators O_n (Eq. (163)), the previous expression can be simulated by a stochastic dynamics in phase-space given by

$$d\rho_1 = \frac{dt}{i\hbar}[h_{MF}, \rho_1] + \sum_n d\xi_n^{[2]}(1-\rho_1)O_n\rho_1 + \sum_n d\eta_n^{[2]}\rho_1 O_n(1-\rho_1), \tag{210}$$

where $d\xi_\lambda^{[2]}$ and $d\eta_\lambda^{[2]}$ are two sets of independent stochastic variables with mean zero and verifying $d\xi_n^{[2]} d\xi_{n'}^{[2]} = \delta_{nn'}\frac{dt}{i\hbar}\lambda_n$ and $d\eta_n^{[2]} d\eta_{n'}^{[2]} = -\delta_{nn'}\frac{dt}{i\hbar}\lambda_n$. This stochastic master equation is exact and can equivalently be replaced by a Stochastic Schrödinger equation for single-particle wave-functions given by

$$\begin{aligned} d\,|\alpha_i\rangle &= \Big(\frac{dt}{i\hbar}h_{MF} + \sum_n d\xi_n^{[2]}(1-\rho_1)O_n\Big)\,|\alpha_i\rangle \,, \\ d\,\langle\beta_i| &= \langle\beta_i|\,\Big(-\frac{dt}{i\hbar}h_{MF} + \sum_n d\eta_n^{[2]}O_n(1-\rho_1)\Big). \end{aligned}$$

This stochastic equation preserves the property $\langle \beta_j \,|\, \alpha_i \rangle = \delta_{ij}$. Therefore, it corresponds in many-body space to a Monte-Carlo procedure which transforms the initial set of densities into another set of densities with identical properties.

Using the present method, quantum Monte-Carlo approach to a closed system can be rather easily guessed. Application of QMC remains very challenging. First, in most physical cases, statistical fluctuations around the mean trajectory become very large for long time evolutions. As a consequence, the number of trajectories necessary to properly describe the problem increases very fast and prevent from using such a technique. Specific methods, that explicitly use the QMC flexibility, can however be proposed to reduce statistical fluctuations (Lacroix, 2005b). Second, implementation of QMC requires to solve non-linear stochastic equations. It turns out that trajectories can make large excursion in unphysical regions of the phase-space leading to unstable trajectories (also called spikes). This is a problem which seems to be recurrent in the context

of quantum stochastic mechanics both with Stochastic Schroedinger Equation (Carusotto *et al.*, 2001) or stochastic evolution in phase-space (Gardiner and Zoller, 2000). Therefore, to take full advantage of these techniques one should develop specific numerical methods. This has been done for instance in refs. (Carusotto *et al.*, 2001; Deuar and Drummond, 2002; Plimak *et al.*, 2001) using the fact that stochastic equations are generally not unique.

I. Summary

In this section, we have summarized some of the possible ways to extend TDHF, some of them are able to incorporate pairing correlations (like TDHFB or TDDM) whereas others concentrates on direct nucleon-nucleon collisions (ETDHF, STDHF) or initial correlation effects (SMF). Table I gives an overview of the theory introduced in this section while figure 8 illustrates the differences between the three stochastic methods, namely Stochastic TDHF, SMF and QMC. While very promising applications of these theories to the nuclear many-body problem remain very challenging and some of the above theories have never been used. A first difficulty is the computational effort required to treat time dependent methods beyond mean-field. However, besides numerical difficulties, more fundamental problems persist. Indeed, a second critical aspects which has not been discussed up to now is that all applications of dynamical quantum transport theories to nuclear reactions are nowadays possible thanks to the introduction of effective interactions (essentially Skyrme like). These interactions have led to the more general concept of Energy Density Functional (EDF) and are expected, in a similar way as Density Functional Theory (DFT) in condensed matter, to incorporate most of the correlations already at the mean-field level. Then, the very notion of "mean-field " and/or "beyond mean-field" framework becomes ill defined. All theories presented in this chapter (extended, stochastic...) start from a Many-Body Hamiltonian. In the EDF context, such an Hamiltonian, although it exists, is not simply connected to the EDF itself. As a consequence, the Hamiltonian derivation could only serve as a guideline and a proper formulation in the EDF framework is mandatory. Large debates exist nowadays on the validity and foundation of the nuclear EDF applied to static properties of nuclei. The EDF approach is introduced in next chapter while its time-dependent version is discussed in section VI.

V. THE NUCLEAR ENERGY DENSITY FUNCTIONAL THEORY

In previous sections, theories based on mean-field (Hartree-Fock) or beyond mean-field have been introduced in a rather academic way starting from a many-body Hamiltonian. Unfortunately, such theories can often not be applied to realistic nuclear systems where nucleons interact through the strong interaction. Indeed, application of the strict Hartree-Fock (or Hartree-Fock-Bogolyubov) theory to "vacuum" nucleon-nucleon Hamiltonian does lead to very bad (if any) results at least due to the presence of the short range repulsive core. This makes the nuclear many-body problem highly non-perturbative with respect to the independent particle approach. On the other hand, the recently proposed soft-core interaction, based on renormalization group techniques (Kehrein, 2006), does make the nuclear many-body problem perturbative (Bogner *et al.*, 2003a,b, 2005). Still, one must go beyond lowest order to obtain close to converged results and the strict independent particle and/or independent quasi-particle approximation is not quantitatively viable.

The nuclear Energy Density Functional (EDF) is very close in spirit to the Density Functional Theory (DFT)widely applied to electronic systems (Dreizler and Gross, 1990; Fiolhais *et al.*, 2003; Koch and Holthausen, 2001; Parr and Yang, 1989). The great technical advantage of DFT (and EDF) is to establish a mapping between the original, most often intractable, many-body problem of interacting particles and a functional theory that can be solved using the independent particle method. The introduction of EDF in nuclear system in the early 70's was a major breakthrough (Negele and Vautherin, 1972; Vautherin and Brink, 1972). Today, EDF has become the only tool able in a microscopic framework to address the diversity of phenomena taking place in nuclei from nuclear structure to nuclear reactions: nuclear spectroscopy, small and large amplitude dynamics, equilibrium and non-equilibrium thermodynamics (see illustration in figure 9)...

The aim of this section is to highlight the present status of current EDF. Here, we concentrate on EDF devoted to static properties of nuclei. Time-dependent aspects will be presented in next chapter. The section is organized as follows: first, a brief introduction of the EDF used in the static case is given. This introduction will be helpful to understand the specific aspects of the nuclear many-body problem compared for instance to electronic systems. Important concepts like spontaneous symmetry breaking largely influence the strategy used to apply the EDF. Second, recent discussions related to correlations "beyond mean-field" are presented. Examples of application as well as the difference between an "Hamiltonian" and a functional theory will be discussed. Finally, the Density-Matrix Functional Theory, that has been recently proposed to improve current EDF, is discussed.

A. DFT versus EDF: common aspects and differences

The nuclear EDF has many aspects in common with the DFT theory. DFT is a very powerful approach that can be applied to a wide range of physical problems. A complete description of all the ramifications of DFT is certainly out of the scope of the present document (for details see excellent the textbooks (Dreizler and Gross, 1990; Fiolhais *et al.*, 2003; Koch and Holthausen, 2001; Parr and Yang, 1989)). Nevertheless, to understand connections between EDF and DFT a brief overview of DFT is given below.

1. Selected aspects of DFT

At first sight, Density Functional Theory might appear as a nice trick to find properties like the ground state energy, the local density of a complex system of interacting electrons without solving the associated N-body problem. In reality, "Density functional theory is a completely different, formally rigorous, way of approaching any interacting problem, by mapping it exactly to a much easier-to-solve non-interacting problem"(Burke and friends, 2003). Some of the theorems and aspects of DFT relevant for the present discussion are listed below:

- **Hohenberg-Kohn theorem:** The DFT concept has been introduced to describe electrons interacting through the well known repulsive *Coulomb interaction* and *bound by the surrounding Ions*. The starting point is the Hohenberg-Kohn (HK) theorem (Hohenberg and Kohn, 1964; Kohn, 1999): The HK theorem demonstrates that the problem of interacting electrons in an external field (surrounding ions) can be replaced by a problem where the energy is

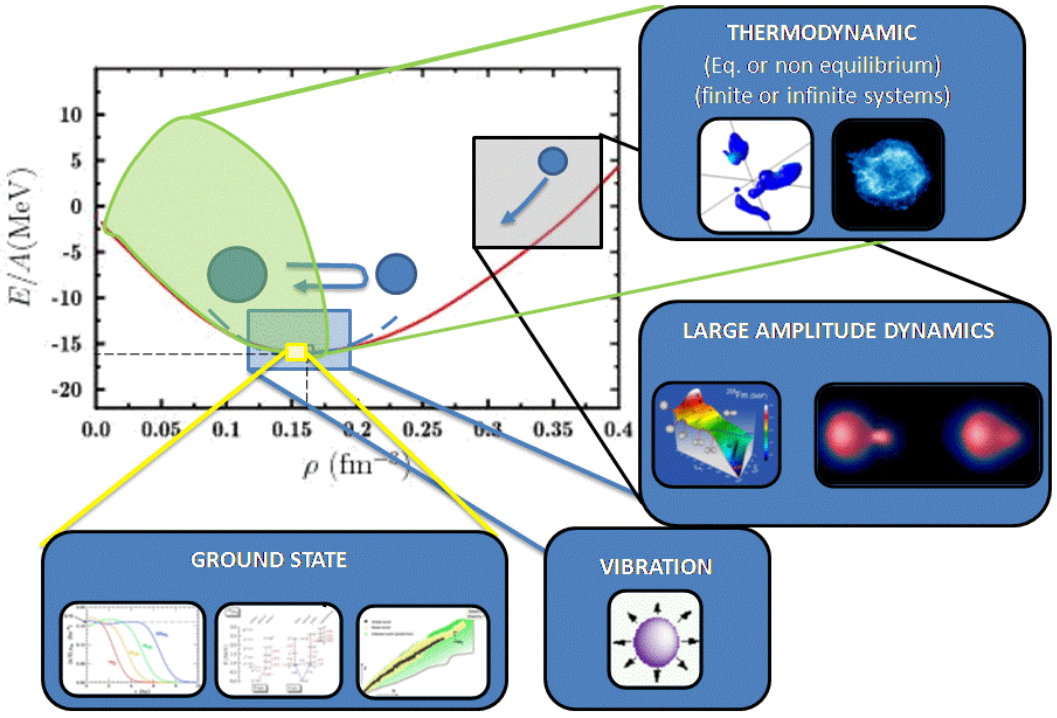

FIG. 9: Range of applications of the nuclear EDF: *(Color online) The red curve represents the equation of state in symmetric nuclear matter as a function of the system density. In the EDF theory, the energy is directly parametrized as a functional of the density. Nuclear structure study focus on or around the minimum. EDF is used extensively to get information on the ground state (yellow box) as well as excited state (see discussion in the text). It could also be used when the system is slightly shifted from the minimum leading to the onset of small amplitude vibrations (blue box). Time-Dependent version of the EDF also provides a description of nuclear dynamics like fusion or fission when the system is far away from the minimum (large amplitude collective motion [LACM]). Finally, EDF can also be extended to treat systems at finite temperature or entropy and provide information on the full phase-diagram and associated phase-transition.*

replaced by a functional of the local density. Eventually, in some cases (v-representability), the complex interacting system can be replaced by an ensemble of non-interacting electrons in a local external field $v(\mathbf{r})$. This potential can be written as a functional of the local density $n(\mathbf{r}) \equiv \rho(\mathbf{r},\mathbf{r})$. At the minimum of the functional, the energy of the non-interacting system matches the energy of the interacting one and the local density matches the local density of the exact ground state.

- **Kohn-Sham state and equation:** Kohn-Sham introduced the notion of auxiliary state (Kohn and Sham, 1965). In the KS approach, a Slater determinant denoted by Φ is introduced to compute the local density (see also discussion (Perdew and Zunger, 1981)). Associated single-particle states (Kohn-Sham orbitals), denoted by φ_α are solution of the Kohn-Sham equation:

$$\Big\{ -\frac{\hbar^2 \bigtriangledown^2}{2m} + v(\mathbf{r}) \Big\} \varphi_\alpha(\mathbf{r}) \;=\; \varepsilon_i \varphi_\alpha(\mathbf{r}). \tag{211}$$

Note that the auxiliary state itself has no specific physical meaning. This leads to the following sequence of mapping:

$$\Phi = \mathcal{A}(\{\varphi_\alpha\}_{\alpha=1,N}) \Longrightarrow n(\mathbf{r}) \Longrightarrow v(\mathbf{r}) \Longrightarrow \mathcal{E}[n(\mathbf{r})] \Longleftrightarrow E = \frac{\langle\Psi|H|\Psi\rangle}{\langle\Psi|\Psi\rangle} \tag{212}$$

- **Construction of the functional:** The difficulty of course is to construct the "exact" functional. Many techniques and degrees of approximation to it have been proposed, starting from the Local Density approximation (LDA), where the functional depends only on the local density, to the Gradient Expansion Approximation (GEA), Generalized Gradient Approximation (GGA), to Meta-GGA, where different orders of density gradients are introduced progressively (Fiolhais *et al.*, 2003). Note that alternative methods like Optimized Effective Potential (OEP) are also extensively used (see for instance (Capelle, 2006)).
- **Additional theorems and extensions:** Starting from the pioneering work of Hohenberg, Kohn and Sham, many theorems useful in DFT have been proven. Some of them are specially related to the discussion on EDF are quoted below:
  - **Density Matrix Functional Theory (DMFT):** Gilbert (Gilbert, 1975) has shown that the one-body density matrix (OBDM) $\rho(\mathbf{r}, \mathbf{r}')$ can be used instead of the local density to construct the functional. The functional can equivalently be written either in terms of the OBDM or in terms of occupation numbers n_α and natural orbitals φ_α. One of the advantages of this approach, compared to the Kohn-Sham scheme, is that single-particle states and occupations identifies with the exact ones at the minimum, and therefore carry the information on all one-body degrees of freedom.
  - **Pairing:** DFT has been generalized to account for pairing correlations in ref. (Oliveira *et al.*, 1988b).
  - **Time-Dependent Density-Functional Theory (TDDFT):** The possibility to describe non-equilibrium dynamics of electrons has been initiated by the Runge-Gross (RG) theorem (Runge and Gross, 1984). The proof of the theorem has shown in particular that the current vector $\mathbf{j}(\mathbf{r})$ should also be introduced and that the functional for time-dependent process might be highly non-local in time.
  - **Excited states:** Using a generalization of the Rayleigh-Ritz theorem given in (Gross *et al.*, 1988b), the Ensemble Kohn-Sham theory has been proposed to access not only the ground state but also excited states (Gross *et al.*, 1988a; Oliveira *et al.*, 1988a). Note that TDDFT is nowadays a tool of choice to get information on excited states (Marques and Gross, 2004; Marques *et al.*, 2006).

2. Selected aspects of EDF

A detailed description of formal aspects related to EDF will be given in the following. The goal of the present section is to introduce some of the important features of what is nowadays called Energy Density Functional. These features are introduced in order to follow as much as possible the concepts introduced for DFT in section V.A.1 and underlines resemblances and differences.

- **EDF for nuclei:** The EDF concept has been introduced to describe nucleons in nuclei interacting through the *strong nucleon-nucleon interaction*. Contrary to electronic systems, nuclei are *self-bound* systems for which the original HK theorem does not apply. In its simplest form, the EDF theory corresponds to the replacement of the initial complex many-body problem by a energy functional of the density. Historically, the EDF theory has been empirically introduced in the 70's without relying on a firm theorem. However, recently, theorems for self-bound systems have been proven where the laboratory density is to be replaced by the density in the intrinsic frame (Engel, 2007; Giraud, 2008; Messud *et al.*, 2009).
- **Single-Reference EDF and symmetry breaking:** in its simplest form, called hereafter Single-Reference (SR)-EDF, similarly to DFT, an auxiliary (Reference) state is introduced to construct the different quantities entering in the functional. When pairing is neglected, the reference state is a Slater determinant. When pairing is included, a quasi-particle vacuum is constructed (written generically as $|\Phi\rangle = \prod \beta_i|-\rangle$ below). Following notations from section III, observables (normal and anomalous densities, gradients of the densities ...) entering in the functional are denoted generically by $\{\langle A_\alpha \rangle\}$. SR-EDF can then be schematically

represented by the sequence:

$$|\Phi\rangle = \prod \beta_i|-\rangle \Longrightarrow \langle A_\alpha\rangle \implies v(\langle A_\alpha\rangle) \implies \mathcal{E}_{\rm EDF}[\langle A_\alpha\rangle] \iff E = \frac{\langle\Psi|H|\Psi\rangle}{\langle\Psi|\Psi\rangle} \qquad (213)$$

Two important remarks are in order. First, properties of the auxiliary state like single-particle energies are often used to get physical insight in nuclei. However, having in mind the strict density functional theory framework, it is to be clarified if the auxiliary state could be used to get such physical information. Second, an important aspect of the SR-EDF level is to explicitly use reference states that explicitly break some symmetries of the original bare Hamiltonian. Allowing the reference state to break the symmetries is a way to incorporate *static* long-range correlations associated with collective modes, as for example deformation and pairing, with very moderate effort. However, the breaking of symmetries (translational, rotational, parity, particle number, to name the most current ones) forbids a trivial connection of the nuclear SR-EDF formalism to the original existence theorems (Engel, 2007; Giraud, 2008; Messud *et al.*, 2009). Indeed, the density that minimizes the exact HK energy functional must reflect the symmetries of the exact ground state of the system. In fact, the appearance of symmetry-breaking solutions in nuclear EDF calculations underlines two important elements (i) it is crucial and numerically not too difficult to grasp the most important *static* correlations using rather simple approximate functionals and a single-determinantal reference state (ii) kinematic correlations associated with the corresponding symmetry modes (Goldstone modes) as well as the correlations due to the fluctuation of their order parameters are extremely difficult to incorporate into a single-determinantal approach. In other words, correlations associated with highly non-local processes such as large-amplitude collective motions can hardly be described within a SR approach based on a standard, nearly-local EDF. Last, it is important to keep in mind that broken symmetries like pairing or deformation are directly observed experimentally for instance in odd-even mass effects or through the observation of rotational bands.

- **Effective interaction and Construction of the SR-EDF functional:** current EDF used are mainly based on on zero-range (Skyrme like) or finite range (Gogny like) effective interactions. The use of zero range Skyrme interaction (Skyrme, 1956) has been originally proposed to obtain a functional form in (Vautherin and Brink, 1972). In this reference, starting from the Skyrme interaction including three-body forces, the Hartree-Fock approximation is used to get a functional of the local density ρ, the kinetic density τ, etc. Parameters of the functional have then been directly adjusted on specific properties of infinite nuclear matter (energy, saturation density and incompressibility) and finite nuclei. Due to the use of effective interactions and many-body techniques very similar to HF or HFB, EDF are sometimes themselves confused with HF or HFB theory which might be misleading. A list of reason why the EDF should not be mixed with such theories are given below:

  ♢ Original Skyrme interaction, restricted to two and three-body terms, do not provide a proper description of nuclear systems close to the saturation point. For this reason, density dependent effective interactions have been introduced in ref. (Decharge and Gogny, 1980; Negele, 1970). Strictly speaking, one cannot speak anymore about a Hamiltonian and Hartree-Fock approximation if the underlying interaction depends itself on the trial state on which it is applied.

  ♢ The exchange term in the Coulomb interaction is rarely treated exactly and most often the Slater approximation is made.

  ♢ When pairing is included, different effective interaction are often used in the mean-field and pairing channels respectively, showing that the very notion of an underlying Hamiltonian on which the Hartree-Fock approximation is made does not exist.

  ♢ In practice the functional parameters are directly adjusted on experimental observations. Since experiments include complex correlations in nuclei, one expect that coefficients contain much more physics than the simple Hartree-Fock approximation made with the bare nuclear Hamiltonian.

These are few examples emphasizing the difference between HF and EDF. Obviously, one can eventually continue to use terminology like "Skyrme HF" but things might become very

confusing in the near future. Indeed, with new soft interactions, it is now possible to make the true HF approximation of the vacuum nuclear Hamiltonian. This HF approximation has nothing to do with EDF theory. In this report, SR-EDF will be systematically used to not confuse with the HF theory.

Finally, it is important to realize that there are several advantages in constructing a functional from an effective interaction. EDF deduced in this way are very rich and automatically contain many density dependent terms as well as term depending on gradients... of the density. As a direct consequence, even original EDF can already be classified at least as a Meta-GGA approach. In addition, time-odd terms as well as specific combinations of terms that automatically ensure some physical properties like Galilean invariance, naturally appear in the functional (Bender *et al.*, 2003).

- **Extensions:** Similarly to DFT many extensions of SR-EDF have been proposed:
  - **Density Matrix Functional Theory (DMFT):** Following the idea of Gilbert (Gilbert, 1975), the possibility to enrich the functional by using functional of the one-body density matrix (OBDM) or occupation numbers n_α and natural orbitals φ_α has been recently rediscussed (Lacroix, 2009; Papenbrock and Bhattacharyya, 2007). DMFT might in particular be a way to conciliate the physical interpretation of single-particle energies used in EDF since in that case single-particle states are meaningful and should be identified with the exact natural orbitals.
  - **Pairing:** As mentioned above, pairing correlations are often included by considering functionals not only of the normal density but also of the anomalous density (see for instance (Bender *et al.*, 2003)).
  - **Time-Dependent Energy Density Functional (TD-EDF):** Right after first applications of EDF to study static properties of nuclei, the dynamics of nuclei using TD-EDF has been developed (Bonche *et al.*, 1976). The next section will be devoted to the application of transport theories based on EDF (Lacroix *et al.*, 2004a; Negele, 1982; Simenel *et al.*, 2008). Note that, a first step towards the proof of a functional theory for time-dependent processes is made in ref. (Messud, 2009).
  - **Restoration of broken symmetries and Multi-Reference EDF (MR-EDF):** At the SR-EDF level several symmetries are explicitly broken (see discussion above). In a Hamiltonian case, those symmetries could be restored through configuration mixing using the Generator Coordinate Method (GCM) (Ring and Schuck, 1980). Guided by the Hamiltonian case, configuration mixing techniques are nowadays used to incorporate correlations associated with large amplitude collective motion beyond the static ones. In that case, a new many-body state, denoted by $|\Psi\rangle$ and written as

$$|\Psi\rangle = \sum_Q f_Q |\Phi(Q)\rangle \tag{214}$$

    is introduced, where $|\Phi(Q)\rangle$ corresponds to a set of reference states function of some collective parameters $Q = \langle Q\rangle$. Configuration mixing within EDF, called hereafter Multi-Reference EDF, is not only used to restore symmetry but also provides a tool of choice to access excited states of the nucleus. Recent studies (Bender *et al.*, 2009; Dobaczewski *et al.*, 2007; Duguet *et al.*, 2009; Lacroix *et al.*, 2009) have pointed out some deficiencies in combining functional theory and configuration mixing technique as well as the necessity to develop a clear theoretical framework for MR-EDF approach (see discussion below).

B. Actual strategy to construct SR-EDF and MR-EDF

It is clear from the above discussion that nuclear EDF shares several features with DFT. However, the strategy used to construct the functional is different as it embraces two successive levels of description. These two levels are strongly guided by the Hamiltonian case, see illustration in Fig. 10). A brief outline of the nuclear EDF construction is given below. On the SR-EDF level, one product state Φ_0 provides the normal (ρ^{00}) and anomalous (κ^{00}) density matrices the many-body

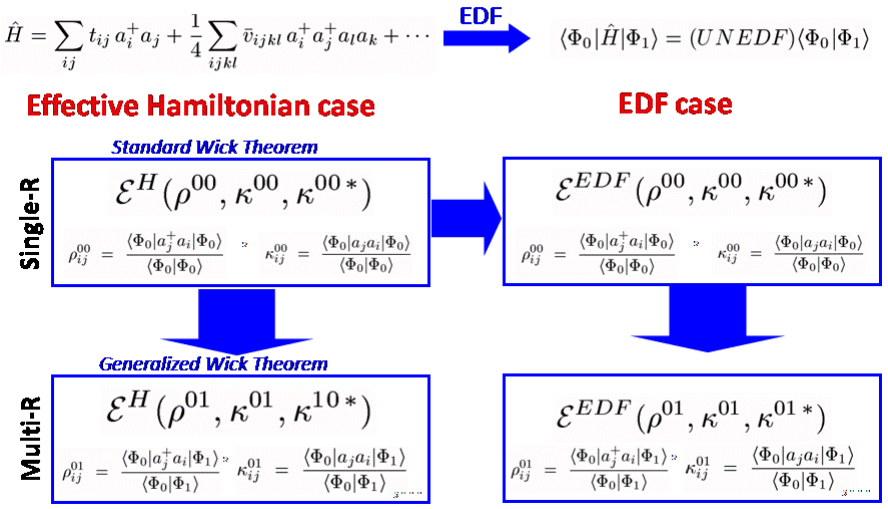

FIG. 10: *Illustration of the strategy used to construct universal nuclear EDF (UNEDF). Left : the use of the Standard Wick Theorem (SWT) (Wick, 1950) applied to a true Hamiltonian gives an example of functional of the density only in the HF case or of the normal and anomalous density in the HFB case. SR-EDF functional are deduced in analogy with the Hamiltonian case by replacing the true interaction by the effective vertex in different channels. MR-EDF : Configuration mixing calculations performed at the MR-EDF rely on extending the SR energy functional into non-diagonal EDF kernels. In the Hamiltonian case, using the Generalized Wick Theorem (GWT) (Balian and Brezin, 1969), one deduce that the functional should be the same except that the normal and anomalous density are replaced by the transition densities. Again, in analogy with the Hamiltonian case, most MR-EDF simply take the SR-EDF functional where densities are replaced by transition densities.*

energy is a functional of. In the following, $\mathcal{E}_{SR}[\Phi_0] = \mathcal{E}_{SR}[\rho^{00}, \kappa^{00}, \kappa^{00\,*}]$ denotes the associated functional. Although such a restriction is not necessary, one usually builds the EDF from an effective vertex (of the Skyrme or Gogny type), whose parameters are adjusted to reproduce a selected set of experimental observations. Independently of the starting point, the EDF can be written as in any arbitrary basis as

$$\begin{aligned}\mathcal{E}_{SR}[\rho^{00}, \kappa^{00}, \kappa^{00\,*}] \;=\; & \sum_{ij} t_{ij}\,\rho^{00}_{ji} + \tfrac{1}{2}\sum_{ijkl}\bar{v}^{\rho\rho}_{ijkl}\,\rho^{00}_{ki}\,\rho^{00}_{lj} + \tfrac{1}{4}\sum_{ijkl}\bar{v}^{\kappa\kappa}_{ijkl}\,\kappa^{00\,*}_{ij}\,\kappa^{00}_{kl} \\ & + \tfrac{1}{6}\sum_{ijklmn}\bar{v}^{\rho\rho\rho}_{ijklmn}\,\rho^{00}_{li}\,\rho^{00}_{mj}\,\rho^{00}_{nk} + \tfrac{1}{4}\sum_{ijklmn}\bar{v}^{\rho\kappa\kappa}_{ijklmn}\,\rho^{00}_{li}\,\kappa^{00\,*}_{jk}\,\kappa^{00}_{mn} + \dots \;,\end{aligned} \tag{215}$$

where the first term accounts for the uncorrelated kinetic energy, whereas $\bar{v}^{\rho\rho}$, $\bar{v}^{\kappa\kappa}$, $\bar{v}^{\rho\rho\rho}$, ... denote effective vertices associated with the different terms of the EDF. Again, although it formally resembles it, Eq. (215) should not be confused with the expectation value of a Hamiltonian containing two-body, three-body, ... interactions in the Hartree-Fock-Bogolyubov state Φ_0. For this to be true, specific properties, e.g. $\bar{v}^{\rho\rho}_{ijkl} = \bar{v}^{\kappa\kappa}_{ijkl}$ and $\bar{v}^{\rho\rho}_{ijkl} = -\bar{v}^{\rho\rho}_{ijlk}$ for all (i,j,k,l), would have to be satisfied, which is usually not the case in the EDF context (see discussion in section V.A.2) [10].

While static collective correlations, e.g. pairing and deformation, can be accounted for within the SR EDF formalism through the symmetry breaking of the auxiliary state Φ_0, dynamical collec-

[10] Note that most popular and performing EDF cannot be written under the form of Eq. (215) as they contain a dependence on a non-integer power of the (local) normal density (Bender *et al.*, 2003). Due to the pathologies recently observed in MR-EDF (see discussion below and ref. (Duguet *et al.*, 2009)), it is to be anticipated, however, that future MR-EDFs will be constructed under such a form, typically truncated at forth or fifth power.

tive correlations requires to perform Multi-Reference (MR) calculations, traditionally denoted as "beyond-mean-field". Such an extension, built by analogy with the Generator Coordinate Method (GCM) in the Hamiltonian formalism (Ring and Schuck, 1980), allows one not only to incorporate additional correlations but also to describe low-energy spectroscopy and transition probabilities between states characterized by symmetry-restored quantum numbers. In strict analogy with the Hamiltonian formalism, a new trial state Ψ is introduced that corresponds as a mixing of several independent particle (or quasi-particle) state. It is here written generically as

$$|\Psi\rangle = \sum_{0\in \mathrm{MR}} f_0 |\Phi_0\rangle, \tag{216}$$

while the MR EDF is written as

$$\mathcal{E}[\Psi] \equiv \frac{\sum_{\{0,1\}\in \mathrm{MR}} f_0^* \, f_1 \, \mathcal{E}_{MR}[\Phi_0,\Phi_1] \, \langle\Phi_0|\Phi_1\rangle}{\sum_{\{0,1\}\in \mathrm{MR}} f_0^* \, f_1 \, \langle\Phi_0|\Phi_1\rangle} \ , \tag{217}$$

where non-diagonal matrix elements $\langle\Phi_0|\hat{H}|\Phi_1\rangle/\langle\Phi_0|\Phi_1\rangle$ have been replaced by their EDF counterpart $\mathcal{E}_{MR}[\Phi_0,\Phi_1]$. The weight functions f are determined either by symmetry considerations, by diagonalization, or both. The product states Φ_i belonging to the MR set are chosen according to the collective modes one wants to describe. In the absence of a well-founded prescription to build $\mathcal{E}_{MR}[\Phi_0,\Phi_1]$, only specific constraints can be imposed. For a number of reasons (Robledo, 2007), it is necessary to impose that

$$\mathcal{E}_{MR}[\Phi_0,\Phi_0] \equiv \mathcal{E}_{SR}[\Phi_0] \qquad \text{and} \qquad \mathcal{E}_{MR}[\Phi_1,\Phi_0] = \mathcal{E}^*_{MR}[\Phi_0,\Phi_1] \tag{218}$$

Following the Hamiltonian formalism, the most natural guidance is provided by the generalized Wick theorem(Balian and Brezin, 1969) which tells us that $\mathcal{E}_{MR}[\Phi_0,\Phi_1]$ is obtained by replacing SR density matrices by transition ones in Eq. (215). Transition density matrices, denoted by $[\rho^{01},\kappa^{01},\kappa^{10\,*}]$ are defined through:

$$\rho^{01}_{ij} \ \equiv \ \frac{\langle\Phi_0|a^+_j a_i|\Phi_1\rangle}{\langle\Phi_0|\Phi_1\rangle} \ , \qquad \kappa^{01}_{ij} \equiv \frac{\langle\Phi_0|a_j a_i|\Phi_1\rangle}{\langle\Phi_0|\Phi_1\rangle} \ , \qquad \kappa^{10\,*}_{ij} \equiv \frac{\langle\Phi_0|a^+_i a^+_j|\Phi_1\rangle}{\langle\Phi_0|\Phi_1\rangle} \ , \tag{219}$$

An illustration of the EDF application is shown in Fig. 11 (Adapted from (Bender *et al.*, 2006)). Each point of the black curve corresponds to a SR calculation with a constraint on the axial quadrupole moment to deform more or less the ^{76}Kr nucleus. This nucleus presents two minima at non-zero deformation favored energetically compared to the spherical configuration, indicating that the spherical symmetry is explicitly broken. The MR-EDF is performed with the subset of these SR states, giving an additional gain of energy of 3.5 MeV (for the $J = 0$ state).

C. Difficulties and Pathologies observed in configuration mixing calculations

Recently, several groups have pointed out difficulties, namely appearance of divergences and finite steps in MR-EDF in the context of Particle-Number Restoration (PNR) (Almehed *et al.*, 2001; Anguiano *et al.*, 2001; Dobaczewski *et al.*, 2007; Dönau, 1998; Flocard and Onishi, 1997). A pathology that resembles the one identified for PNR has recently been seen in EDF calculations, without explicit treatment of pairing, aiming at restoring angular momentum (Zduńczuk *et al.*, 2007), whereas a similar problem was identified much earlier in the GCM-type mixing of zero- and two-quasi-particle states (Tajima *et al.*, 1992). An illustration of these pathologies is given in Figure 12.

At first sight, these pathologies might be thought of as a numerical artifact. However, in a trilogy of papers (Bender *et al.*, 2009; Duguet *et al.*, 2009; Lacroix, 2009), it has been shown that the difficulty encountered in MR-EDF are deeply rooted in the strategy used to perform MR-EDF depicted in Fig. 10. In these works, characteristics and origin of the difficulties have been carefully analyzed. Using many-body techniques, a minimal solution to the problem has been proposed. A guideline for recent discussions in MR-EDF is given below.

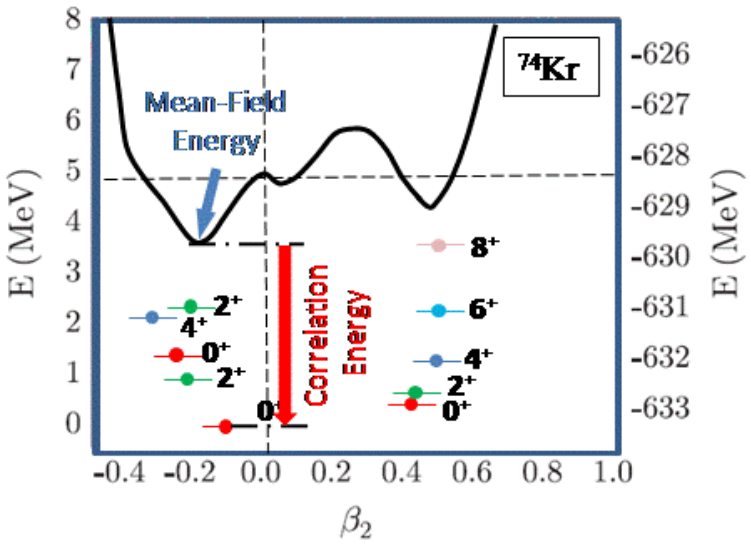

FIG. 11: *Illustration of application of SR-EDF (Black curve) and MR-EDF (Levels) in the case of ^{76}Kr (adapted from (Bender* et al.*, 2006)). The minimum of black curve correspond to a deformed nucleus indicating indicating that deformation is favored energetically. The red arrow indicates the gain in energy (of the order of 3.5 MeV) when using MR-EDF.*

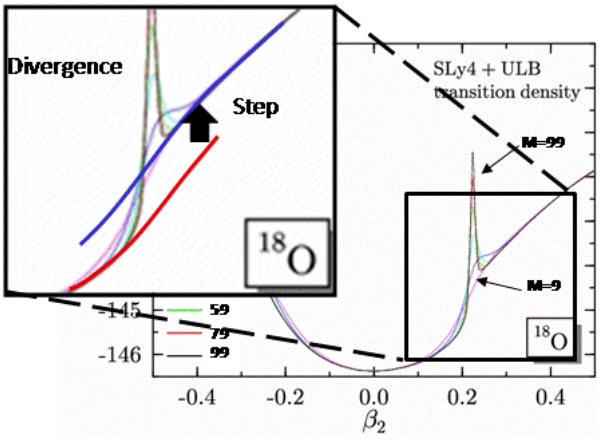

FIG. 12: *Illustration of the divergence and finite step in particle-number projected binding energy of ^{18}O calculated with the Skyrme interaction SLy4 and a density-dependent pairing interaction as a function of the quadrupole deformation. Different curves correspond to the number M of reference states taken to perform the PNR. (adapted from (Bender and Duguet, 2007)). We clearly see that the curves significantly depend on M and does not seems to converge as M increase (with the presence of finite steps and divergences).*

1. Characteristics of steps and divergences

PNR is one of the simplest cases of configuration mixing and where pathologies can be unambiguously identified. Some aspects that have initiated the discussion on difficulties in MR-EDF for restoration of particle number are listed below. Starting from a SR-EDF built from the auxiliary quasi-particle state Φ_0, dynamical pairing correlations associated with PNR can be incorporated through a MR EDF calculation. Building the MR set from product states rotated in gauge space

$|\Phi_\varphi\rangle = e^{i\varphi\hat{N}}|\Phi_0\rangle$, Eq. (217) specified to PNR reads

$$\mathcal{E}^N \equiv \int_0^{2\pi} d\varphi \, \frac{e^{-i\varphi N}}{2\pi \, c_N^2} \, \mathcal{E}_{MR}[\Phi_0, \Phi_\varphi] \, \langle \Phi_0 | \Phi_\varphi \rangle \, . \tag{220}$$

In practice, Eq. (220) is often evaluated numerically using the Fomenko (Fomenko, 1970) discretization procedure. The illustration in Fig. 12 has been obtained using different number of mesh points in the discretization. Obvious pathologies are visible, i.e. (i) the estimate of the energy landscape does not converge everywhere and (ii) non-physical steps appear at particular deformations as the number of mesh points is increased. Several groups have discussed various aspects of these pathologies:

- divergences in PNR may appear when either a proton or neutron single-particle level crosses the Fermi energy, as pair of states differing by $\pi/2$ are orthogonal in this case, i.e. $\langle \Phi_0 | \Phi_\varphi \rangle = 0$ (Anguiano *et al.*, 2001).
- When the same (density-independent) vertices are used in the p-h and p-p channel and the exchange is properly taken into account, problems were shown to disappear.
- The problem has been characterized more precisely with a complex plane analysis(Dobaczewski *et al.*, 2007; Duguet *et al.*, 2009), demonstrating in particular the less obvious, but more profound, occurrence of steps. This technique, however, cannot be extended straightforwardly to the restoration of other symmetries, and does not lead to a practical solution to the problem.
- The fact that divergences occur at $\langle \Phi_0 | \Phi_\varphi \rangle = 0$ has been recognized rather earlier as a problem of the MR-EDF deduced from a direct mapping of the Hamiltonian EDF based on the Generalized Wick Theorem (Anguiano *et al.*, 2001). This early hypothesis has been confirmed later (Bender and Duguet, 2007) by avoiding the use of the GWT in the PNR case.
- This problem is not specific to PNR but seems to be generic for any MR-EDF calculation. For instance, it has been seen when performing angular-momentum restoration (Zduńczuk *et al.*, 2007).

2. Minimal solution to the problem

Two remarks are at the heart of the proposed solution: (i) actual MR-EDF are strongly guided by the Hamiltonian case (ii) The use of Generalized Wick Theorem, which does not lead to any specific difficulty in the Hamiltonian case, seems to be at the origin of the problem in the EDF case. The recent study of pathologies have indeed confirmed that the GWT, applied beyond its strict domain of validity, leads to ill-defined calculations when performed within the EDF approach. The starting point of the solution recently proposed is to avoid the GWT at the first place.

A careful analysis of ref. (Balian and Brezin, 1969), underlines that the proof of the GWT passes through the use of the Thouless theorem that connects two quasi-particle vacuum Φ_0 and Φ_1 through an exponential of a second order polynomial of quasi-particle creation/annihilation operator. Strictly speaking, the Thouless theorem does not hold for orthogonal states, i.e. $\langle \Phi_0 | \Phi_1 \rangle = 0$.

In order to avoid the use of the GWT on one hand and of the Thouless strategy to connect two vacuum one the other hand, the following trick was used: given a pair of quasi-particle vacua, denoted by $|\Phi_0\rangle$ and $|\Phi_1\rangle$ (with possibly $\langle \Phi_0 | \Phi_1 \rangle = 0$), one can always find a simple "BCS like" expression connecting these two states (Ring and Schuck, 1980), i.e.:

$$|\Phi_1\rangle = \tilde{\mathcal{C}}_{01} \prod_{p>0} \left(\bar{A}^*_{pp} + \bar{B}^*_{p\bar{p}} \, \tilde{\alpha}^\dagger_p \, \tilde{\alpha}^\dagger_{\bar{p}} \right) |\Phi_0\rangle \ . \tag{221}$$

The operators $\tilde{\alpha}_{p/\bar{p}}$ are pairs of quasi-particles states associated to $|\Phi_0\rangle$ and have been obtained by performing the Bloch-Messiah-Zumino (BMZ) (Bloch and Messiah, 1962; Zumino, 1962) decomposition on the Bogoliubov transformation between the two sets of quasi-particle operators associated to the states Φ_0 and Φ_1. $\tilde{\mathcal{C}}_{01}$ is a factor that depends explicitly on the convention used to express the vaccua before the BMZ decomposition. Properties of this expression have been extensively

discussed in ref. (Lacroix *et al.*, 2009) and only a brief summary is given here. Essentially, once a simple expression like Eq. (221) is obtained, many manipulations, properties, proofs of theorems become straightforward. Few examples are given below:

- **Expectation values of operators and GWT proof:** for any operator O, we can write

$$\langle\Phi_0|O|\Phi_1\rangle = \tilde{\mathcal{C}}_{01}\prod_{p>0}\langle\Phi_0|O\left(\bar{A}^*_{pp} + \bar{B}^*_{p\bar{p}}\,\tilde{\alpha}^\dagger_p\,\tilde{\alpha}^\dagger_{\bar{p}}\right)|\Phi_0\rangle. \tag{222}$$

  Since any operator can be decomposed in the specific quasi-particle basis $\{\tilde{\alpha}^\dagger_\nu, \tilde{\alpha}_\nu\}$, expectation values $\langle\Phi_0|O|\Phi_1\rangle$ reduces to the use of the standard Wick theorem for the state Φ_0. Using this property, a more direct proof of the GWT compared to ref. (Balian and Brezin, 1969) can be given simply using the SWT.

- **Overlaps:** Taking $O = 1$ gives

$$\langle\Phi_0|\Phi_1\rangle = \tilde{\mathcal{C}}_{01}\prod_{p>0}\bar{A}^*_{pp} = \tilde{\mathcal{C}}_{01}\sqrt{\det A^*} \tag{223}$$

  which is nothing but the Onishi-Yoshida formula (Onishi and Yoshida, 1966).

- **Proof of the Thouless theorem:** When $\langle\Phi_0|\Phi_1\rangle$, i.e. when all A_{pp} are different from zero, one can introduce new parameters $\bar{Z}_{\bar{p}p} = (\bar{B}_{\bar{p}p}/\bar{A}^{-1}_{pp})^*$ such that:

$$\begin{aligned}|\Phi_1\rangle &= \tilde{\mathcal{C}}_{01}\prod_{p>0}\left(\bar{A}^*_{pp} + \bar{B}^*_{p\bar{p}}\,\tilde{\alpha}^\dagger_p\,\tilde{\alpha}^\dagger_{\bar{p}}\right)|\Phi_0\rangle \\ &= \langle\Phi_0|\Phi_1\rangle\prod_{p>0}\left(1 + \bar{Z}_{p\bar{p}}\,\tilde{\alpha}^\dagger_p\,\tilde{\alpha}^\dagger_{\bar{p}}\right)|\Phi_0\rangle = \langle\Phi_0|\Phi_1\rangle\, e^{\sum \bar{Z}_{p\bar{p}}\,\tilde{\alpha}^\dagger_p\,\tilde{\alpha}^\dagger_{\bar{p}}}|\Phi_0\rangle\end{aligned}$$

  which is nothing but the Thouless theorem (Thouless, 1960) written in a specific basis.

The new quasi-particle basis is particularly suitable to analyze the origin of pathologies. In this basis, a new expression of the multi-reference functional is obtained (restricting here to bilinear EDF and omitting the kinetic term) as

$$\mathcal{E}_{MR}[\Phi_0,\Phi_1] = \frac{1}{2}\sum_{\nu\mu}\bar{v}^{\rho\rho}_{\varphi_\nu\varphi_\mu\varphi_\nu\varphi_\mu} + \frac{1}{4}\sum_{\nu\mu}\bar{v}^{\kappa\kappa}_{\varphi_\nu\phi_{\bar{\nu}}\varphi_\mu\phi_{\bar{\mu}}} \tag{224}$$

$$+\frac{1}{2}\sum_{\nu\mu}\bar{v}^{\rho\rho}_{\varphi_\nu\varphi_\mu\phi_\nu\varphi_\mu}\,\bar{Z}_{\nu\bar{\nu}} + \frac{1}{4}\sum_{\nu\mu}\bar{v}^{\kappa\kappa}_{\varphi_\nu\varphi_{\bar{\nu}}\varphi_\mu\phi_{\bar{\mu}}}\,\bar{Z}_{\nu\bar{\nu}} \tag{225}$$

$$+\frac{1}{2}\sum_{\nu\mu}\bar{v}^{\rho\rho}_{\varphi_\mu\varphi_\nu\varphi_\mu\phi_\nu}\,\bar{Z}_{\nu\bar{\nu}} + \frac{1}{4}\sum_{\nu\mu}\bar{v}^{\kappa\kappa}_{\varphi_\mu\phi_{\bar{\mu}}\phi_\nu\phi_{\bar{\nu}}}\,\bar{Z}_{\nu\bar{\nu}} \tag{226}$$

$$+\frac{1}{2}\sum_{\nu\mu}\bar{v}^{\rho\rho}_{\varphi_\nu\varphi_\mu\phi_\nu\phi_\mu}\,\bar{Z}_{\nu\bar{\nu}}\,\bar{Z}_{\mu\bar{\mu}} + \frac{1}{4}\sum_{\nu\mu}\bar{v}^{\kappa\kappa}_{\varphi_\nu\varphi_{\bar{\nu}}\phi_\mu\phi_{\bar{\mu}}}\,\bar{Z}_{\nu\bar{\nu}}\,\bar{Z}_{\mu\bar{\mu}}\ , \tag{227}$$

where $(\mu,\bar{\mu})$ denote a canonical pair in the specific quasi-particle representation while φ_μ and ϕ_μ stand for the upper and lower components of the quasi-particle states. The Expressions (224-227) is convenient as it separates the contributions remaining in the SR limit (line 224) from the rest. It also allows to identify the different sources of problems:

(i) Self-interaction: Well-kown from DFT, self-interaction relates to the fact that a particle should not interact with itself, which, however, happens when the vertices $\bar{v}^{\rho\rho}$ are not anti-symmetric(Lacroix *et al.*, 2009). This is almost always the case in actual EDFs at least because of the approximations often used to treat Coulomb exchange. Such a self-interaction, if present at the SR level, further contributes at the MR level (lines (225-226)).

(ii) Self-pairing: this new concept(Bender and Duguet, 2007; Bender *et al.*, 2009) is specific to EDFs treating pairing correlations explicitly and relates to the fact that two paired particles should not generate correlation energies, beyond their direct interaction, by scattering onto themselves. Again, such a spurious contribution appears at both SR and MR levels.

(iii) Steps and divergences: As the energy kernel is multiplied by $\langle\Phi_0|\Phi_1\rangle \propto \prod_\nu \bar{A}^*_{\nu\nu}$ in the MR energy (see Eq. (217)), only terms with $\nu = \mu$ or $\nu = \bar{\mu}$ in line (227) can lead to divergences and steps when $\bar{A}^*_{\nu\nu} = 0$. In the pure Hamiltonian case, i.e. $\bar{v}^{\rho\rho}_{ijkl} = \bar{v}^{\kappa\kappa}_{ijkl}$ and $\bar{v}^{\rho\rho}_{ijkl} = -\bar{v}^{\rho\rho}_{ijlk}$ for all (i, j, k, l), the dangerous contributions coming from the two terms in Eq. (227) exactly cancel out and no divergence or step occurs. However, when different or non-antisymmetrized vertices are used, as in the EDF context, divergences and/or steps are observed, as illustrated in Fig. 12.

The quasi-particle basis introduced above allows one to proceed to the analogy with the Hamiltonian formalism on the basis of the standard Wick theorem rather than on the generalized one. Comparing the results of the two schemes, one proves(Lacroix *et al.*, 2009) that terms with $\nu = \mu$ or $\nu = \bar{\mu}$ in line (227) should be zero in the first place and must be removed altogether. This not only solves problem **(iii)** entirely but also removes finite spurious contributions to the MR energy kernel. Such a regularization technique can be applied to any type of configuration mixing performed in terms of an EDF depending on integer powers of the densities. It has been successfully applied to PNR(Bender *et al.*, 2009), as is exemplified on the left panel of Fig. 13 using the SIII Skyrme EDF. The correction not only removes the dependence on the number of mesh points and the non-physical steps, but also corrects the energy landscape *away* from those steps. The case

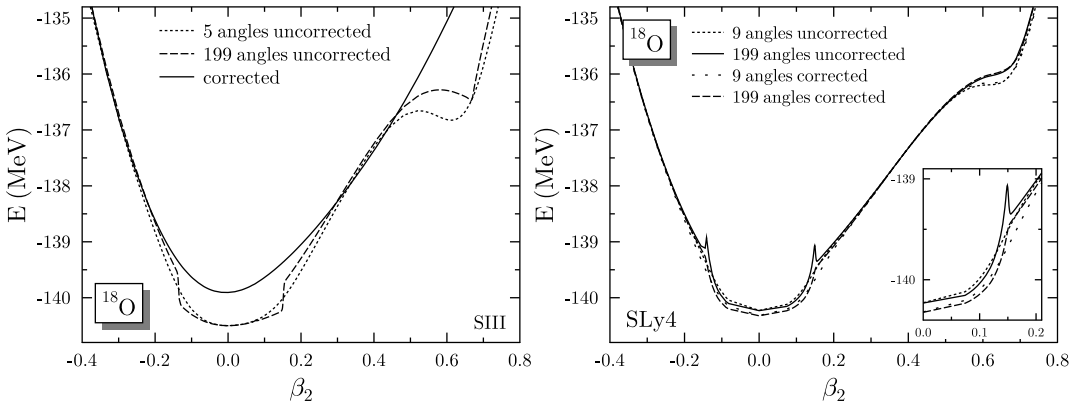

FIG. 13: *Left: Uncorrected (dotted and dashed lines) and corrected (solid line) particle-number restored quadrupole deformation energy obtained for ^{18}O with SIII and calculated with $M = 5$ and 199 discretization points of the integral in gauge space. The two corrected curves are superimposed. Right: attempt to regularize the particle-number restored energy of ^{18}O obtained with SLy4 that contains a non-integer power of the (local) normal density.*

of EDFs depending on non-integer powers of the density matrix has also been analyzed(Duguet *et al.*, 2009). Although divergences can be removed using a variant of the method proposed in Ref.(Lacroix *et al.*, 2009), the complex-plane analysis demonstrates that the left-over fractional power ρ^γ with $0 < \gamma < 1$ is ill-defined as it generates cusps in the PNR energy l andscape, (see right panel of Fig. 13). Generally speaking, one cannot use a functional that is multi-valued over the complex plane. This has important consequences on the present and future of EDF methods.

3. Summary and consequences for future MR-EDF

Above discussion shows that a minimal solution to recently observed pathologies can be found for EDF depending on integer powers of the density and applies to any kind of configuration mixing. These difficulties clearly underline the frontier between a many-body theory based on a Hamiltonian and a functional theory with phenomenological inputs. Nuclear physics models are strongly guided by the Hamiltonian theory. However specific care has to be made when concepts perfectly valid in the Hamiltonian case are exported to the functional framework. Besides the specific solution found, the study of pathologies has underlined important aspects to be taken into account both in formal and practical aspects of MR-EDF:

♢ Studies in refs. (Dobaczewski *et al.*, 2007; Duguet *et al.*, 2009) have clearly pointed out that functional with non-integer powers of the densities are ill defined in MR-EDF calculation and cannot be regularized. Most of the actual functionals based on Skyrme and/or Gogny do contain such non-integer dependence. Therefore, in the near future, three possibilities exist (a) either we stick to the SR-EDF level and no MR-EDF should be performed anymore. It is however difficult to believe that dynamical correlations associated for instance to strong deformation can be grasped easily in that way. (b) One can also try to use alternative methods that incorporate approximately configuration mixing without a direct diagonalization of the MR energy kernels. One can for instance use Lipkin-Nogami method (Lipkin, 1960; Nogami, 1964), Kamlah expansion (Kamlah, 1968) or RPA corrections (Blaizot and Ripka, 1986). (c) or one could finally try to design functional based on effective interactions without non-integer powers of the density. If the last option is pursued, in the near future, new generations of EDF have to be proposed with eventually higher powers of the densities.

♢ Correction to pathologies implies to perform Bloch-Messiah-Zumino decomposition for all pairs of reference states and then to work in a specific basis of quasi-particles. Therefore major modifications of existing codes are anticipated. Work is actually in progress to implement the present correction not only in the PNR case, but also in other configuration mixing calculations (Bender, 2010).

♢ Besides the discussion on numerical aspects and on the specific form of the functional, recent discussions on difficulties in MR-EDF approaches have clearly pointed out the absence of a well defined theoretical framework to construct excited states using a MR theory. An effort to clarify theoretical issues related to symmetry breaking and their restoration in functional theory, excited states... should be made in the near future.

D. Beyond mean-field with density matrix functional theory

As discussed above, there are technical and conceptual difficulties related to the use of MR-EDF within the nuclear context. Although MR-EDF is certainly one of the most powerful tools to incorporate correlations that are important in nuclear structure, it is still very costly numerically and cannot easily be applied in some cases. For instance, configuration mixing is often used after the variation (Projection After Variation-PAV) while the Reference state should a priori be projected before variation (Variation After Projection -VAP), see for instance (Sheikh and Ring, 2000). VAP is much more involved numerically than PAV and remains even nowadays very difficult. In addition, only few applications of MR-EDF, restricted to the adiabatic limit, have been made for time-dependent processes (Goutte *et al.*, 2005). Again, extensive applications of MR-EDF able to describe the richness of time-dependent phenomena seem impossible today. For these reasons, it is important to consider alternative methods able to incorporate more correlations than the SR-EDF framework. The Density-Matrix Functional Theory (DMFT) has been recently proposed as a candidate (Lacroix, 2009; Papenbrock and Bhattacharyya, 2007). The DMFT is summarized and illustrated below.

1. The Density Matrix Functional Theory

The concept of Density Matrix Functional Theory is a generalization of the Hohenberg-Kohn theorem (Hohenberg and Kohn, 1964) formulated in (Gilbert, 1975). It relies on a theorem showing that the ground state energy could be written as a functional of the one-body density matrix (OBDM) $\rho(\mathbf{r},\mathbf{r}')$ (instead of the local one-body density $\rho(\mathbf{r})$). In DMFT, the Single-Reference concept is replaced by the eigenvalues n_i and eigenvectors φ_i, called hereafter resp. occupation numbers and natural orbitals, of the OBDM, i.e. $\rho = \sum_i |\varphi_i\rangle n_i \langle\varphi_i|$. The variation of the functional

$$\mathcal{F}[\{\varphi_i\},\{n_i\}] \;=\; \mathcal{E}[\{\varphi_i\},\{n_i\}] - \mu\{Tr(\rho) - N\} - \sum_{ij}\lambda_{ij}(\langle\varphi_i|\varphi_j\rangle - \delta_{ij}), \tag{228}$$

with respect to one-body state components $\varphi_i^*(\mathbf{r})$ and occupation numbers (with the additional constraint $0 < n_i < 1$) is then performed to obtained the optimal φ_i, n_i and associated ground

state energy. The set of Lagrange multipliers μ and $\{\lambda_{ij}\}$ are introduced to insure particle number conservation and orthogonality of the single-particle states. Here, $\mathcal{E}[\{\varphi_i\},\{n_i\}]$ is the functional that has to be guessed. In electronic systems, the functional is generally separated into the Hartree, denoted by $\mathcal{E}_H$, (eventually Hartree-Fock, $\mathcal{E}_{HF}$) part and the exchange-correlation part, denoted here by $\mathcal{E}_{XC}$ (eventually correlation only $\mathcal{E}_C$).

While the DMFT has been studied theoretically for a rather long time (Gilbert, 1975; Mller, 1984; Valone, 1980a,b; Zumbach and Maschke, 1985), only recently explicit functionals of the OBDM or directly to natural orbitals have been proposed and applied to realistic situations(Cioslowski and Pernal, 2005; Cioslowski *et al.*, 2003; Csányi and Arias, 2000; Csányi *et al.*, 2002; Goedecker and Umrigar, 1998; Gritsenko *et al.*, 2005; Kollmar, 2004, 2006; Lathiotakis and Marques, 2008; Lathiotakis *et al.*, 2005; Leiva and Piris, 2005; Marques and Lathiotakis, 2008; Pernal and Cioslowski, 2004; Yasuda, 2002). There are nowadays extensive works to test functionals especially in infinite systems, the so-called Homogeneous Electronic Gas (HEG) (Cioslowski and Pernal, 1999; Lathiotakis *et al.*, 2007).

2. Nuclear DMFT: general aspects

EDF presents specific aspects and the introduction of new theories should definitely take advantage of the expertize accumulated during 30 years. The strategy to obtain actual EDF starting from the SR framework extended to the MR theory has been extensively discussed in section V.B. In Figure 14, this strategy is presented from a different perspective. Starting from a two-body Hamiltonian, the energy of the system can be regarded as a functional of the OBDM and the two-body correlation matrix C_{12}. The main advantage of the SR-EDF approach is to reduce the relevant information to the normal density and anomalous density if pairing is included. SR functionals with pairing can already be interpreted as a functional of occupation numbers and natural orbitals. Indeed, in that case, the SR-EDF writes

$$\mathcal{E}_{\rm SR}[\{\varphi_i,n_i\}] = \mathcal{E}_{\rm MF}[\{\varphi_i,n_i\}] + \mathcal{E}_{\rm Pair}[\{\varphi_i,n_i\}]. \tag{229}$$

where the notation $\mathcal{E}_{\rm MF}$ has been introduced to denote the SR-EDF without pairing while $\mathcal{E}_{\rm Pair}$ corresponds to the additional contribution associated with the introduction of pairing. Written in the canonical basis, the latter becomes

$$\mathcal{E}_{\rm Pair}[\{\varphi_i,n_i\}] \;\equiv\; \frac{1}{4}\sum_{i,j}\bar{v}^{\kappa\kappa}_{i\bar{i}j\bar{j}}\sqrt{n_i(1-n_i)}\sqrt{n_j(1-n_j)} \tag{230}$$

where $\bar{v}^{\kappa\kappa}$ is the effective interaction in the pairing channels while $(i,\bar{i})$ stands for canonical pairs of single-particle states. Therefore, SR-EDF including pairing can already be regarded as a class of functionals of natural orbitals and occupations. In his pioneering work, Vautherin (Vautherin, 1973) already discussed the possibility to use alternative functionals than the BCS one. Below, properties and illustration of such functionals are discussed.

a. **Rules for the construction of nuclear DMFT:** Although it is not obligatory, to keep actual SR-EDF as a starting point, the following rules are proposed to apply DMFT to the nuclear many-body problem (some aspects of the strategy are illustrated in Fig. 15):

- First, construction of EDF based on effective interaction has important advantages (see discussion V.A.2). Guided by the pairing case (Eq. 229), it is first proposed to write the nuclear density matrix functional as

$$\mathcal{E}[\{\varphi_i,n_i\}] = \mathcal{E}_{\rm MF}[\{\varphi_i,n_i\}] + \mathcal{E}_{\rm cor}[\{\varphi_i,n_i\}]. \tag{231}$$

- $\mathcal{E}_{\rm MF}$ might correspond to the "state of the Art" functional associated to a pure Slater determinant state and extended by replacing the pure state one-body density (with $\rho^2=\rho$) by more general densities with $\rho=\sum_i|\varphi_i\rangle n_i\langle\varphi_i|$. in the following, ρ_0 denotes the density that minimizes $\mathcal{E}_{\rm MF}[\rho]$. Note that, if we assume that any local density can be obtained from a Slater determinant (N-representability), any other density should verify:

$$\mathcal{E}_{\rm MF}[\rho_0] \;\leq\; \mathcal{E}_{\rm MF}[\rho]$$

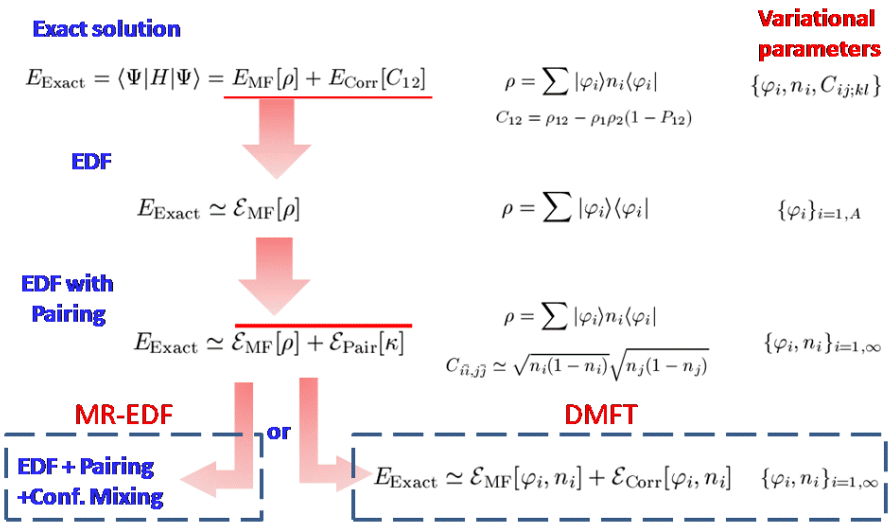

FIG. 14: *Illustration of the "standard" method based on the SR-EDF + MR-EDF used nowadays to incorporate correlations in functional theories. The idea behind DMFT is to try to incorporate correlations beyond the SR-EDF using the one-body density matrix (or equivalently the natural orbitals and occupation numbers) as a variational quantity.*

as depicted in figure 15

- A second natural hypothesis is to assume that the DMFT functional identifies with $\mathcal{E}_{\rm MF}$ when the variation is restricted to Slater determinants. This implies

$$\mathcal{E}_{\rm cor}[\rho^2 - \rho = 0] = 0. \quad \text{or} \quad \mathcal{E}_{\rm cor}[\{n_i = 0, 1\}, \varphi_i] = 0. \tag{232}$$

With this simple hypothesis, currently used functionals might be seen as a more general functional restricted to a specific class of densities. From the additional contribution $\mathcal{E}_{\rm cor}$, we do aspect to gain further energy due to internal correlations like pairing, configuration mixing... For instance, SR-EDF functionals where pairing is included might already be seen as a DMFT functional. In particular, the pairing functional (230) verify all hypothesis described above.

FIG. 15: *Illustration of the strategy proposed to design a DMFT for nuclei starting from the SR-EDF approach restricted to Slater determinants. Assuming simple hypothesis to design density matrix functional (DMF), actual SR-EDF restricted to Slater determinants (dashed blue curve) can be interpreted as the DMF (solid curve) restricted to densities verifying $\rho^2 = \rho$. When the variation is performed over a larger class of one-body density matrices, additional energy is expected to be gained.*

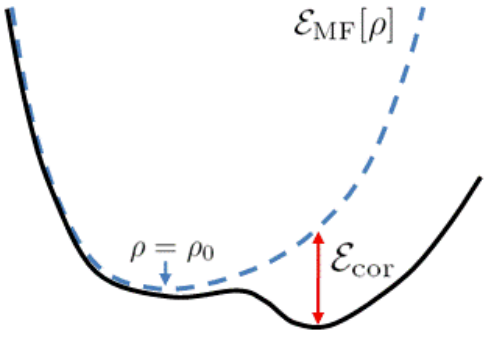

3. Illustration in the two level Lipkin model

The descriptive power of DMFT is illustrated here in the two-level Lipkin model (H. J. Lipkin, 1965). In this model, the Hartree-Fock (HF) theory fails to reproduce the ground state energy

whereas configuration mixing like Generator Coordinate Method (GCM) provides a suitable tool (Ring and Schuck, 1980; Severyukhin *et al.*, 2006). Therefore, the two-level Lipkin model is perfectly suited both to illustrate that DMFT could be a valuable tool and to provide an example of a functional for system with a "shape" like phase-transition. In this model, one considers N particles distributed in two N-fold degenerated shells separated by an energy ε. The associated Hamiltonian is given by

$$H \;=\; \varepsilon J_0 - \frac{V}{2}(J_+J_+ + J_-J_-),$$

where V denotes the interaction strength while J_0, $J_\pm$ are the quasi-spin operators defined as

$$J_0 \;=\; \frac{1}{2}\sum_{p=1}^{N}(c^\dagger_{+,p}c_{+,p} - c^\dagger_{-,p}c_{-,p}), \qquad J_+ = \sum_{p=1}^{N} c^\dagger_{+,p}c_{-,p},$$

and $J_- = J_+^\dagger$. $c^\dagger_{+,p}$ and $c^\dagger_{-,p}$ are creation operators associated with the upper and lower levels respectively. Due to the specific form of the Lipkin Hamiltonian , ρ simply writes in the natural basis as

$$\rho \;=\; \sum_{p=1}^{N}\Big\{|\varphi_{0,p}\rangle n_0\langle\varphi_{0,p}| + |\varphi_{1,p}\rangle n_1\langle\varphi_{1,p}|\Big\}$$

with $n_1 = (1-n_0)$. Introducing the angle α between the state $|-,p\rangle$ and $|\varphi_0,p\rangle$, leads to the following mean-field functional (Lacroix, 2009)

$$\mathcal{E}_{\rm MF}(\{\varphi_{i,p},n_i\}) = \mathcal{E}_{\rm MF}(\alpha,n_0) = -\frac{\varepsilon}{2}N\Big\{\cos(2\alpha)(2n_0-1) + \frac{\chi}{2}\sin^2(2\alpha)(2n_0-1)^2\Big\}. \qquad (233)$$

where $\chi = V(N-1)/\varepsilon$. This expression is easily obtained by generalizing the Hartree-Fock case (recovered here if $n_0 = 1$). The main challenge of the method is to obtain an accurate expression for $\mathcal{E}_{\rm cor}$.

To get the functional, clearly identified cases from which properties of the functional could be inferred have been used(Lacroix, 2009), namely the $N = 2$ case and the large N limit. In the two-particles case, the correlation energy can be analytically obtained and reads

$$\mathcal{E}_{\rm cor}^{N=2}(\alpha,n_0) \;=\; -2V\Big\{\sin^2(2\alpha)n_0(1-n_0) + \big(\sin^4(\alpha)+\cos^4(\alpha)\big)\sqrt{n_0(1-n_0)}\Big\}. \qquad (234)$$

A simple extension of the $N = 2$ case for larger number of particles is to assume that each pair contributes independently from the others leading to $\mathcal{E}_{\rm cor}^{N} = [N(N-1)/2]\,\mathcal{E}_{\rm cor}^{N=2}$. However, such a simple assumption leads to a wrong scaling behavior in the large N limit. Indeed, in this case, $\mathcal{E}_{\rm cor}^{N} \propto N^2$ as N tends to infinity while a $N^{4/3}$ scaling is expected (Dusuel and Vidal, 2004). To obtain the correct limit, a semi-empirical factor $\eta(N)$ can be introduced such that

$$\mathcal{E}_{\rm cor}^{N\geq 3}(\alpha,n_0) = \eta(N)\frac{N(N-1)}{2}\mathcal{E}_{\rm cor}^{N=2}(\alpha,n_0), \qquad (235)$$

with $\eta(N) = cN^{-2/3}$. The value $c = 1.5$ has been retained using a fitting procedure. Examples of results obtained by minimizing the functional given by Eqs. (233) and (235) are shown in Fig. 16 for different particle numbers and interaction strengths. In all cases, a very good agreement, much better than the HF case is found.

4. Functional theory for pairing with finite-size corrections

Functional theories that includes pairing are generally inspired from the BCS or HFB framework. In this case, one directly starts from functional of occupation numbers as already illustrated by Eq. (230). This approach suffers however from the same limitation as BCS and/or HFB case. The theory generally predict the absence of pairing correlation below a certain residual interaction threshold while it is expected to exist for any interaction strength. In nuclei, EDF predicts

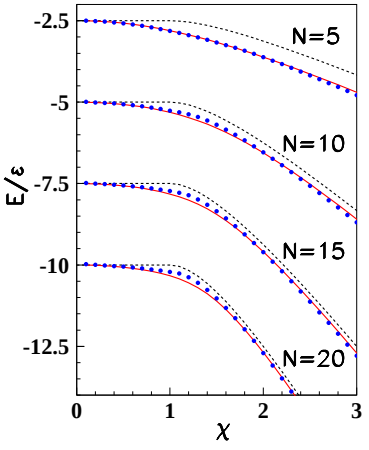

FIG. 16: *Exact ground state energy (solid lines) displayed as a function of χ for $N = 5$ to 20 resp. from top to bottom. In each case, the corresponding HF (dashed line) and DMFT (filled circle) minimum energy are shown. The DMFT calculation is performed using the mean-field and correlation energy resp. given by Eq. (233) and Eq. (235) with $\eta(N) = 1.5\ N^{-2/3}$ (Adapted from (Lacroix, 2009)).*

for instance no pairing correlations for doubly magic nuclei due to the large single-particle gaps. Several methods have been proposed to improve the pairing description like the Lipkin-Nogami method, RPA correction or Kamlah expansion. Alternatively, it is expected that functional based on variation after projection provides a suitable framework. We have however shown previously that projection made through MR-EDF is ill defined. Recently, we have proposed a new functional approach based on DMFT that correct the BCS functional and includes the effect of projection directly (Lacroix and Hupin, 2010).

The new functional approach was tested on the "picket fence" pairing Hamiltonian for which the exact solution is available:

$$H = \sum_i \varepsilon_i (a_i^\dagger a_i + a_{\bar{i}}^\dagger a_{\bar{i}}) - g \sum_{i,j} a_i^\dagger a_{\bar{i}}^\dagger a_{\bar{j}} a_j. \tag{236}$$

As an illustration, results obtained with the standard BCS, and projected BCS [PBCS] frameworks when the projection is made before (Variation After Projection [VAP]) or after the variation (Projection After Variation [PAV]) are shown in figure 17. The projection clearly improves the description of correlation and is almost indistinguishable from the exact result when VAP is performed.

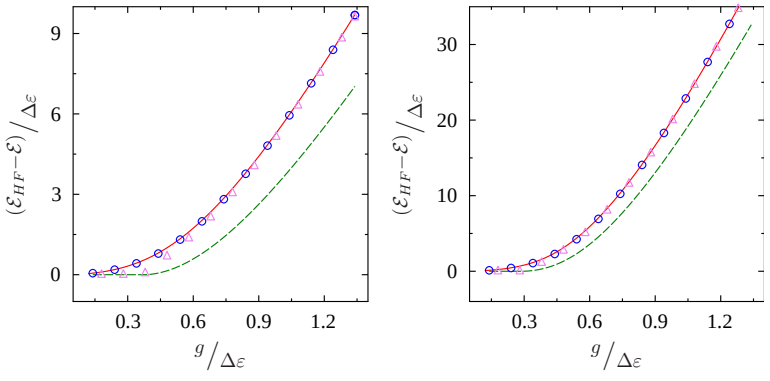

FIG. 17: *Difference between the exact total energy and the Hartree-Fock energy (solid line) obtained in the picket fence Hamiltonian with constant level spacing $\Delta\varepsilon$ for $A = 8$ and $A = 16$ particles. In both case, the BCS (dashed), PAV (open triangle) and VAP (open circles) results are displayed.*

The strategy we have followed to improve the BCS theory is to directly start from the projected state:

$$|N\rangle \equiv \frac{1}{\sqrt{N!}} \left(\sum_i x_i a_i^\dagger a_{\bar{i}}^\dagger \right)^N |-\rangle, \tag{237}$$

and directly write the energy as a functional of the natural orbitals and occupation numbers of this state.

Here $\{a_i^\dagger, a_{\bar{i}}^\dagger\}$ denotes pairs of time-reversed states. It could easily be shown that this state can be obtained by projection of the BCS state, $|\mathrm{BCS}\rangle = \prod(1 + x_i a_i^\dagger a_{\bar{i}}^\dagger)|0\rangle|-\rangle$, onto good particle number $A = 2N$. Note that here N denotes the number of pairs. The PBCS energy for the Hamiltonian (236) reads

$$\frac{\langle N|H|N\rangle}{\langle N|N\rangle} \equiv \mathcal{E}(n_i, C_{ij}) = 2\sum_i \varepsilon_i n_i - g\sum_{ij} C_{ij}, \tag{238}$$

where n_i and C_{ij} are the occupation probabilities and correlation matrix elements defined through

$$n_i \;=\; \frac{\langle N|a_i^\dagger a_i|N\rangle}{\langle N|N\rangle}, \quad C_{ij} = \frac{\langle N|b_i^\dagger b_j|N\rangle}{\langle N|N\rangle}. \tag{239}$$

According to the definition (237), n_i and C_{ij} and therefore $\mathcal{E}(n_i, C_{ij})$ can eventually be written as an explicit functional of the $\{x_i\}$ parameters, which turns out to be too complicated for a direct use as variational parameters. After tedious manipulation, it has been shown in ref. (Lacroix and Hupin, 2010), that these parameters can approximately be written as a functional of the $\{n_i\}$ through:

$$|x_i|^2 \;\simeq\; \left(\frac{n_i}{1-n_i}\right)(a_0 - a_1 n_i) \tag{240}$$

with

$$a_1 \;=\; \frac{1}{N}\left(1 + s_2 + s_2^2 + \cdots + s_2^{N-1}\right) = \frac{1}{N}\frac{1-s_2^N}{1-s_2} \tag{241}$$

and

$$a_0 \;=\; 1 + \frac{(s_2 - s_3)}{N}\left(1 + 2s_2 + \cdots + (N-1)s_2^{N-2}\right) = 1 + (s_2 - s_3)\frac{\partial a_1}{\partial s_2}, \tag{242}$$

and $s_p = 1/N\sum n_i^p$. With these expressions, we can now write the correlation as a functional of single-particle occupancies:

$$C_{ij} \;=\; \sqrt{n_i(1-n_i)n_j(1-n_j)} \times \frac{\sqrt{(a_0 - a_1 n_i)(a_0 - a_1 n_j)}}{\{a_0 - a_1(n_i + n_j - n_i n_j)\}}. \tag{243}$$

The present functional, based on the PBCS trial state, corresponds to a generalization of the BCS ansatz that approximately account for particle number conservation. The BCS limit is obtained for $a_0 = 1$ and $a_1 = 0$ leading to the well know expression $C_{ij} = \sqrt{n_i(1-n_i)n_j(1-n_j)}$. It is worth to mention that a completely different expression is obtained in the weak coupling limit (Hartree-Fock limit) for which $s_2 = s_3 = 1$ and $C_{ij} \to \sqrt{n_i n_j}$.

Illustrations of the new functional accuracy are given in figure 18 where the energy is obtained by a direct minimization of (238) using expression (243). A very good agreement is obtained for any particle number and coupling strength.

By formulating the functional directly using the state projected onto good particle number, we completely change the actual strategy to perform VAP within functional framework. In particular, none of the problems recently encountered in MR-EDF will appear. Application to EDF based on Skyrme effective interaction is underway. First results seem very promising.

5. Discussion on DMFT

The Lipkin and pairing example suggests that DMFT can be a valuable tool for describing the ground state of a many-body system when symmetry breaking plays a significant role. The main challenge is now to propose new functionals able to describe the diversity of ground state

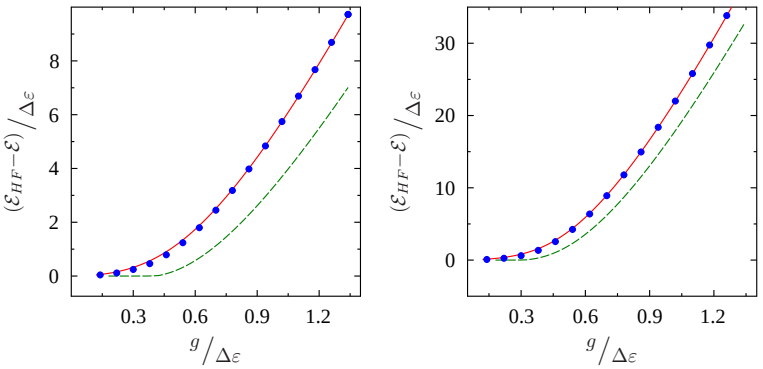

FIG. 18: *Same quantity as in Figure 17 displayed as a function of the coupling strength for the exact (solid line), BCS (dashed line) and the new functional (filled circles) case.*

correlations in nuclei. When the energy can be explicitly written as a functional of the single-particle energies, one can use the Legendre transformation technique (Bertolli and Papenbrock, 2008; Papenbrock and Bhattacharyya, 2007) to get the functional of occupation probability. Another strategy is to directly propose a functional form as it is illustrated in the Lipkin model. For instance, functional dedicated to pairing correlations are being now revisited along this line.

Functional of the one-body density matrix might eventually also break some symmetries of the underlying Hamiltonian. Indeed, the use of symmetry breaking method is certainly a way to provide simpler functional than if no symmetry are broken. the price to pay might be to not be able anymore to restore the symmetry unless a clear theoretical framework is proposed to do so.

E. Summary and discussion

The EDF is nowadays accepted as one of the most powerful tool able to describe in a unique framework the many facets of nuclei. The international community is now trying to organize itself around a unified description of nuclei with energy density functional theory (UNEDF, FIDIPRO project). In the mean time, it has been realized recently that many aspects which have been accepted for many years, need to be revisited. This is for instance the case of symmetry breaking and restoration of broken symmetries that are are the heart of current EDF. The recent discussion on pathologies have clearly pointed out some unclear aspects of broken symmetries in functional theory. In the near future, an effort has to be made to clarify these issues. In the mean time, while EDF was developed in close analogy with Hamiltonian theories, from time to time, this theory is more and more following the spirit of a "true" functional theory. This clearly opens new, yet unexplored, perspectives with the possible emergence of a completely new theoretical framework. An illustration has been given here with the possibility to introduce DMFT.

VI. TIME-DEPENDENT ENERGY DENSITY FUNCTIONAL

In this section, the Time-Dependent version of the Energy Density Functional (TD-EDF) is illustrated through different examples. TD-EDF methods have been introduced in nuclear physics more than 30 years ago (Bonche *et al.*, 1976; Bonche, 2000; Goeke and Reinhard, 1982; Koonin, 1980; Negele, 1982; Simenel *et al.*, 2008). However, even today, the application of full three dimensional time-dependent transport theory with all components of the effective interaction consistent with the static case remains computationally very demanding. In the last ten years, several groups have developed TD-EDF computer program without any restriction (Kim *et al.*, 1997; Maruhn *et al.*, 2006; Nakatsukasa and Yabana, 2005; Simenel *et al.*, 2001; Umar and Oberacker, 2006). For a recent review see (Simenel *et al.*, 2008). The possibility to perform time-dependent calculations fully consistent with nuclear structure models is an important step in the development of microscopic transport theories. Similarly to the static EDF case, dynamical approaches can be generically separated into two classes. The first one is the so-called mean-field framework that essentially corresponds to a direct extension of the SR-EDF restricted to Slater determinant trial states. Other transport theories enter into the category of "beyond mean-field" approaches. A brief description of these two classes and the philosophy behind the construction of dynamical theories within a functional approach is made below. Then, several applications of time-dependent EDF are given: collective motion, fusion, transfer and break-up reactions. In each case, successes and failures of mean-field framework will be illustrated and theories beyond mean-field are introduced to provide a correct description of experimental observations.

A. TD-EDF with a single Reference Slater determinant: basic aspects

As discussed in section V.A.1 and V.A.2, time-dependent processes within functional theory are expected to involve functionals much more complex than for the static case. For instance, the time-dependent functional should be highly non local in time. Most of the TD-EDF applications neglect this possible non-locality and enters into the class of the so-called "adiabatic" approximation. Similarly to the static case, Hamiltonian based theories have largely influenced the choice of functionals taken in the time-dependent theory. Similarly to the Hartree-Fock framework extended to the Time-Dependent Hartree-Fock (TDHF), the TD-EDF directly maps the static SR-EDF (restricted in most cases to Slater determinants) as follows. Starting from a one-body density $\rho(t_0)$, the many-body evolution is replaced by the one-body density evolution written as:

$$i\hbar\frac{\partial}{\partial t}\rho = [h(\rho),\rho] \tag{244}$$

where $h[\rho] \equiv \partial\mathcal{E}_{SR}(\rho)/\partial\rho$ denotes the mean-field Hamiltonian. Again, although this approach is traditionally called Time-Dependent Hartree-Fock, it should not be confused with TDHF derived from a two-body Hamiltonian (section III). At least because the parameters of the effective vertex are directly adjusted to experimental observations, EDF incorporates much more correlations than a pure Hartree-Fock theory. It is easy to verify that the unitary evolution (244) preserves the relation $\rho^2 = \rho$ along the path. Therefore, if initially the density is associated to a pure Slater determinant $|\Phi(t_0)\rangle = \mathcal{A}(\{\varphi_\alpha(t_0)\})$, this remains valid at any time. As a consequence, the concept of auxiliary state is automatically transposed to the time dependent EDF. At all time, the one-body density writes $\rho(t) = \sum_\alpha |\varphi_\alpha(t)\rangle\langle\varphi_\alpha(t)|$. Its evolution can be replaced by the set of coupled self-consistent evolutions: $i\hbar\partial_t|\varphi_\alpha\rangle = h(\rho)|\varphi_\alpha\rangle$ which could be integrated using standard techniques (Simenel *et al.*, 2008).

One of the ultimate goal of a time-dependent functional theory based on the local one-body density is to provide a description of the evolution where the local one-body density matches the exact density along the dynamical path. Many experimental observations can be understood through the evolution of local one-body quantities that only require $\rho(\mathbf{r},\mathbf{r})$. TD-EDF obtained by a direct mapping of the static SR-EDF has met some interesting successes in the description of such observables. For instance, mean frequencies of giant resonances or nucleus-nucleus potentials extracted from a mean-field approach, discussed respectively in section VI.C and VI.D, are in very good agreement with the experimental ones. It should however be kept in mind that these agreements can partially be attributed to the static EDF powerfulness. For instance, the collective frequency can be understood as the curvature of a constrained EDF along a given deformation

(the case of monopole resonance is illustrated in Fig. 9). Similarly, nucleus-nucleus potentials can roughly be understood in the frozen density approximation. This mainly reflects the balance between Coulomb and nuclear part of the effective interaction, on one side, and the density profile of each partner of the collision, on the other side. Both are properly treated in the static EDF. Still, it is quite amazing that these aspects come out naturally while some of them have not been used to constraint the static EDF. For instance, while only the monopole vibration which is connected to the incompressibility modulus is used as a constraint from dynamics, collective frequencies are properly predicted for other multipoles.

Unfortunately, the predicting power of the simple approach described here is rather limited. Nuclear dynamics reflect a fantastic diversity. Even though some aspects can sometimes be understood with a surprising simplicity, most often, careful analysis of experiments uncover rather complex phenomena. Mean-field theories generally catche simple aspects but badly miss the complexity.

B. Beyond mean-field theory in time-dependent transport theory

Similarly to the static EDF case, a second level of functional theory also called "beyond mean-field" is introduced to describe these complex phenomena. The strategy used for this second level significantly differs from the static one based on configuration mixing. Functional theories beyond the first SR-EDF level are generally guided by the different theories, introduced in section IV, by replacing the bare interaction by effective vertex in different channels. Then, the solution retained depends on the goal:

- In most cases, the aim is to properly describe only one-body observables. The difficulty is that other degrees of freedom that are not described by the one-body density affect the one-body dynamics. To avoid the explicit treatment of these extra degrees of freedom, a closed equation for the one-body density is used where the effect of surrounding complex degrees of freedom are approximately accounted for. The spirit in that case is the same as the one used in Open Quantum System (section II) and the resulting equation resembles the Extended TDHF one (section IV.E). Such functional has marked differences from the original mean-field level (i) The resulting theory is a functional theory of the one-body density matrix closer to the DMFT presented in section V.D.1. Accordingly, the use of an auxiliary Slater determinant state is not possible anymore. (ii) At a given time t, the kernel entering in the density evolution depends a priori on the full history of the density from time t_0 to t. It is therefore highly non-local in time and enters the class of non-adiabatic functionals.

- The importance of configuration mixing in nuclear structure studies underlines the fact that a nucleus Many-Body wave-function can hardly be described by a single Slater determinant. Multi-Reference EDF, used in the static case, can hardly be extended to the dynamical case at least due to its numerical complexity. Nevertheless, assuming that the initial fluctuations in one-body space induced by the configuration mixing are the main effect on the dynamic, a theory similar to the Stochastic Mean-Field theory presented in section IV.F.3 has been introduced. This theory, directly transposed to the functional case, turns out to be rather effective to catch the physics of fluctuations in collective space without solving explicitly a two-body problem.

- Finally, when not only one-body observables but also two-body observables are of interest, new functional theories are proposed. In that case, similarly to the TDDM theory (equation (IV.C)), not only the one-body density but also the two-body correlation matrix is explicitly followed in time.

The introduction of theories beyond the mean-field level is rather empirical but rather efficient as will be illustrated in the following. In particular, while theories presented in section IV have generally clear physical interpretation depicted in Fig. 6, effects beyond TDHF are present in both levels of TD-EDF. Still, the different examples given below will show that the introduction of a second level beyond mean-field significantly improves the description of physical phenomena.

C. Collective motion in nuclei

Giant resonances (GR) in nuclei, also called phonons, reflect the capability of a complex many-body system to self-organize into a rather simple collective motion. This effect is shared with many other mesoscopic systems such as zero sound phonons in helium-3 fluid or plasmons in metallic clusters (Bertsch and Broglia, 1994; Chomaz, 1996). There exists a large diversity of GR in nuclei depending on their multipoles and on the fact that proton/neutron are moving in phase (isoscalar) or in opposite phase (isovector). A complete discussion of the GR richness could be found in ref. (Harakeh *et al.*, 2001). Here, I will concentrate on the generic properties of a collective mode.

Experimentally, GR are probed by exciting the nucleus with an external perturbation (for instance a nucleus passing by). In a time-dependent microscopic approach, an initial perturbation is applied to the system. Its response to the perturbation is then followed in time. An illustration of the nucleus time evolution after a dipole boost is given in figure 19. The response function corresponding to the Fourier transform of the evolution is generally used to understand the GR features.

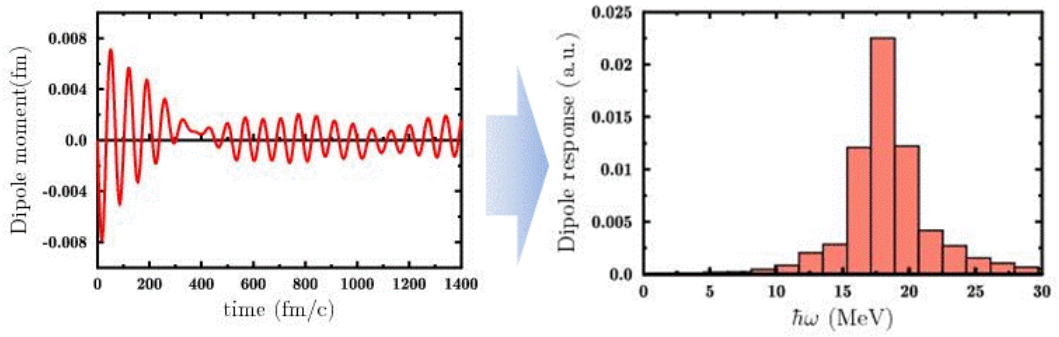

FIG. 19: *Left: Time evolution of the dipole moment in ^{40}Ca obtained in a mean-field approach where the proton and neutrons have been boosted in opposite direction initially (dipole boost). Right: The Fourier transform of the time evolution gives access to the Isovector Giant Dipole Resonance (GDR) response.*

A GR is usually characterized by a mean energy and a width. An example of response function of the Giant Quadrupole Resonance (GQR) in lead deduced from $^{208}\mathrm{Pb}(p,p')$ experiment (Lisantti *et al.*, 1991) is displayed in Fig. 20. While the experiment presents two spread bumps respectively around 11 and 14 MeV, mean-field calculations lead to a single highly collective narrow peak around 12 MeV (Lacroix *et al.*, 2001). While the mean energy of the resonance is globally well understood at the mean-field level, the width often reflects the coupling of one-body degrees of freedom with more complex internal excitations that could not be treated at the first level of TD-EDF. Fig. 20 reveals that the width alone is not sufficient to characterize the complexity in nuclear response especially with the appearance of fine structure on top of a global spreading.

1. Unraveling different scales in the response of nuclei

In order to get deeper insight in the nuclear response, a technique similar to image processing using wavelet analysis has been proposed in ref. (Lacroix and Chomaz, 1999). The original aspects of the method is to define a global quantity, denoted by $K(\delta E)$ and called entropy index, that focus on fluctuations at various scales of energy and changes abruptly when a physical scale is reached. Technical details are given in ref. (Lacroix and Chomaz, 1999; Lacroix *et al.*, 2000). An illustration of the entropy index evolution as a function of energy scale is given in Fig. 21 for the GQR response of $^{208}\mathrm{Pb}$ deduced from the (e,e') and (p,p') experiments. The entropy index method provides additional information compared to previously analysis of fine structure. First, up to now, the comparison of both experimental probes presented in figure 21 was very qualitative and most of the time limited to the comparison of peaks position. The fact that both curves perfectly

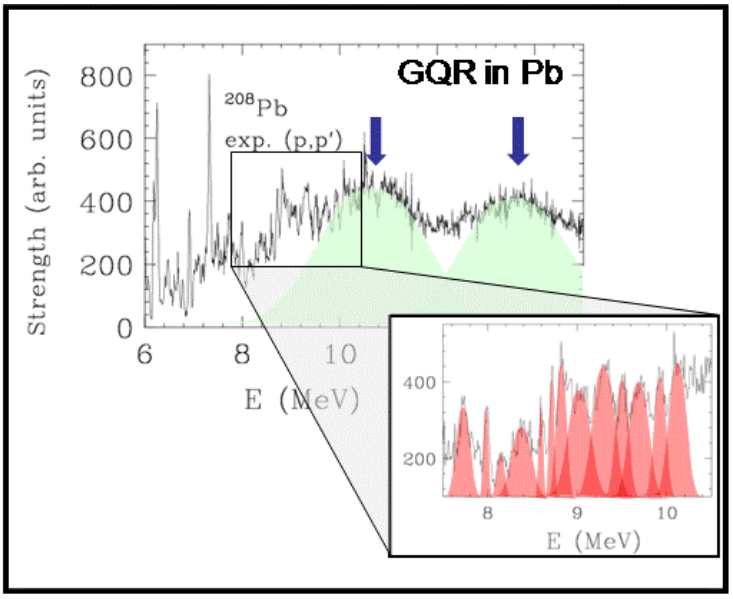

FIG. 20: *Giant quadrupole response deduced from inelastic proton scattering (Lisantti* et al., *1991). In this experiment the resolution is of the order of 50 keV. A focus on the collective energy region reveals fine structure at very small scales, which has also been observed by means of electron scattering experiments(Schwierczinski* et al., *1975).*

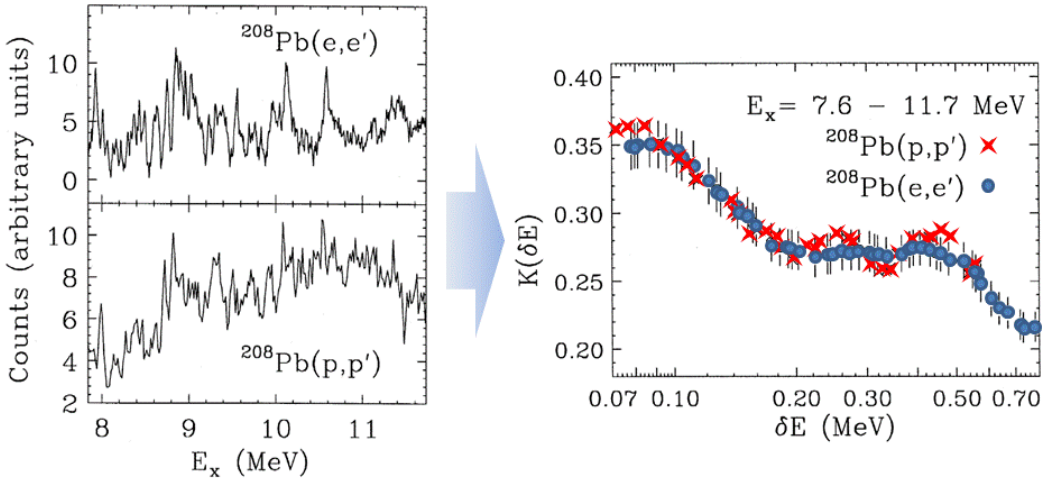

FIG. 21: *Left: Comparison between the GQR response obtained from the* (e, e') *(top) and* (p, p') *(bottom) experiment. In the former case, the high-resolution part of the experimental spectrum is limited to* $E_x = 7.6 - 11.7$ *MeV. Right: Evolution of the entropy index as a function of the energy scale for the* (e, e') *(circles) and* (p, p') *(crosses) case (adapted from (Lacroix* et al., *2000)).*

superimpose points out that the same information is contained in the two spectra. Second, with the help of wavelets analysis, physical energy scales around 125 keV and 460 keV associated to sudden jump of $K(\delta E)$ have been extracted. The analysis has been extended to a wider range of energy revealing an additional scale around 1.1 MeV. The method has been recently improved to provide two dimensional imaging of the GR (Shevchenko *et al.*, 2004, 2009) and essentially has confirmed the appearance of several scales of interest.

2. Physical interpretation of the Giant Resonance Fragmentation

As illustrated in figure 20 and 21, the response function of a nucleus is highly fragmented with well defined energy scales. This fragmentation signs the dissolution of a well ordered motion into a disordered almost chaotic movement of increasing complexity internal degrees of freedom. Several phenomena contribute to the width and more generally to the fragmentation of GR (Lacroix *et al.*, 2004a):

- **Landau fragmentation:** GR corresponds to a coherent superposition of particle-hole (p-h) excitations. When many p-h states have energies close to the collective energy, this might induce a fragmentation called Landau fragmentation (Bertsch and Broglia, 1994). This effect is properly accounted for in a mean-field microscopic method. This is best illustrated in the small amplitude limit of equation (244) (Random-Phase Approximation [RPA] (Ring and Schuck, 1980)) where the small variation of the density, denoted by $\delta\rho$, is directly decomposed onto p-h states. An illustration of Landau damping is given in figure 19 with the beating of several collective modes with close energy.
- **Evaporation width:** due to the high energy of GR, well above the neutron or proton emission threshold, particle are evaporated while the nucleus surface oscillates. The finite lifetime of particle states is associated to a width (of the order of few hundreds of keV) that smooths the GR response function. The evaporation process is automatically included in time-dependent approaches solving eq. 244 or equivalently when the RPA is directly solved in the continuum.
- **Coupling to 2p-2h states:** p-h states represent a small fraction of the possible states on which the nucleus wave-function can be decomposed. As was illustrated in section IV, the Born term initiates the departure from the single-particle. In the small amplitude limit, this term reflects the coupling between p-h states and 2p-2h states. More generally, the BBGKY hierarchy (section IV.B) gives the feeling that a hierarchy exists in the importance of many-body states on which the nucleus wave-function decomposes, i.e. p-h, 2p-2h, 3p-3h ... This hierarchy is indeed empirically verified. For instance, there is no need to incorporate three-body states to understand the fragmentation of the GQR in Fig. 20. Coupling to 2p-2h is properly treated if the Born term is included in the theory. In the Hamiltonian case, this is true for the Extended TDHF and more generally with TDDM based theory. At the functional level, effects of 2p-2h coupling has been incorporated consistently in the EDF framework along the line of Extended TDHF in ref. (Lacroix *et al.*, 1998) at zero and finite temperature. However, the coupling to 2p-2h is strongly suppressed at zero temperature due to Pauli blocking and is insufficient to explain the strong fragmentation of GR.
- **Coupling to p-h $\otimes$ phonon:** A more efficient way to damp out a GR built on top of the nucleus ground state is to consider two-body states that are themselves constructed from a collective excitation of the nucleus, this states are generally called p-h$\otimes$phonon states. According to simple energetic consideration only collective states at low energy (around 3-10 MeV) might contribute significantly to the fragmentation. States constructed from the low lying 2^+, 3^- and 5^- are the most important. As illustrated below, this coupling is the main source of damping of GR. This effect is also crucial to properly describe single-particle state fragmentation (Bertsch *et al.*, 1983).

3. Understanding damping, fragmentation and fine structure of Giant resonances

Although the precise reproduction of energy scales observed is still under discussion (Shevchenko *et al.*, 2009), the understanding of their physical origin at least up the experimental energy resolution is now rather well understood (Lacroix *et al.*, 2004a).

An illustration of the transport theory beyond mean-field developed in ref. (Lacroix *et al.*, 2000) able to incorporate all effects discussed above is shown in figure 22. In this approach, the one-body density evolves according to:

$$i\hbar\frac{d\rho}{dt} = [h(\rho),\rho] \quad + \quad \underbrace{K(\rho)}_{\text{2p}-\text{2h}} \quad + \quad \underbrace{\delta K(\rho)}_{\text{p}-\text{h}\otimes\text{phonon}} \tag{245}$$

where $K(\rho)$ and $\delta K(\rho)$ plays the role of the Born term and initial fluctuation effects introduced in equation (144) for the Hamiltonian case. To study small amplitude collective motion, Eq. (245)

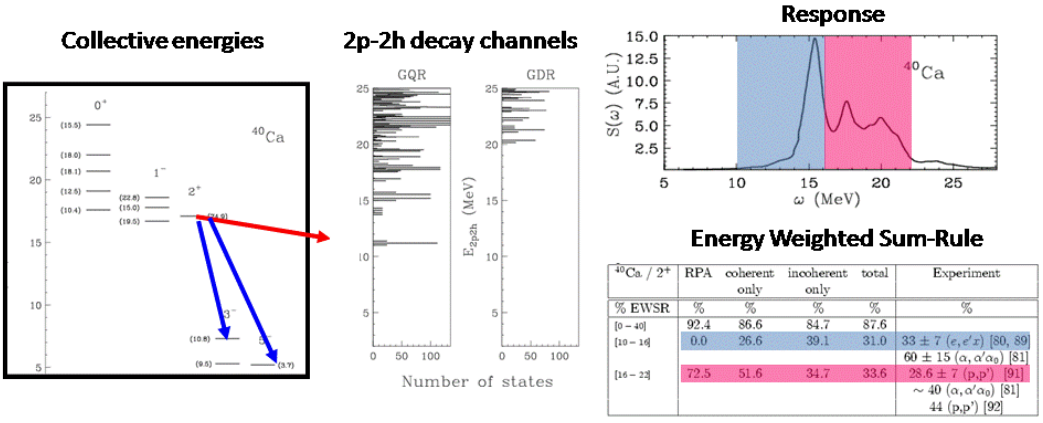

^{40}Ca / 2$^+$	RPA	coherent only	incoherent only	total	Experiment
% EWSR	%	%	%	%	%
[0 – 40]	92.4	86.6	84.7	87.6	
[10 – 16]	0.0	26.6	39.1	31.0	33 ± 7 ($e,e'x$) [80, 89
					60 ± 15 ($\alpha,\alpha'\alpha_0$) [81]
[16 – 22]	72.5	51.6	34.7	33.6	28.6 ± 7 (p,p') [91]
					∼ 40 ($\alpha,\alpha'\alpha_0$) [81]
					44 (p,p') [92]

FIG. 22: *Left: Different collective modes of ^{40}Ca obtained by linearizing the first TD-EDF level. The use of beyond mean-field with Born like term and initial fluctuations leads to a coupling with 2p-2h (blue arrow) and p-h⊗phonon (red arrows) states respectively. Energies of the collective states and 2p-2h states that are coupled to the GQR and GDR are given in left and middle panels respectively. These couplings induce a strong fragmentation of the GQR response presented in the (top-right) panel. Bottom-right: The integrated response (Energy Weighted Sum Rule [EWSR]) for the two intervals* $[10, 16]$ *MeV and* $[16, 22]$ *MeV are compared to the experimental observation. "Coherent only" , "Incoherent only" and "Total" refer respectively to cases where p-h⊗phonon only, 2p-2h only or both couplings are accounted for.*

has been linearized in ref. (Lacroix *et al.*, 2000). As expected, the Born term accounts for the 2p-2h effect on the decay of giant resonances. More surprisingly, the introduction of a statistical ensemble to simulate initial correlations, propagates into the self-consistent mean-field and gives rise after averaging over different initial conditions to a coupling to the p-h⊗phonon. Note that, the direct application of TDDM in the small amplitude limit, i.e. second RPA, also contains these effects. However, eq. 245 is a one-body theory and therefore greatly simplifies the problem. In addition, it has the advantage that the two effects expected to be important add up in a coherent way, while they can hardly be disentangled in second RPA.

This theory has been systematically applied for the monopole, dipole, quadrupole giant resonances in doubly magic nucleus in ref. (Lacroix *et al.*, 2000) and further pursued in ref. (Lacroix *et al.*, 2004a). A special analysis have been made in the GQR of ^{40}Ca and ^{208}Pb where several high precision measurements exist. The case of ^{40}Ca is shown in figure 22 as an illustration. The following important conclusions can be drawn:

- First, correlations beyond mean-field change the mean collective energy up to 1 MeV. This effect is of particular importance for the GMR which is used to extract the incompressibility modulus.
- In all cases, correlations induce a greater fragmentation of the response function compared to the mean-field case. This fragmentation is particularly large in the GQR case (see figure 22[top-right]).
- The main source of fragmentation is the coupling to p-h⊗phonon. When only this coupling is accounted for, a rather good agreement is already obtained. However, in all case the introduction of 2p-2h effects improve further the description of experiments underlying the necessity to treat both (see table in figure 22 and table II).
- Appearance of fine structure is properly described in the present theory. This is illustrated in table II where peaks positions reported in the literature for the ^{208}Pb GQR are compared

(e,e')	(p,p')	(p,p')	Total	coherent only	incoherent only
8.9	8.9	8.9			
9.4	9.3	9.4	9.3	9.3	9.3
9.6		9.6	9.9	9.9	
10.1		10.1	10.2	10.3	
10.7	10.6	10.7	10.7	10.8	
11.5		11.0	11.0	11.3	
					11.9

TABLE II: Experimental energies of peaks position observed in the GQR of ^{208}Pb using (p,p') and (e,e') experiments (Bertrand *et al.*, 1986; Kamerdzhiev *et al.*, 1997; Kuhler *et al.*, 1981). Comparison with calculated fine structures when the coherent only (p-h⊗phonon), incoherent only (2p-2h) or both coherent and incoherent self-energies (Total) are accounted for. The table is taken from (Lacroix *et al.*, 2004a)

to theoretical calculations. Such an agreement is quite amazing in view of the degree of phenomenology in EDF framework.

- A careful analysis shows that positions of peaks is a subtle combination of two-body state energies and couplings matrix elements between these states and the GR under interest.

D. Fusion and transfer reactions

Contrary to Giant resonances, during a reaction between two atomic nuclei, the nuclear many-body system encounters Large Amplitude Collective Motion (LACM). The description of Fusion reactions within a fully microscopic time-dependent EDF framework was a major step forward (Bonche *et al.*, 1976; Negele, 1982). However, it has been very fast realized that the description of Fusion and more generally Deep Inelastic Collisions (DIC) could only be achieved by including beyond mean-field effects into TD-EDF (Goeke and Reinhard, 1982). To underline the complexity of the problem, it is important to realize that, more than 30 years after first TD-EDF application, a complete description of DIC with a fully quantum transport theory is not yet achieved. In view of this complexity and the necessity to describe Heavy-Ion reactions around the Fermi energy, semi-classical models have been preferred during more than twenty years (Ayik and Gregoire, 1988, 1990; Baran *et al.*, 2005; Bertsch and Gupta, 1988; Chomaz *et al.*, 2004).

Here, reactions involving beam energies close to the Coulomb barrier, namely transfer reaction and fusion, are considered. These physical mechanisms are presented schematically in figure 23. For low energy reactions, the de Broglie wavelength becomes comparable to the typical scale of the problem and quantum effects cannot be neglected. Numerous macroscopic models have been developed (see the review (Lacroix, 2002b) and references therein) to describe DIC. However, to get a deeper insight into the reaction mechanism, the use of microscopic theory where internal degrees of freedom are explicitly treated is mandatory. Extensive study of DIC with mean-field EDF have shown that it generally provides a good description of the mean-value of one-body observables: mean number of exchanged particle, mean energy loss, mean angular momentum ... However it completely underestimates fluctuations around the mean value (Koonin, 1980; Negele, 1982). Large theoretical efforts have been made to overcome this difficulty. However, most of the proposed extensions of mean-field were not applied because of formal and/or practical difficulties (see for instance (Lacroix *et al.*, 2004a; Simenel *et al.*, 2008)).

Nuclear reactions around the Coulomb barrier are a perfect test bench for nuclear transport model. In particular, contrary to higher energies, the number of entities involved during the collisions is rather limited (one in case of complete fusion and two in case of transfer without particle emission). In addition, at beam energy close to the Coulomb barrier energy, direct nucleon-nucleon collisions are strongly suppressed and can be neglected. Physically, as the two nuclei approach from

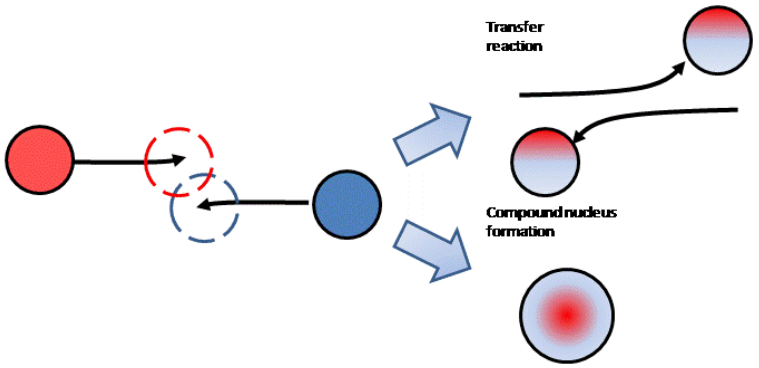

FIG. 23: *Schematic representation of a reaction leading either to a partial exchange of nucleons (transfer reactions) or to the formation of a compound nucleus through the fusion of the collision partners. Here, the possible pre-equilibrium particles is not considered.*

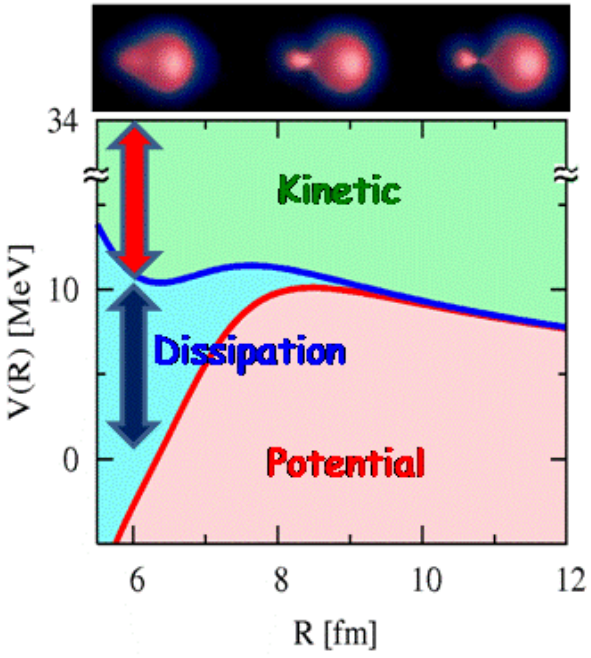

FIG. 24: *Schematic illustration of the energy balance during the approaching phase. During the approaching phase, the initial beam energy is shared between kinetic energy, the potential energy (nuclear + Coulomb) and the dissipated energy that is then transformed into internal excitation.*

each other (approaching phase), nucleons reorganize in time inducing a transfer of the initial relative kinetic energy to internal excitation. This transfer can be understood as a coupling of few collective degrees of freedom (relative distance between the two nuclei, deformation...) to the large set of internal degrees of freedom leading to the onset of dissipation in collective space. Such a picture is schematically represented in figure 24 for the relative distance collective variable. Most often, fusion and/or transfer reactions have been analyzed using macroscopic models having important phenomenological input like nucleus-nucleus potentials, dissipation kernels or diffusion transport coefficients. Recently, our group have mas an effort to connect the microscopic EDF approach to parameters used in macroscopic models (Lacroix, 2002a; Washiyama and Lacroix, 2008).

1. Nucleus-nucleus potential, one-body dissipation and internal excitation from TD-EDF

As in the giant resonance case, the mean-field approximation of TD-EDF is first considered. In this case, the information on the system is contained in the one-body density matrix. The original idea developed first in (Lacroix, 2002a) is to further reduce the information by focusing on few selected collective variables. In the case of fusion, the simplest choice is to focus on the relative distance between nuclei, denoted by R and its canonical conjugated P. Starting from the density evolution, Eq. 244, the evolution of any observable can a priori be written explicitly. This direct estimate and the recognition of specific terms entering in macroscopic models turns out to be rather cumbersome. A different strategy is to directly map the evolution onto a "reasonable" macroscopic equation of motion and verify a posteriori the validity of the approximation. The simplest guess for the relative distance evolution that account for dissipative aspects is

$$\begin{aligned} \frac{dR}{dt} &= \frac{P}{\mu(R)}, \\ \frac{dP}{dt} &= -\frac{dV}{dR} + \frac{1}{2}\frac{d\mu(R)}{dR}\dot{R}^2 - \gamma(R)\dot{R}, \end{aligned} \tag{246}$$

where $V(R)$ and $\gamma(R)$ denote respectively the nucleus-nucleus potential and friction coefficient. In this macroscopic equations, R, $\dot{R}$, P and $\mu(R)$ can directly be computed from TD-EDF. Following the method proposed in ref. (Koonin, 1980) and improved in ref. (Lacroix, 2002a), the nucleus-nucleus potential and one-body friction coefficient have been systematically extracted for different symmetric and asymmetric reactions as well as different beam energies in ref. (Washiyama and Lacroix, 2008; Washiyama *et al.*, 2009b). An example of potential and reduced friction extracted from the ^{40}Ca+^{40}Ca is given in figure 25. From these studies, the following important conclusions

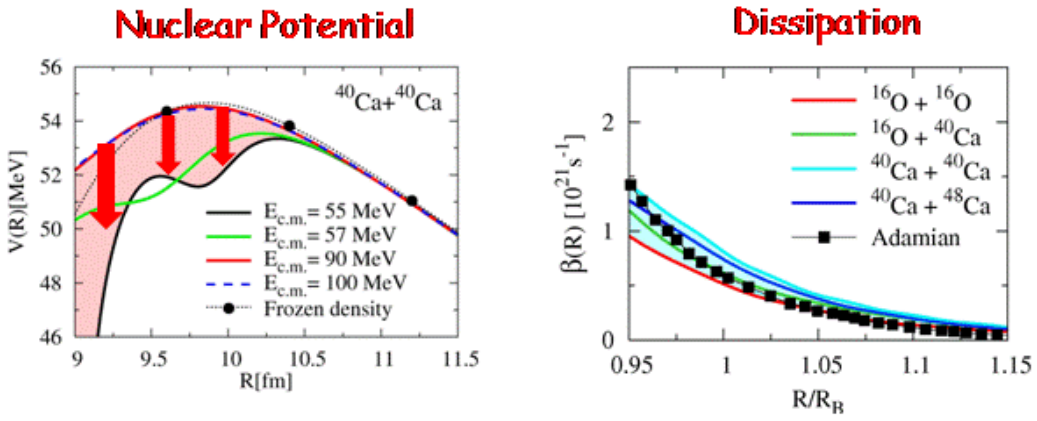

FIG. 25: *Left: Example of nucleus-nucleus potential extracted from TD-EDF for the central ^{40}Ca+ ^{40}Ca reaction. Different curves correspond to different initial center of mass energies. Right: Reduced friction, defined as $\beta(R) = \gamma(R)/\mu(R)$, deduced from the macroscopic reduction of the microscopic dynamics. Each curve corresponds to a different system.*

have been drawn:

- **Nucleus-nucleus potential:**
  - ◇ As expected, the nucleus-nucleus potential identifies with the frozen density (FD) approximation when the center of mass energy is much higher than the Coulomb barrier energy. Indeed, at this energy, nucleons have no time to reorganize. In addition, a good agreement is found with another technique called Density-Constraint TDHF (Umar and Oberacker, 2006).
  - ◇ As the beam energy decreases, the extracted potential deviates from the the FD case and a reduction of the apparent barrier is observed. This reduction which is due to

dynamical effect (i) is consistent with the fusion threshold already extracted from TD-EDF (Simenel and Avez, 2008), (ii) significantly improves the comparison with the barrier height extracted from experimental data.

- **Dissipation:**
  - ◇ The reduced friction coefficient has been systematically extracted showing a rather universal behavior independent of the system considered. The values extracted are in good agreement with previously deduced values of ref. (Adamian *et al.*, 1997). This, in addition with the different remarks made above for the potential, gives good confidence in the macroscopic equation used to reduce the microscopic dynamics.
  - ◇ During the approaching phase, nucleon exchange is the main source of dissipation in TD-EDF.
  - ◇ The internal excitation after the touching of the two nuclei has been estimated and perfectly matches the dissipated energy. This indicates that the dissipated energy can indeed be interpreted as an energy transfered to the internal degrees of freedom leading to excited nucleus.

The present method, based on TD-EDF, is a promising tool to provide physical insight in the fusion process. In addition, it removes some ambiguities in the choice of parameters values used in macroscopic models.

2. Fluctuation of one-body observable from Stochastic Mean-Field

Values extracted previously for nucleus-nucleus potentials and dissipative kernels are consistent with experimental observations and macroscopic input. This is not surprising since both are obtained from the evolution of one-body observables that are expected to be properly described at the mean-field level. However, two important issues have to be clarified:

- dissipation in one-body space is due to a further reduction of the information contained in the complete mean-field evolution to a set of collective variables. However, to any dissipative process, one could a priori associate a fluctuating process consistent with the fluctuation/dissipation theorem. How this fluctuation can be introduced in a mean-field approach is far from being obvious.
- A related question is how to describe the dispersion around the mean trajectory? Fluctuations of one body observables correspond to two-body objects that are out of the scope of a functional theory based only on the one-body density.

The Stochastic Mean-Field theory introduced in section IV.F.3 (Ayik, 2008) for the Hamiltonian case provides clues (i) to understand how fluctuations can be properly introduced (ii) to improve the description of diffusion process in collective space. This theory has recently been applied to fusion and transfer reactions within the EDF approach in ref. (Ayik *et al.*, 2009; Washiyama *et al.*, 2009a). In SMF, fluctuations are introduced at initial time to mimic the effect of initial correlation on the dynamics. The initial density is then replaced by a statistical ensemble of one-body density, each of them being associated to a Slater determinant. Performing the same macroscopic reduction as above, central collisions leading to fusion have been mapped to a one-dimensional macroscopic Langevin evolution on the relative distance R between the two nuclei (Ayik *et al.*, 2009):

$$\frac{d}{dt}P^{\lambda} \;=\; \frac{d}{dR}V(R^{\lambda}) - \gamma(R^{\lambda})\dot{R}^{\lambda} + \xi_P^{\lambda}(t). \tag{247}$$

where λ is a label associated to the initial density sampling. $\xi_P^{\lambda}(t)$ is a Gaussian random force acting on the relative motion reflecting stochasticity in the initial value. This fluctuating part leads to diffusion in collective space which can be approximated by

$$\overline{\xi_P^{\lambda}(t)\xi_P^{\lambda}(t')} \simeq 2\delta(t-t')D_{PP}(R) \tag{248}$$

where $D_{PP}(R)$ denotes the momentum diffusion coefficient. The latter term is nothing but the one that is missing in the original theory and is of primer importance to properly describe observables

fluctuations. The SMF theory has been first applied to fusion reactions in ref. (Ayik *et al.*, 2009). Using a semi-classical expansion of the one-body density, an explicit form of both the dissipation kernel γ and the diffusion coefficient D_{PP} has been obtained and evaluated. This work was the first estimation of diffusion transport coefficient from a fully microscopic theory. In addition, the use of a semi-classical approximation was particularly useful (i) to show that the friction and fluctuations obtained in that way are consistent with the fluctuation/dissipation theorem (ii) to further underline the importance of nucleon exchange in the dissipation. In particular, expressions similar to the nucleon exchange model ones (Feldmeier, 1987) have been obtained. The case of fusion reactions, although quite interesting cannot serve as a quantitative test of the theory. Indeed, even if the dispersion in relative kinetic energy is enhanced in the entrance channel, the reaction leads to the formation of a compound nuclei where all the energy will be transformed into excitation.

Transfer reactions are a much more drastic benchmark. In that case, the results of the reactions are the two nuclei with varying masses due to event by event fluctuations. Fragment mass distributions deduced from Heavy-Ion reactions have been extensively studied. It is seen that the dispersion in mass scales approximately with the average number of exchanged nucleons. While mean-field properly describes the latter, it miserably fails to account for the dispersion. This phenomenon is rather well understood in macroscopic models but has not been yet reproduced microscopically. To address this issue, we have considered head-on collisions below the Coulomb barrier. In that case, nuclei approach, exchange some nucleons and then re-separate. Similarly to the relative distance case, a macroscopic reduction onto the projectile (resp. target) mass, denoted by A_P^λ (resp. A_T^λ) can be made leading to:

$$\frac{d}{dt}A_P^\lambda = v(A_P^\lambda, t) + \xi_A^\lambda(t), \tag{249}$$

where $v(A_P^\lambda, t)$ denotes the drift coefficient for nucleons transfer. Again, the fluctuating term $\xi_A^\lambda(t)$ is linked to the diffusion in mass through $\overline{\xi_A^\lambda(t)\xi_A^\lambda(t')} = 2\delta(t-t')D_{AA}$. Mass dispersion can then directly be estimated using:

$$\sigma_{AA}^2(t) \simeq 2\int_0^t D_{AA}(s)ds. \tag{250}$$

An illustration of $\sigma_{AA}^2(t)$ evolution for ^{40}Ca+^{40}Ca transfer reactions at different center of mass

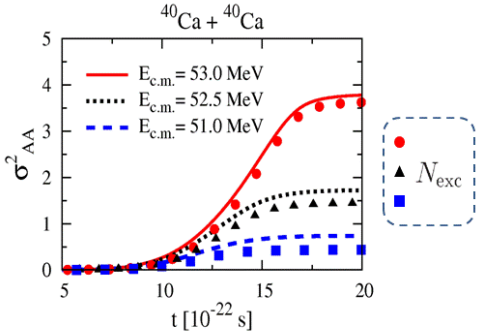

$E_{c.m.}$(MeV)	σ^2_{TDEDF}	N_{exc}	σ^2_{SMF}
51.0	0.004	0.432	0.730
52.5	0.008	1.441	1.718
53.0	0.008	3.634	3.790

FIG. 26: *Left: Evolution of the mass dispersion as a function of time for the central ^{40}Ca+^{40}Ca reaction at three center of mass energies just below the Coulomb barrier. The mass dispersion increases suddenly after the touching and saturates once the two partners of the reaction re-separates. In all cases, the number of exchanged particle evolution is superimposed. Right: Final Mass dispersion in the original TD-EDF (Left) and SMF (Right). In both cases, the mass dispersion is compared to the net number of exchanged particle between the two nuclei (Middle).*

energies is given in Fig. 26 (Left) and compared to the number of exchanged nucleons, denoted by $N_{\rm exc}$. At all center of mass energy, both quantities are very close from each other in agreement

with what is expected experimentally. As a comparison, the final mass dispersion obtained in SMF is compared to the results from the original TD-EDF without fluctuations. As mention above, TD-EDF alone is much smaller than the number of exchanged particle. This was recognized in the 80's as one of the major limitation of mean-field theory. The introduction of SMF approach clearly provides a formal and practical way to cure this problem. This numerical test is a strong support for the validity of the stochastic mean-field approach and clearly opens new perspectives for improving the predicting power of time-dependent microscopic approaches at low beam energy.

E. Nuclear break-up

The last example presented here to illustrate the powerfulness of time-dependent models is the nuclear break-up where a particle of one nucleus is emitted to the continuum due to the presence of a strong short-range attractive nuclear field created by the other nucleus involved in the reaction. This study has been initially motivated by the observation of a specific mechanism in ref. (Scarpaci *et al.*, 1998) called by the author "Towing-Mode". This mechanism is schematically presented in Fig. 27. Experimentally, it has been observed that, when a projectile passes by a target at the

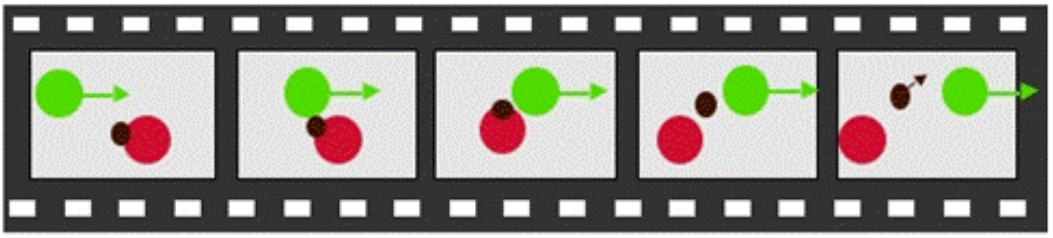

FIG. 27: *Schematic illustration of the towing mode. As the projectile passes by the target, the last bound single-particle state in the target is strongly attracted by the nuclear potential of the projectile but has not the time to be transferred, leading to an emission into the continuum.*

grazing impact parameter and beam energy close to the Fermi energy (20-50 MeV/A), a nucleon of the target can be emitted with rather specific properties: (i) the nucleon is emitted on the same side as the projectile (ii) its velocity is more or less half of the velocity of the projectile, i.e. mid-rapidity emission (iii) it leaves the emitter either in its ground state or in one of its first excited state. An interpretation of this mechanism in terms of incomplete transfer has been immediately proposed and confirmed by theoretical calculations (Lacroix *et al.*, 1999b). During 10 years, experimental investigations conjointly to the development of appropriate models have been made to promote this mechanism at the level of a tool for nuclear structure studies. In particular, spectroscopic factors, configuration mixing and pairing correlations have been investigated using the Towing mode. A summary of recent advances is given below.

1. Time-dependent description of one-nucleon emission

A great advantage of microscopic theories like EDF is that many physical effects are included. It should however be kept in mind that the experimental setup often select specific channels. In order to perform a proper comparison between theory and experiment one should be able to disentangle in the calculation the phenomena that has been selected experimentally. There are two strategy to do so: either the full calculation with all channels is performed and then the specific phenomena are selected a posteriori or channels which are not desired are blocked in the theory not to pollute the signal under interest. In most practical situation, the second option is much easier and has been retained to describe nucleon emission.

The towing-mode is a "gentle" phenomena where one of the least bound nucleon is emitted while the remnant nucleus is left with almost zero excitation. To describe this mechanism, it has been proposed to consider the time evolution of one single-particle wave-function initially in the target

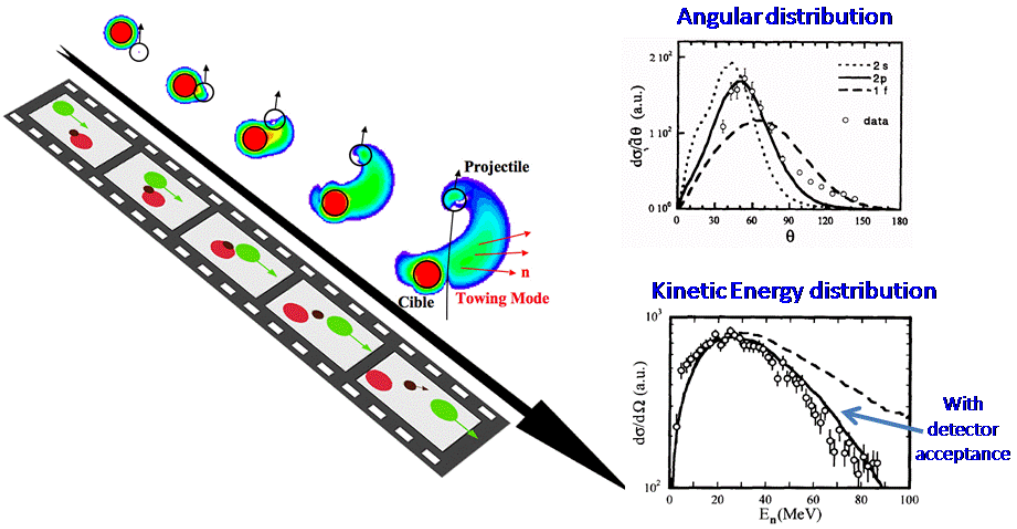

FIG. 28: *Left: Description of the wave-function evolution of the least bound nucleons in the target as the projectile passes by (Adapted from (Lacroix* et al.*, 1999b)). Top-Right: Experimental angular distribution of the nucleon emitted to the continuum during the reaction* $^{40}Ar+^{58}Ni$ *compared to theoretical prediction assuming initially a 2s, 2p or 1f single-particle state. Bottom-Right: Kinetic energy distribution of the nucleon deduced for an emission of a 2p nucleon.*

potential and perturbed by the projectile potential passing close by. The equation of motion for this wave-function reads:

$$i\hbar\frac{d}{dt}\varphi_\alpha(\mathbf{r},t) \;=\; \left\{\frac{\mathbf{p}^2}{2m} + V_T(\mathbf{r}-\mathbf{R}_T(t)) + V_P(\mathbf{r}-\mathbf{R}_P(t))\right\}\varphi_\alpha(\mathbf{r},t) \tag{251}$$

where V_T and V_P correspond to the target and projectile mean-field potentials resp. (most often taken as fixed Wood-Saxon potentials). The centers of mass evolution, $\mathbf{R}_T(t)$ and $\mathbf{R}_P(t)$ are chosen to properly describe peripheral collisions.

An illustration of single-particle wave-function evolution is given in figure 28 (Left). In this figure, the final wave-function separates into three parts: part of the wave-function stays in the initial nucleus, part is transfered to the target while the rest is emitted. From the latter, properties (angular distribution, kinetic energies...) of nucleons escaping the target can be calculated and compared to the experimental distributions (figure 28 (Right)). A perfect agreement is obtained when the nucleon is supposed to be emitted from the $2p$ level which is the last occupied state for a ^{58}Ni. This study has confirmed the intuitive picture of the towing mode phenomena given in Fig. 27 and has shown that the mechanism can be perfectly understood using a rather simple time-dependent approach.

Besides the understanding and description of the towing-mode, figure 28 illustrates that the observed distributions are expected to be sensitive to the quantum properties of the initial state: quantum numbers, initial binding energy, extension of the wave-packet... In view of this sensitivity, the simplicity of the mechanism as well as its high cross-section (of the barn order), the Towing-Mode has been proposed as a tool to infer structure properties of nuclei.

2. Nuclear break-up of one neutron halo nuclei: role of configuration mixing

Exotic nuclei that are produced in new Radioactive Ion Beam (RIB) facilities are a perfect playground to benchmark new experimental methods. The nuclear break-up of ^{11}Be has been studied at GANIL (Fallot *et al.*, 2002; Lima *et al.*, 2007). ^{11}Be is a weakly bound one neutron halo (with neutron separation energy equal to 503 keV). Its description is however more complex than

the previous case. Its ground state is indeed expected to be a mixing between two configurations written as:

$$|^{11}\mathrm{Be} : \mathrm{GS}\rangle \;=\; \alpha|0^+ \otimes 2s_{1/2}\rangle + \beta|2^+ \otimes 1d_{5/2}\rangle \tag{252}$$

where the first configuration stands for a spherical ^{10}Be core surrounded by a $2s_{1/2}$ nucleon while the second is a strongly deformed core ($\beta_2 = 0.74$) coupled to a $1d_{5/2}$ state. The description of such a configuration mixing is a priori beyond the scope of an independent particle framework. However, neglecting the interference between configurations, it could be assumed that the spherical and deformed configurations give independent contributions with probabilities $|\alpha|^2$ and $|\beta|^2$ respectively. With this simple assumption, effect of configuration mixing on nuclear break-up can be simulated by performing two independent single-particle evolutions properly weighted to approximately account for the initial mixing. The final wave-functions of nucleons initially respectively in the $2s_{1/2}$ and $1d_{5/2}$ are presented in figure 29. Experimentally, contributions of the two configurations can also be disentangle by noting that only the emission from the deformed core will be accompanied by γ emission. The experimental setup has thus been designed to provide coincidence measurement between the ^{10}Be, neutrons and γ. Shapes of the emitted neutron kinetic energies distributions when no γ are detected or when γ are observed, are in very good agreement with the calculation assuming respectively a $2s_{1/2}$ or a $1d_{5/2}$ initial wave-function. In addition, by comparing absolute cross-sections between experiment and theory, the mixing probabilities $|\alpha|^2$ and $|\beta|^2$ have been extracted in relatively good agreement with previous estimates (Lima *et al.*, 2007).

3. Probing spatial correlations in nuclei with the nuclear break-up

The ^{11}Be study was the first example pointing out that the nuclear break-up can not only provide information on single-particle properties but also be useful to get information on many-body effects taking place in nuclei. A second type of correlations, namely pairing correlations, has been recently analyzed with the nuclear break-up tool. Due to static and dynamical pairing correlations, short and long range correlations coexist in nuclei (see discussion in section V). Accordingly, very specific spatial correlations between nucleons are expected (Zhukov *et al.*, 1993). The case of the borromean ^{6}He nucleus where two spatial correlations have been predicted, is the subject of strong debate (Assié, 2008). In that case, it is expected that a configuration where the two neutrons are very close in space (the so-called di-neutron conf.) coexists with a configuration where they are far away from each other (the so-called cigar conf.). Two intuitive scenarios (presented in figure 30) have been proposed (i) If the two neutrons are initially close in position, both will feel the strong short range nuclear attraction of the reaction partner and will be emitted simultaneously at small relative angles. (ii) If the two nucleons are far away in r space, only one will undergo nuclear breakup. Then, the other nucleon might eventually be emitted isotropically from the daughter nucleus. Accordingly, large relative angles are expected between the two nucleons transmitted to the continuum in this sequential emission. Contrary to previous cases, a simple independent particle description cannot be used to confirm this intuitive picture. Indeed, since the aim is to probe initial correlations between nucleons, the relevant information on this phenomenon is not only contained in the one-body density matrix but also the two-body correlation C_{12}. Therefore, the transport theory able to describe coincidence experiments should explicitly treat C_{12} in the dynamics. The use of a functional theory based on the TDDM (see section IV.C) appears as a good candidate. However, due to the increase of computational effort and lack of numerical stability, the full TDDM theory cannot directly be applied in full three dimensions within a reasonable computational time. To overcome this difficulty, an approximation guided by the BCS theory has been recently proposed (Assié and Lacroix, 2009). Pairing correlations are expected to play an important role on spatial correlations in ground state nucleus. To reduce the size of the two-body correlation matrix and focus on pairing, it is assumed that the dominant correlations (and two-body interaction matrix elements) are between pairs of time-reversed states, denoted by $\{\alpha, \bar{\alpha}\}$.

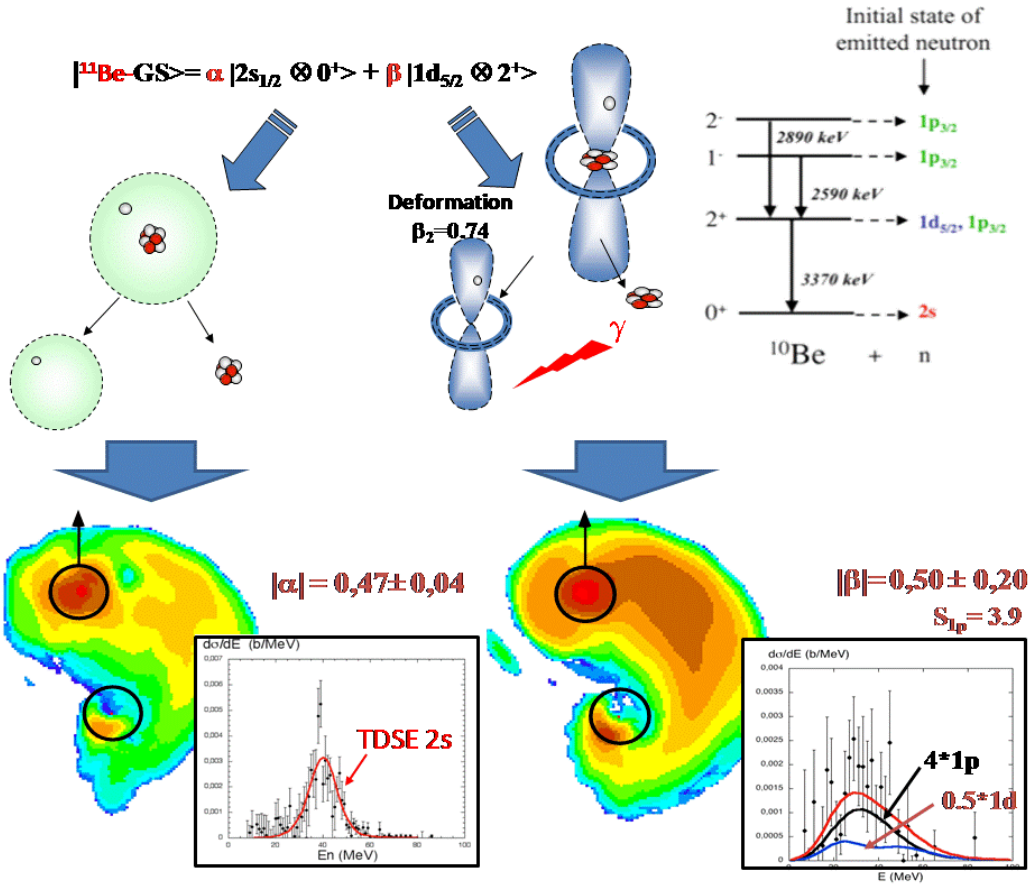

FIG. 29: *To simulate the nuclear break-up ^{11}Be, it is assumed that each configurations of the ground state contributes independently to the particle emission. The wave-functions presented in the bottom corresponds respectively to the result of the Time-Dependent Schrödinger equation assuming a $2s_{1/2}$ wave-function in a spherical mean-field and a $1d_{5/2}$ wave-function in a deformed mean-field. Experimentally, contributions of the two configurations have been disentangled by detecting neutrons in coincidence with γ or by imposing that no γ are detected. Indeed, it is expected that γ can be emitted only in the case of the deformed configuration, or if the neutron comes from the ^{10}Be core leading to a cascade ending with a 3.37 MeV γ. Experimental kinetic energy distribution are systematically compared to theoretical prediction and are found to be in very good agreement with each other. Note that, when γs are observed, the possible contribution of the emission from a 1p state has also been taken into account.*

Then, in the canonical basis where $\rho = \sum_\alpha |\alpha\rangle n_\alpha \langle\alpha|$, the evolution reduces to

$$i\hbar\partial_t|\alpha\rangle = h[\rho]|\alpha\rangle \tag{253}$$

$$\dot{n}_\alpha = \frac{2}{\hbar}\sum_\gamma \Im\left(\mathbf{V}_{\alpha\gamma}\mathbf{C}_{\gamma\alpha}\right) \tag{254}$$

$$i\hbar\dot{\mathbf{C}}_{\alpha\beta} = \mathbf{V}_{\alpha\beta}((1-n_\alpha)^2 n_\beta^2 - (1-n_\beta)^2 n_\alpha^2) + \sum_\gamma \mathbf{V}_{\alpha\gamma}(1-2n_\alpha)\mathbf{C}_{\gamma\beta} - \sum_\gamma \mathbf{V}_{\gamma\beta}(1-2n_\beta)\mathbf{C}_{\alpha\gamma} \tag{255}$$

where $\mathbf{V}_{\alpha\beta} \equiv \langle\alpha\bar{\alpha}|v_{12}^c(1-P_{12})|\beta\bar{\beta}\rangle$, $\mathbf{C}_{\alpha\beta} \equiv \langle\alpha\bar{\alpha}|C_{12}|\beta\bar{\beta}\rangle$ and where the degeneracy of time-reversed states, i.e. $n_\alpha = n_{\bar{\alpha}}$, has been used. The present theory is called TDDM$^{\rm P}$ hereafter.

These coupled equation are much more tractable than the original TDDM theory and can easily be implemented on top of existing 3D TD-EDF codes. Note again that such theory could not

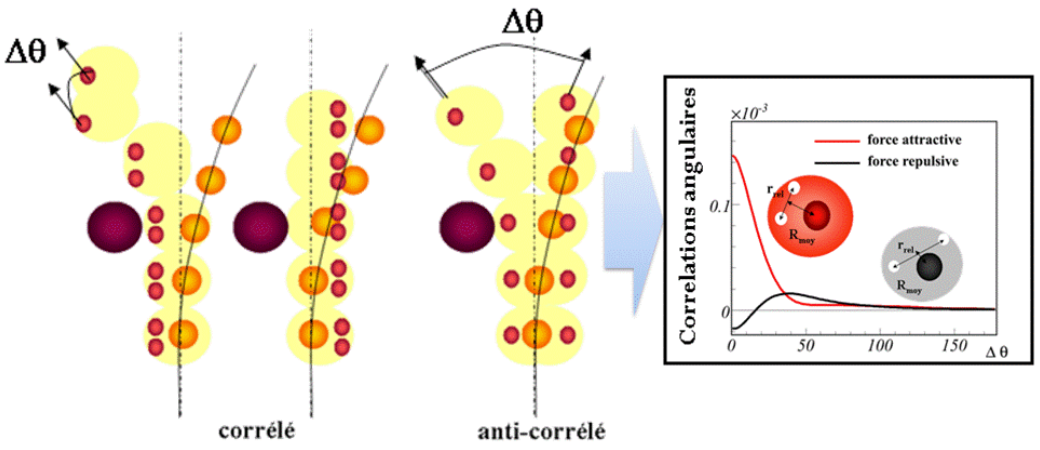

FIG. 30: *Schematic illustration of the two nucleons nuclear break-up for initial nucleons very close in r-space (Left) or far away from each other (Right). According to these scenarios, the relative angles between emitted nucleons are expected to be peaked at zero for the former case while an emission at larger angle is expected in the latter case.*

easily be linked to the TDDM theory derived from a Hamiltonian due to the replacement of the bare interaction by effective two-body interaction v_{12}^c. It is finally worth to mention that TDDM$^{\mathrm{P}}$ not only contains pairing correlation but also account partially for 2p-2h correlation through the Born term. This has important consequences. For instance, while a pure pairing theory based on a quasi-particle vacuum leads to zero correlation energy in doubly magic nuclei, a non-zero correlation has been obtained for instance in ^{16}O (Assié and Lacroix, 2009).

As a test case for the two scenarios, an ^{16}O has been initialized with different initial correlations between the last bound neutrons. Two residual interactions have been chosen, one attractive with strength equivalent with the one retained in standard pairing theories and one repulsive. The former leads to strong spatial correlation of the two last bound nucleon while for the latter a strong spacial anti-correlation is obtained (see figure 31).

Starting from an initially correlated system, the nuclear break-up of two nuclei is simulated by perturbing the nucleus with a time-dependent external potential. Since the information on two-body correlations is explicitly followed in time, final angular correlations of particles emitted in coincidence can be constructed (figure 31-Right). The theoretical prediction confirms the scenario depicted in figure 30. Conjointly to the theoretical investigation, an experiment has been done at GANIL with a high intensity ^{6}He Spiral. The experimental setup as well as the experimental angular correlation are shown in figure 32. The experimental data, which is still being finalized (Assié *et al.*, 2009), supports the strong dominance of neutrons very close from each other. The presence and/or the influence of a cigar configuration seems to be completely absent in the experiment.

F. Summary and discussion

In this section, different physical processes have been discussed: giant resonances, fusion, transfer and break-up reaction. In all cases, the use of a transport model based on mean-field only failed to account for the richness of nuclear dynamics. The strategy most often followed is to start from the mean-field approach and include beyond mean-field components. The choice of these components: pairing, 2p-2h or configuration mixing is most often strongly guided by the observation. Several extensions of mean-field, in each case specifically designed to the physical problem, have been presented here. In all cases, theories have been pushed to provide deep insight in the understanding of experiments. One may regret the absence of a unique framework able to describe all phenomena. However, it should be kept in mind that any of the beyond mean-field approach presented here corresponds to a very large increase of the numerical complexity compared to the original mean-

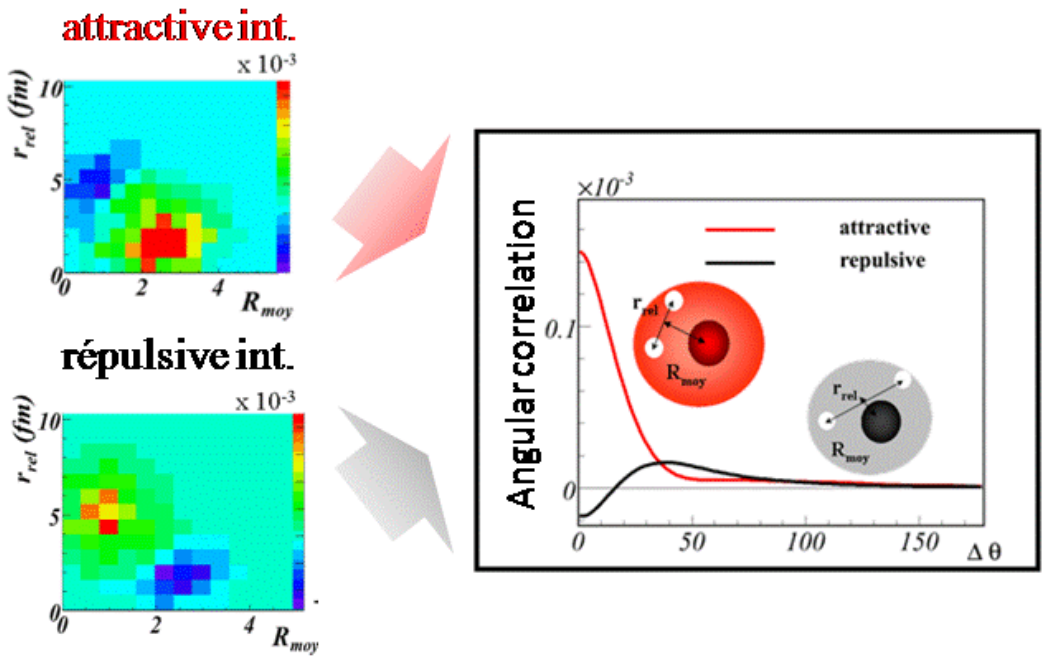

FIG. 31: *Left: Initial spatial correlations represented as a function of the center of mass position R_{moy} of the two neutrons relative to the core and relative distance r_{12} between the last bound neutrons in ^{16}O obtained using an attractive (top) and repulsive (bottom) residual interaction. For the attractive part, correlation is strongly peaked at small relative distance and large distance from the core, while the opposite is obtained for the repulsive case. Right: Angular distribution of two-nucleons nuclear break-up deduced from the TDDM^{P} simulation. As expected, strong spatial correlation leads to small relative angles while larger relative angles have been obtained in the repulsive case.*

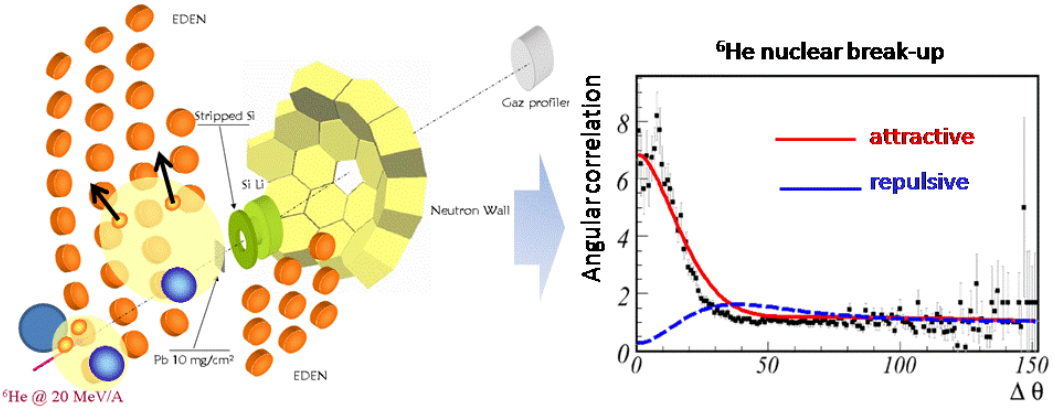

FIG. 32: *Left: Experimental setup of the ^{6}He nuclear break-up performed at GANIL. In this experiment the two emitted neutrons are detected in EDEN and/or the Neutron Wall in coincidence with the recoil alpha particle in the Si-Li detector. Right: Reconstructed angular correlation obtained from the two-neutron + α coincidence measurement. As a reference, curves obtained with TDDM^{P} for repulsive (black curve) and attractive (red curve) interaction are superimposed.*

field. This increase also explains why only few applications of beyond mean-field quantum transport theories have been made so far.

VII. PHENOMENOLOGY OF VIOLENT NUCLEAR REACTIONS: PHASE-SPACE METHODS

Heavy-Ion reactions around Fermi energies have revealed that nuclei under collisions may break into several pieces of different sizes, the so-called multifragmentation. A striking feature of experimental observation is the large number of charge and energy partitions that can be accessed. In order to understand statistical aspects of the explored phase-space, several physical origin have been proposed. Among them, the nuclear liquid-gas phase transition appears as one of the best candidate. However due to the complexity of nuclear reactions that mixes impact parameters, pre-equilibrium emission and thermal decay, to trace-back the true origin of cluster formation is a hard quest.

For instance, the complexity of experimental analysis increases constantly. Conjointly, more and more elaborated models have been proposed to simulate reactions. Despite this complexification, *"How clusters are formed?"* remains a highly debated question. Within this short note, we would like to contribute to the discussion on cluster formation during the pre-equilibrium stage. Previous chapters present an overview of microscopic transport models used to describe nuclear reactions. Several applications have illustrated the powerfulness of such an approach. It should however be noted that these applications are only few examples of the different mechanisms that might appear during a reaction. A more complete picture is given in Figure 33. While already rather involved, microscopic models are still far from giving a unified description of the nuclear reaction diversity. In particular, important questions or aspects are way beyond the capabilities of nuclear transport models:

- To apply transport theories, it is most often necessary to neglect some aspects of nuclear systems which should not be neglected: quantum effects, internal correlations (two-body or more)...
- Experiments, like fragmentation data, reveal the crucial role of simple effects like nuclear masses on the abundance of produced fragments. Actual accuracy of up to date microscopic EDF is not less than few hundreds of keV for ground state nuclei, not mentioning excited states. This accuracy is still insufficient to predict cross sections.
- Microscopic transport theories are not able to describe long time dynamics and generally focus on the first stage of the reaction (pre-equilibrium stage). After this stage, it is expected that "entities" involved in the reactions are thermalized. Even if the expected mechanism leading to thermalization, namely direct nucleon-nucleon collisions, is known, its description in terms of a fully quantum non-equilibrium transport model is still missing.
- Since microscopic theory provides only the description of the initial stage of the reaction additional inputs are necessary to make a comparison with experiment possible:
  - ◇ The output of the first stage of a reaction in a quantal or semi-classical density functional theory is a density profile while the input of a secondary stage (decay) should be a set of definite clusters each of them having a temperature. To bridge the two stages, a clusterization method is necessary. The onset of clustering is certainly beyond the scope of a theory based only on the one-body density matrix. In practice, specific algorithms are retained to form clusters from the density. Clustering methods add new physics on top of the functional theory and have to be carefully controlled.
  - ◇ Secondary decay has an important role and tends to further wash out physical signals of the first stage of the reaction.

The impossibility to treat the whole reactions up to the detector in a unique framework has led to a description where different building blocks (microscopic transport models, clustering models and decay models) are added on top of each other with sometimes some difficulties to make them fully consistent. The net effect of the actual strategy is that (i) the description of the full reaction is often very difficult (ii) current models are not able to describe all reaction channels and generally focus on specific aspects (ii) complex effects observed experimentally are often assigned to the complexity of the physics. However, the interpretation of observations is often made difficult due to the rather complex models used at each stage of the reaction.

In view of this complexity, in parallel to the use of microscopic model, we have developed a phenomenological approach with the following leitmotivs:

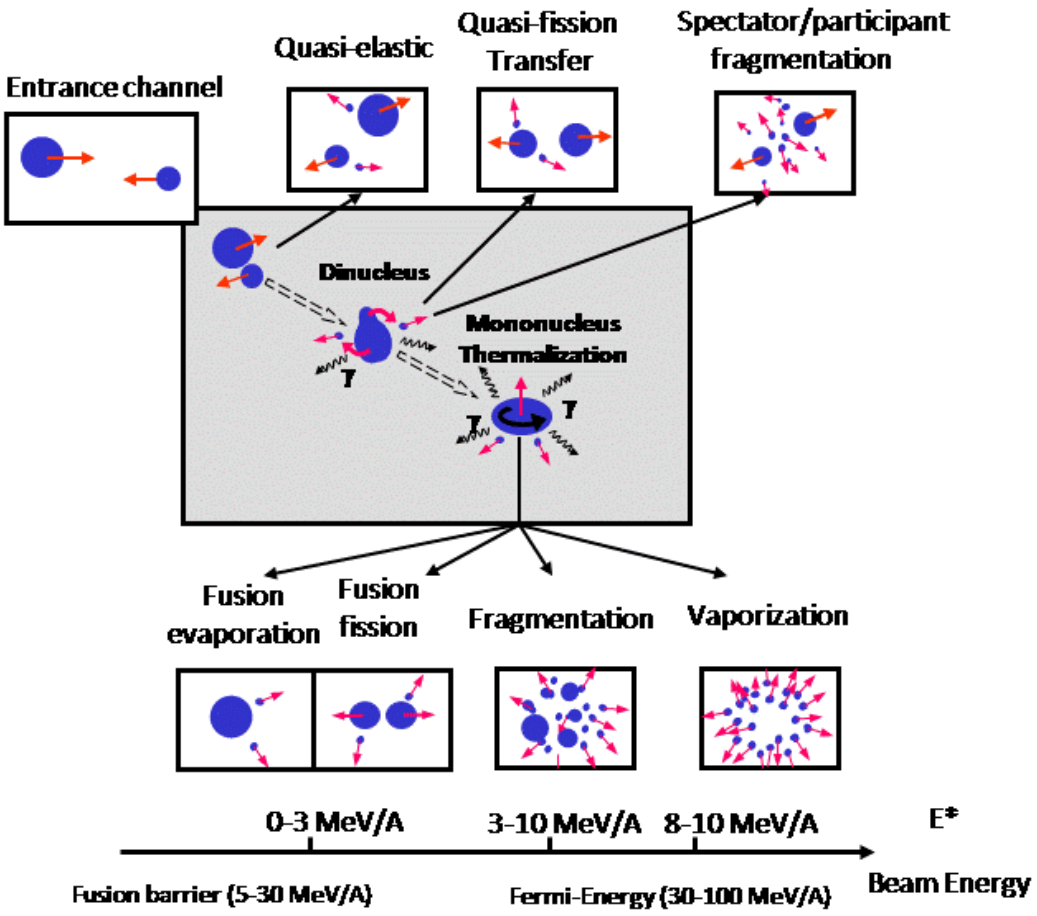

FIG. 33: *Illustration of the diversity of reaction mechanisms. Top: competing phenomena where fossil quasi-target and quasi-projectile survive. Middle: competing phenomena where a compound nucleus is eventually formed at the intermediate reaction stage. The excitation energy and/or beam energy for which these mechanisms appear are given in the bottom part (Adapted from (Lacroix, 2002b)).*

- Is is possible to propose a model where all stage of the reaction are introduced consistently? In particular, the very notion of clusters should be introduced from the very beginning to the very end. The price to pay is to stay at the macroscopic level. This is clearly a step backward but it avoids difficulties inherent to actual microscopic models. For instance, masses of clusters that are often poorly described microscopically can now be introduced exactly.
- Last and most importantly, what are the minimal hypotheses that should be made to describe all mechanisms observed experimentally from low (10 MeV/A) to high beam energy (100 MeV/A), or said differently can the simplicity be identified in so complex spectra?

During the last years, we have tested a large number of hypotheses on the formation of clusters in the nuclear medium, in order to provide event generators for reactions. Guided by the experimental observation, rather surprising conclusions have been reached concerning the way cluster might be formed. As a matter of fact, the most striking conclusion is that rather simple rules have emerged from our study for cluster formation and emission. The hypotheses retained are not only fully compatible with experiments on multifragmentation (Lacroix *et al.*, 2004b), but appear also adequate for spallation where a single nucleon collide a nucleus in the same range of beam energy (Lacroix *et al.*, 2005).

A. Rules for cluster formation and emission

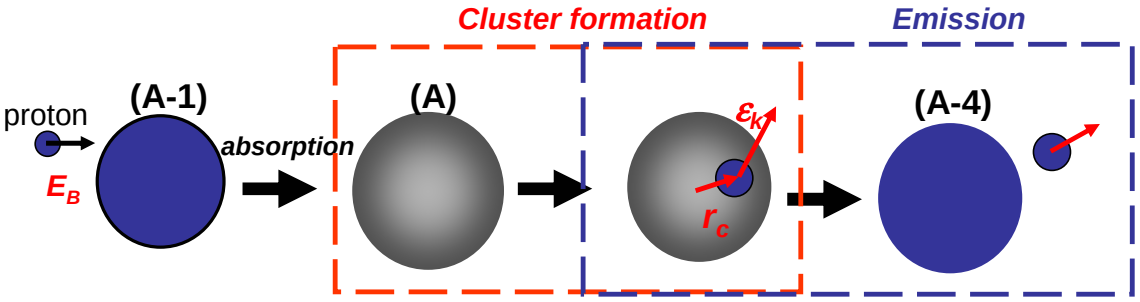

FIG. 34: *Schematic representation of a three steps nucleon-induced reaction. In this simplified experiment, a nucleon with beam energy close to the Fermi energy is absorbed by a nucleus. Then, we assume that the cluster emission occurs in two steps, first the cluster is formed in the medium and then it escape.*

Here, rules for the cluster formation and partition are discussed. These rules are described in a simplified scenario of nucleon-induced reaction depicted in figure 34. Let us consider a incident nucleon with beam energy close to the Fermi energy [11] colliding a heavy target. Here, we disregard the reaction mechanism influence and focus on collisions where the nucleon is absorbed by the target[12]. This defines the first step of a three step scenario for the reaction. The second step described in Fig. 34 corresponds to the cluster formation in the medium while the last step is its emission to the continuum.

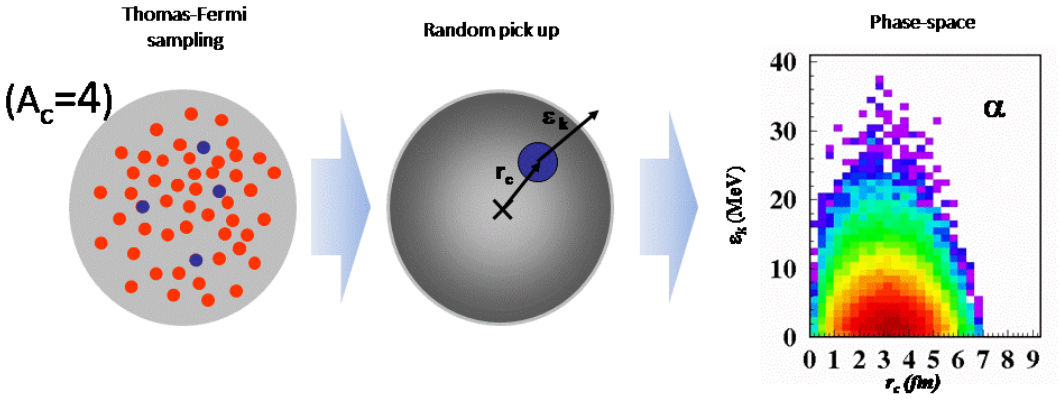

FIG. 35: *Left: Schematic illustration of the Thomas-Fermi sampling. To form an alpha particle, 4 nucleons (2 neutrons-2 protons) are picked up randomly. The phase-space is obtained by choosing 4 nucleons repeatedly and by computing the alpha properties from the nucleons properties. Right: The correlation between the position and kinetic energy per nucleon is obtained for the α particles using a random sampling assumption for the nucleons forming the α. This two-dimensional distribution corresponds to the total "accessible" phase-space to the α.*

We are interested here in the last two stages of the reaction, which are referred below as the

[11] The energy is chosen is that way in order to avoid strong influence of direct two-body nucleon-nucleon collisions
[12] Again this assumptions corresponds to a simplification that will be very helpful for the discussion, in particular for the energetic forthcoming considerations

cluster formation and cluster emission. The hypotheses retained to describe these stages can be summarized as follows:

- **Cluster formation:** Considering a cluster of mass A_c and charge Z_c formed in the medium, it is assumed that the cluster is formed from nucleons chosen randomly in a Thomas-Fermi distribution corresponding to the quasi-target. Due to the energy involved and to the fact that we use a heavy target, the Thomas-Fermi distribution is simply supposed to be the one of the target (this corresponds to the sudden approximation, as we will see in the following the sudden approximation is partially relaxed in a more realistic collision). The cluster properties is then deduced from the properties of their constituent nucleons. This defined the *"total accessible phase-space"* to the cluster (A_c, Z_c) in the medium. An example of total phase-space accessible for an α particle in a lead nucleus is presented in figure 35. In this figure, correlation between the position r_c and the kinetic energy ε_k is shown.

- **Cluster emission:** Here, the total accessible phase-space is dissociated from the explored phase-space accounting for the reaction constraints. Indeed, while the random rule described above leads to a large set of configurations, all configurations will not necessarily lead to an emitted clusters. Two energetic constraints on the emission are essentially identified. The first one, which is independent from the entrance channel, is due to the mutual interaction between the light cluster and the heavy emitter [13]. An example of interaction between an α and a ^{204}Hg nucleus is shown in figure 36. In a classical picture, the cluster could not escape from the heavy nucleus if its energy is below the barrier of emission. Noting $V_{A+A_c}(r_c)$ the interaction potential and V_B the associated barrier. The condition reads [14]

$$\varepsilon_k(r_c) \geq V_B - V_{A+A_c}(r_c) \tag{256}$$

  This leads to a "local" lower limit on the cluster kinetic energy. The second constraint depends directly on the reaction type and is due to the energy balance. Indeed, the accessible configuration is further reduced due to the finite energy available. In the simplified scenario presented here (accounting from the fact that the initial nucleon is absorbed), the second inequality

$$E_B - Q - V_{A+A_c}(r_c) \geq \varepsilon_k(r_c) \tag{257}$$

  is deduced that gives an upper limit for cluster emission. Here E_B denotes the beam energy while Q is the Q-value associated to the specific reaction. It is worth to notice that the second condition depends not only on the beam energy but also on the configuration itself. Therefore, only a fraction of the total phase-space accessible for the cluster will indeed lead to an emission to the continuum. This fraction corresponds to the *"explored phase-space"* accounting for the reaction constraint.

The two constraints are illustrated in top left of Fig. 36 for the specific case of a proton colliding a heavy target at beam energy $E_B = 39$ MeV. In that case, an α particle could only be emitted in a small window of kinetic energy (called "escape window" in the following). This window restricts significantly the phase-space that indeed lead to a cluster emission. The fraction of the phase-space leading to an emission is shown in top-right side of figure 36. According to the energy constraint, all configurations between the two lines leads to emission of an α.

a. **Direct Application of the rules:** The striking aspect of these 'rather simple' rules comes from their compatibility with experimental observation. Indeed, let us directly apply them to the proton

---

[13] Since, a rather low beam beam energy leading to small available energy is considered here, we do not expect here that two clusters are emitted at the same time, thus the outgoing channels are essentially binary. In addition, the use of an heavy target is very helpful since in that case, due to the small available energy in entrance channel, no particle can be emitted in the secondary decay stage. Therefore, in experimental data, detected clusters are issued from the pre-equilibrium state only.

[14] Due to the very asymmetric nature of the emission process, we assume for simplicity that the heavy target is at rest in the laboratory frame.

incident reaction at $E_B = 39$ MeV. Assuming for the moment, that the proton is absorbed by the target, a Monte-Carlo sampling is performed (using the cluster creation rules) of the α particle in order to obtain its initial configurations in the medium. Then, using the emission rules, we retain only configurations authorized by the energetic constraint. Finally, each retained configuration is propagated in the quasi-target potential. With this strategy, a final distribution of kinetic energy for the emitted α is deduced that could be directly compared with experiments. Such a comparison is displayed in bottom part of figure 36 where the calculated spectra (open square) is compared to experimental data (filled circles) of ref. (Bertrand and Peelle, 1973). This figure indicates that the shape of the distribution is perfectly reproduced by simply applying the rules. A similar agreement is found for proton, deuteron and triton emission (see Fig. 37). However in that case, in addition to the Monte-Carlo sampling, direct reactions are also present in the experimental data leading to contribution at high energy.

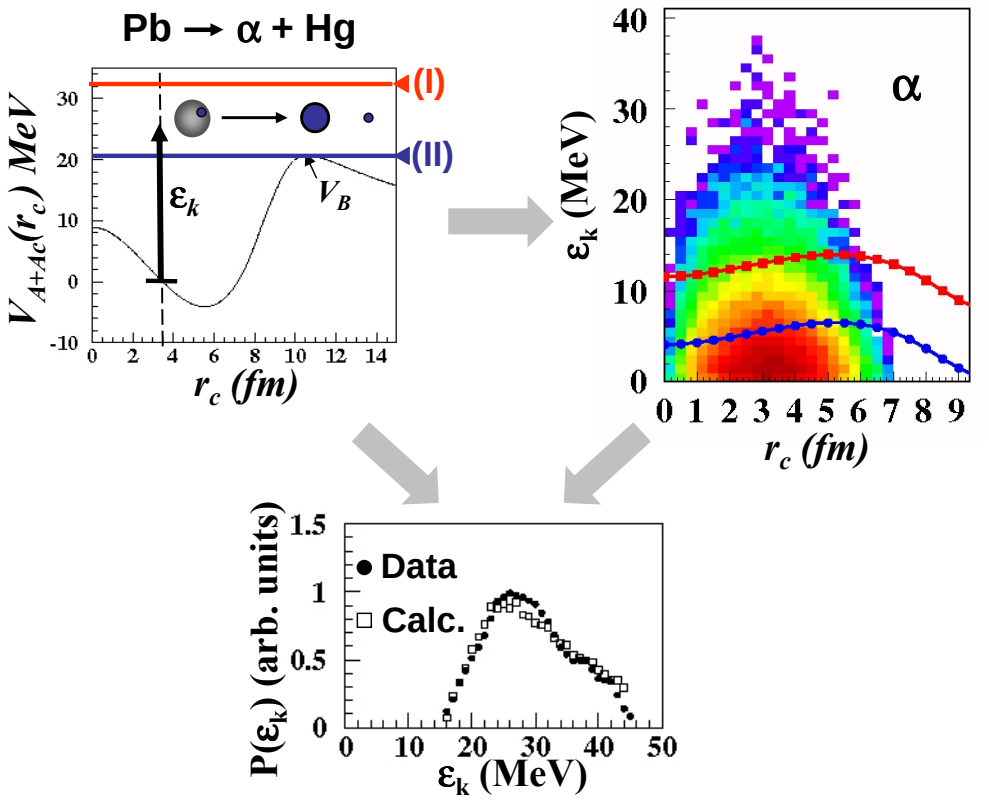

FIG. 36: *Top-left: Two-body Potential between the α and the emitter. Above the line (I), the cluster could not be emitted. This upper limit is directly given by the energy balance of the reaction. Below the line (II), the cluster does not pass the barrier (since here, we do not consider quantum tunneling). In between these two lines, a small windows escape exists where the cluster is authorized to be emitted. Top-right: Total available phase-space of the cluster. This phase-space is significantly reduced due to the two energy constraint. The two curves correspond respectively to the lower and upper limit in the kinetic energy. The constraint phase-space corresponds to the accessible phase-space of the cluster accounting for the reaction constraints. Bottom: Calculated kinetic energy distribution (open square) of the α particle emitted obtained by propagating each configuration in the accessible phase-space up to infinity. The calculated spectra is compared to the experimental data (clack circles).*

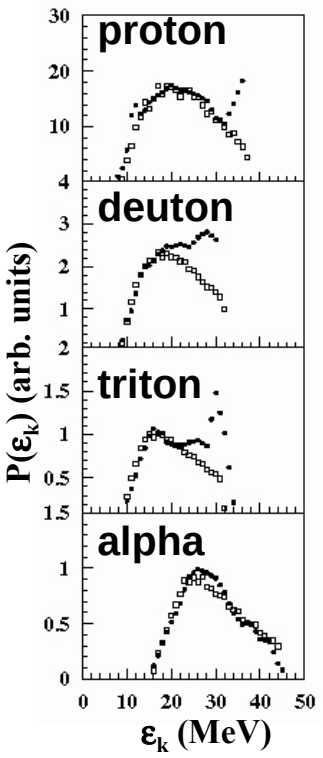

FIG. 37: *From top to bottom, calculated kinetic energy distribution (open squares) obtained for proton, deuteron, triton and alpha. Distributions are systematically compared to experimental data (open circles).*

B. Description of nuclear reactions with simple rules.

Direct application of the rules to the simplified three steps scenario described above can only provide qualitative comparisons with observation. In order to be more quantitative, additional effects related to the reaction should be introduced. In the context of nucleon-induced reaction, this has been done in ref. (Lacroix *et al.*, 2005), while a description of Heavy-Ion reactions can be found in ref. (Lacroix *et al.*, 2004b) leading to two phenomenological models (called n-IPSE[15] and HIPSE[16] respectively) based on the very same assumptions and able to reproduce experiments. Below, a summary of physical effects that should be added on top of the rules are listed:

- **Definition of a participant-spectator region:** After the approaching phase, the two partners of the collisions overlap. The overlapping region defines the participant zone. The remaining parts correspond to the "preformed" quasi-target and quasi-projectile that will behave more like spectators. Nucleons that will encounter nucleon-nucleon collisions, that will be exchanged between the two collision partners and that will serve to form clusters belong to the participant region. For the case of nucleon induced reactions, the concept of overlap has been replaced by the influence radius around the colliding nucleon in ref. (Lacroix *et al.*, 2005) .
- **nucleon-nucleon collisions:** When beam energy is below Fermi energy, effect of two-body collisions is negligible. However, as the beam energy increases direct nucleon-nucleon

[15] n-IPSE: nucleon-Ion Phase-Space Exploration
[16] HIPSE: Heavy-Ion Phase-Space Exploration

collisions should be accounted for. Accordingly, Thomas-Fermi distributions of nucleon that serves for the Monte-Carlo sampling are distorted by two-body effects.

- **Mixing of impact parameters:** in Heavy-Ion collision, geometric aspects of the collision associated to the impact parameter are naturally accounted for by using a Participant-Spectator picture. In nucleon-induced reaction, this picture is replaced by the 'influence area' (equivalent to the participating region) notion which defines a number of nucleons of the quasi-target affected by the projectile.

- **Exchange of particle or nucleon absorption:** Depending on the beam energy more or less particles are exchanged by the two ions. In nucleon induced collisions, this exchange is replaced by a probability of the nucleon to be absorbed by the target.

- **Application of** *cluster formation rules* **and nucleosynthesis in the medium:** We have described previously a rule to obtain cluster properties when a single cluster is formed in the medium. However, the number of clusters is not a priori fixed. In order to solve this difficulty in both models a coalescence algorithm is used to form clusters from nucleon in the participant region. In the nucleon-induced reaction case, it was possible to show explicitly that this coalescence is equivalently to a random sampling assumption.

- **Application of** *cluster emission rules* **and Final-State interaction (FSI)**: After the coalescence stage, many configurations might be accessible, however due to the energy-balance generalized to the many cluster case, only part of the accessible phase-space is really explored. In addition, if the relative energy between two clusters is lower than the barrier associated to their mutual they will not separate during the expansion. In a realistic model, recombination of fragments should be authorized. In HIPSE, possible re-fusion of fragments is accounted for before the freeze-out configuration is reached. This aspect might lead to important FSI and may relax completely the participant-spectator picture.For instance, the quasi-target and quasi-projectile may fuse.

- **Freeze-out and after-burn stage:** When the available energy is big, fragments are excited and once the chemical and thermal freeze-out is reached, the possible in-flight de-excitation of each cluster should be accounted for. This last stage induces a complex mixing of pre- and post-equilibrium emission.

Based on this scenario, two event generators dedicated respectively to nucleon-Ion and Heavy-Ion reactions have been proposed. More technical details can be found in ref. (Lacroix *et al.*, 2004b, 2005). One of the goal was to end with a minimal number of parameters (only three in practice) that should depend only on the beam energy, i.e. they should remain the same as the collision partners change. This is a key issue to make the model predictive. Comparisons with a large set of experiments are given below.

1. Nucleon-Ion reaction: the n-IPSE event generator

The rules described above as well as the identified different steps of the reaction have been applied to nucleon-ion reactions and nucleus-nucleus reactions. The former is first illustrated here. The n-IPSE (nucleon-Ion Phase-Space Exploration) model has been optimized on a large set of neutron induced and proton induced reactions on medium and heavy nuclei for a wide range of beam energy from 37 MeV to 135 MeV (Lacroix *et al.*, 2005). In the n-IPSE model, the remaining three parameters whose values are optimized in the original publication are related to (i) the size of the participating region (ii) the number of direct nucleon-nucleon collisions (iii) the probability of the incident nucleon to be absorbed by the collision partner.

As an illustration, a comparison between the absolute kinetic energy differential cross-section of light clusters calculated with n-IPSE (here spectra are directly compared and no specific normalization has been done) are shown in Fig. 39. As a reference, we also show in left side calculated spectra obtained with GNASH(Young *et al.*, 1992). The n-IPSE calculation is in good agreement with experiments. Similar agreement was found for all the other reactions considered.

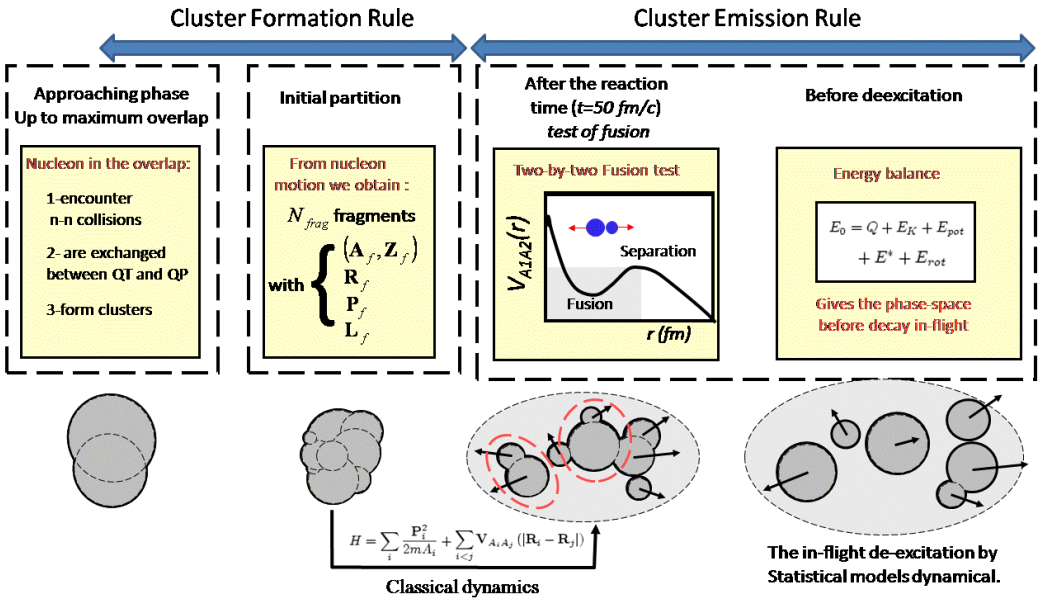

FIG. 38: *Illustration of the different steps to describe nuclear collisions. From left to right are shown: (i) the definition of the participant region after the approaching phase. (ii) the cluster formation. Properties of clusters are directly deduced from properties of nucleons issued from the Thomas-Fermi sampling and eventually distorted by the nucleon-nucleon direct collisions. (iii) Once clusters are formed and after some expansion, a test is made to check if they escape from the attraction of surrounding clusters. If not, the two attracting clusters fuse. (iv) Once the chemical freeze-out is reached, a global energy balance is made to check that the partition is energetically accessible. Then the excitation energy deduced from the energy balance is shared between clusters (v) The in-flight decay is performed. Calculation is stopped once all fragments are cold.*

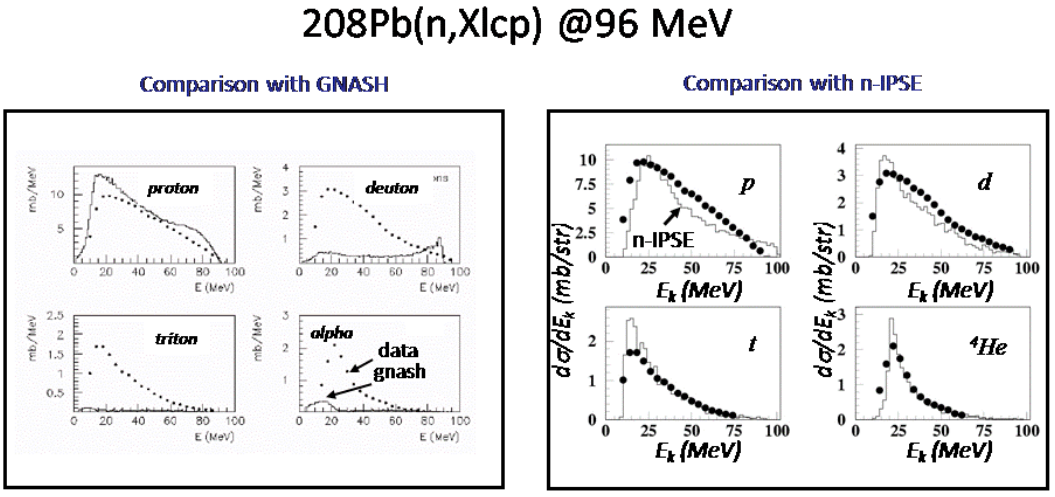

FIG. 39: *Right: Kinetic energy differential cross-section of proton, deuton, triton and alpha particles, obtained with the n-IPSE model calculation (solid line) for neutron induced reaction on ^{208}Pb at beam $E_B = 96$ MeV (from ref. (Lacroix* et al., *2005)). Left: for comparison the distributions obtained using the GNASH model are also shown(Young* et al., *1992).*

2. Comparison with Heavy-Ion reactions: the HIPSE event generator

Similarly to the the nucleon-Ions case, the HIPSE (Heavy-Ion Phase-Space Exploration) model has been designed to provide a description of nucleus-nucleus collisions from the entrance channel to the detector with minimal inputs depending only on the beam energy. The three parameters in that case are (i) the sharpness of the nucleus-nucleus potential in the entrance channel. In particular, depending on the beam energy, this potential is expected to pass from the adiabatic limit (soft potential) to the frozen density case (sharp potential) (ii) the percentage of nucleons in the overlap region participating to the particle exchanged from/to the target to/from the projectile. (iii) the percentage of nucleons in the overlap region participating to direct nucleon-nucleon collisions.

The HIPSE model has been first systematically compared with experiments performed with the INDRA detector. A patchwork of such comparisons is given in Figure 40. The most striking fact that could be noted from this figure is the very good reproduction of many observables. This underlines the compatibility of experiments with the simple rules that have been proposed to understand nuclear reactions are Fermi energy.

To further illustrate the predicting power of the HIPSE model, a second comparison of production yield is given in Figure 92 for experimental data obtained at MSU (Mocko *et al.*, 2008). Again HIPSE gives the best agreement with experiments for the fragment yield. It seems even better than the EPAX parametrization that has directly been adjusted to experiments. In addition, HIPSE is the only model that has the correct description of the quasi-projectile velocity for most peripheral collisions.

The experiment performed at MSU gives also access to isotopic distribution. The reproduction of such a distribution can be used as a benchmark to see if the HIPSE model can be used to predict rare isotopes production in fragmentation reactions. It has been shown that the secondary decay plays a significant role in the estimate of production cross section. In particular, significant improvement is obtained when the original decay code used in HIPSE, i.e. SIMON (Durand, 1992), is replaced by GEMINI(Charity *et al.*, 1988). To further improve cross-section prediction, it is anticipated that an effort has to be made on this secondary decay.

C. Summary and outlook

Simple hypotheses for the formation of clusters during reactions has been a starting point to provide rather simple models able to describe different types of collisions, namely nucleon-Ion or Ion-Ion collisions. Surprisingly enough, lots of observables related to chemical partition or kinematic properties are perfectly reproduced (see for instance figure 40) Such an agreement has never been obtained within a microscopic theory. Besides the simple rules, the HIPSE and n-IPSE model underline the importance of specific features:

- Conservation laws are crucial and should be properly fulfilled at each step of the model.
- Geometric effects are important, in particular through the combination of different impact parameter with the participant/spectator region.
- The Fermi zero point motion of nucleon, used in the Thomas-Fermi sampling is essential to properly describe fluctuations of observables.
- Randomness plays an important role. It leads to a complete exploration of the accessible phase-space under the different constraints of the reaction. It is worth to mention, that even if complete randomness hypothesis appears compatible with data, this do not give any indication on the physical origin of randomness and several effects can be invoked: phase-transition, turbulence, self-organized criticality, quantum decoherence ...

Recently, the HIPSE model has been released to the nuclear physic community. It is now used by different groups worldwide and has been applied to different, sometimes unexpected, studies:

- Multi-fragmentation experiments and associated phase-transition signals (see for instance (Lopez *et al.*, 2005)).
- Fragment yield production for future radioactive beams.

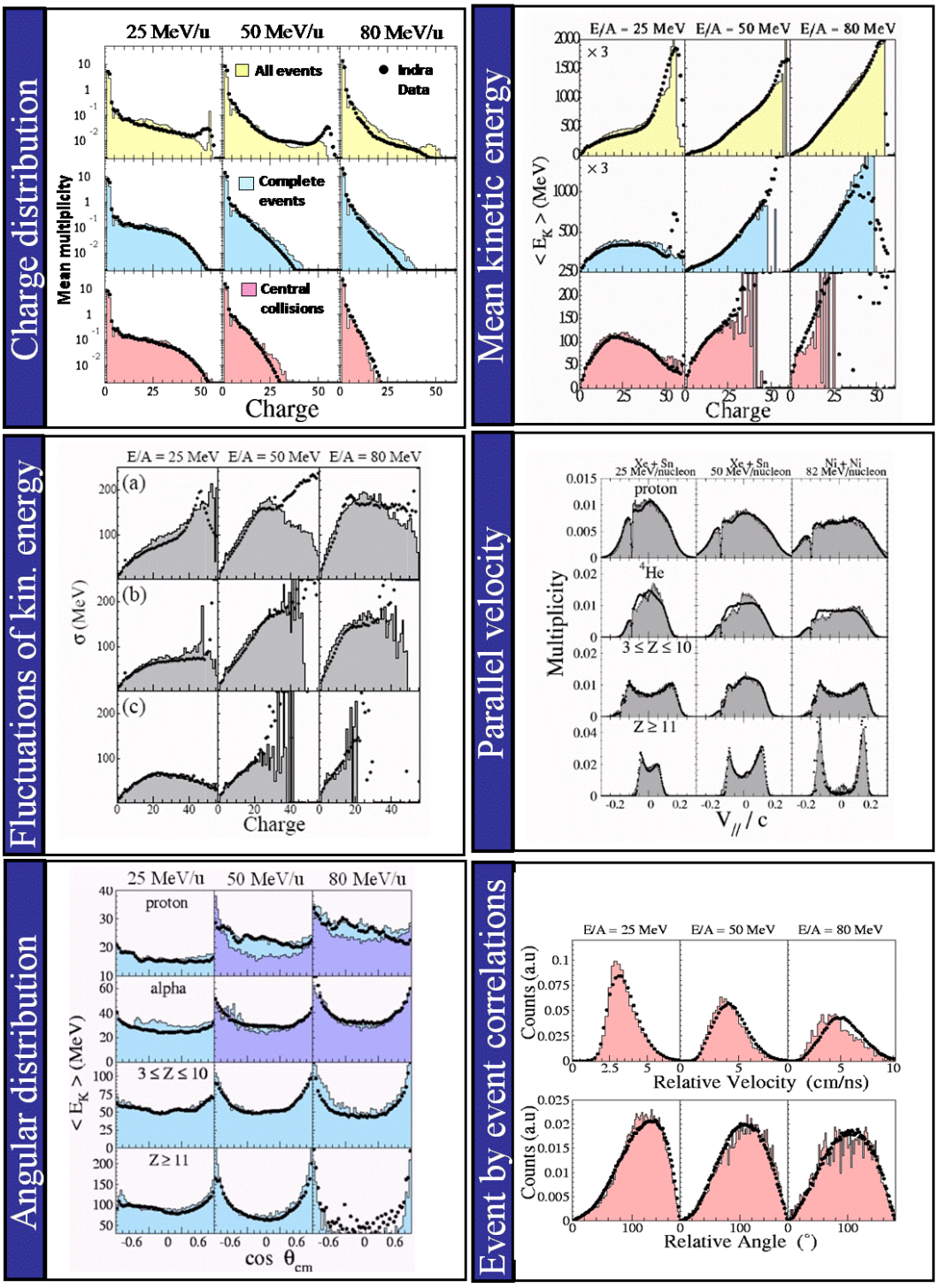

FIG. 40: *Several observables (filled circles) extracted from $^{129}Xe + ^{119}Sn$ experiments at beam energies $E_B = 25$, 50, 80 MeV/A are systematically compared with filtered events generated with the HIPSE model (solid lines). When the selection type of the data is not mentioned, namely "all events", "complete events" or "central collisions", data correspond to complete events, i.e. events where at least 80% of the charge has been detected. Comparison are taken from (Lacroix* et al., *2004b; Van Lauwe, 2003).*

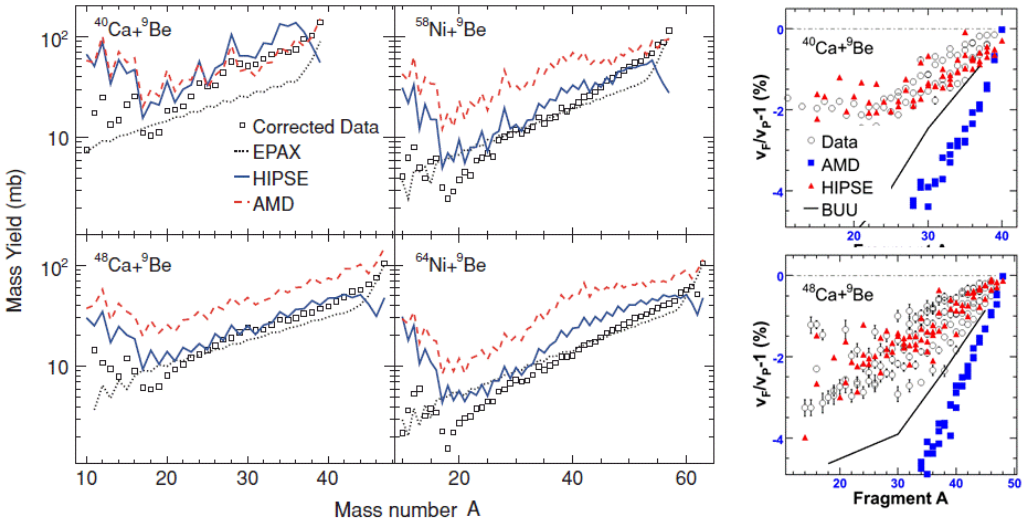

FIG. 41: *Left: Experimental Mass yield (filled circles) obtained for reaction with different calcium and nickel isotopes on ^{9}Be at $E_B = 140$ MeV/A beam energy. In each case, a comparison with the HIPSE model (blue solid line), the microscopic AMD model (red dashed line) (Ono and Horiuchi, 2004) and the empirical EPAX parametrization (dotted line) (Smmerer and Blank, 2002) is made. Right: comparison of the projectile like fragment velocity (normalized to the beam velocity) as a function of its mass. The data (open circles) are systematically compared with different models (adapted from (Mocko* et al.*, 2008)).*

- Tests of detector efficiency.
- Hadron-therapy.

In most cases, the HIPSE model turns out to be a very useful and rather predictive tool. Such a simple approach is rather important to provide practical answer to some physical situation where more microscopic theories cannot be applied. It should however be kept in mind that the goal of the present model is to give simple insight in rather complex observations. On the other hand, microscopic theories have inputs, that are more interesting for fundamental physic like for instance effective interaction. As a consequence, none of the two level of description (macroscopic or microscopic) could be neglected.

VIII. SUMMARY AND DISCUSSION

In this review, I have presented some aspects that have been developed by our group during the past decade. Several topics related to the theory of open quantum and/or many-body interacting systems, transport theories, time-dependent or time-independent density functional theories as well as more phenomenological models for nuclear reactions have been considered during my personal research. I selected below some achievements that, from my point of view are more important than the rest of my contributions:

- New Monte-Carlo method have been proposed that gives an exact reformulation of the Open Quantum System dynamics. Applications of these theories have already given interesting results.

- An effort has been made to clarify the correspondence between a closed system where few relevant degrees of freedom are selected and coupled to the surrounding degrees of freedom and an Open Quantum System. This is a key issue that has strongly guided the development of new methods for non-equilibrium dynamics. For instance, the strict equivalent to the exact Monte-Carlo method has been developed for Many-Body system. In addition, an original formulation of it starting from observables was given.

- Several deterministic or stochastic transport theories have been proposed and applied to the nuclear Many-Body problem. These theories have in common to incorporate effects beyond mean-field (configuration mixing, pairing and direct nucleon-nucleon collisions) that are crucial to understand experiments. Several examples discussed here, like for instance collective motion in nuclei or break-up reactions, points out the importance of these correlations. By mapping Hamiltonian based theories into functional theories, it is now possible to describe properly some of these phenomena. Most of the time, these transport theories were applied for the first time due to their complexity and provides a important step forward for the description of experimental data.

- From the discussion in section V and VI, mean-field theories that are now being used in nuclei, although guided by Hamiltonian theories, should not be confused with them. Thanks to the introduction of such functional theories, important advances have been made recently. With the appearance of pathologies in configuration mixing applied within Energy Density Functional, besides the proposition of a solution, our group has participated actively to the practical and formal formulation of the EDF itself in the nuclear context.

- Different models based on very simple hypothesis have been developed. These models turn out to account for many experimental observation with a precision that has never been met before.

While I am personally rather happy of the above achievements. As often, more remains to be done than what was already achieved. For instance, for the moment, microscopic theories that have been recently developed to treat specific nuclear many-body problem. A description of all effects beyond mean-field fully consistent with nuclear structure model is still missing. It is clear that such a unification can only be done nowadays with the energy density functional framework. Our recent studies have however revealed the necessity to clarify the theoretical framework that justify the introduction of functional theories in nuclear physics. While theories based on effective interaction have been used with success for many years, their justification remains unclear. Density functional theories are a priori introduced to provide an ab-initio formulation of a many-body problem. The separation of mean-field and beyond mean-field levels is far from being trivial in such a context. Related to this, the use of symmetry breaking and associated restoration is an important issue that should be clarified in the near future. More generally, functional theories have been applied to nuclear physics using a very specific strategy (the so-called Single-Reference and Multi-Reference levels discussed in section V). To take advantage of the functional theory powerfulness other strategies have to be explored.

Besides the discussion presented here, a small "revolution" is now taking place in nuclear physics with the possibility to use new generations (less phenomenological) of nucleon-nucleon interaction coming from QCD. Recently important progresses have been made starting from the QCD Lagrangian in the chiral perturbation limit on one side and with the renormalization group technique

on the other side. As a result, nucleon-nucleon interaction can be deduced making the direct connection with underlying constituents. The use of soft interaction opens new perspectives for ab-initio description of nuclei and for the connection of functional theories parameters with more fundamental inputs leading to the so-called bottom-up approach from quarks to nuclei.

Acknowledgments

I would first like to thank members of my HDR defense: M. Bender, F. Gulminelli, P. Schuck, E. Suraud and W. Nazarewicz. I would like to greatly thank M. Assié, B. Avez, M. Bender, J.-A. Scarpaci, C. Simenel for proofreading the manuscript and more specifically G. Hupin who provides some of the figures shown here. Long time research could only be pursued with the help and encouragement of many peoples. I am strongly indebted to all the colleagues, students, members of my family that have contributed from near and far to the research presented in this document.

References

Y. Abe, S. Ayik, P. G. Reinhard, and E. Suraud. On stochastic approaches of nuclear dynamics. *Phys. Rep.*, 275:49, 1996.

G. G. Adamian, R. V. Jolos, A. K. Nasirov, and A. I. Muminov. Friction coefficient for deep-inelastic heavy-ion collisions. *Phys. Rev. C*, 56(1):373, 1997.

D. Almehed, S. Frauendorf, and F. Dönau. Pairing correlations in high-K bands. *Phys. Rev. C*, 63(4):044311, 2001.

M. Anguiano, J.L. Egido, and L.M. Robledo. Particle number projection with effective forces. *Nucl. Phys. A*, 696:467, 2001.

M. Assié and D. Lacroix. Probing neutron correlations through Nuclear Breakup. *Phys. Rev. Lett.*, 102(20):202501, 2009.

M. Assié, J.A. Scarpaci, D. Lacroix, J.C. Angélique, D. Bazin, D. Beaumel, Y. Blumenfeld, W.N. Catford, M. Chabot, A. Chatterjee, et al. Neutron correlations in ^{6}He viewed through nuclear break-up. *Eur. Phys. J. A*, 42:441, 2009.

M. Assié. *Influence des corrélations entre les nucléons sur les réactions de cassure nucléaire : aspects théoriques et expérimentaux*. PhD thesis, Université Paris Sud - Paris XI, 09 2008.

S. Ayik and C. Gregoire. Fluctuations of single-particle density in nuclear collisions. *Phys. Lett.*, B212:269, 1988.

S. Ayik and C. Gregoire. Transport theory of fluctuation phenomena in nuclear collisions. *Nucl. Phys. A*, 513:187, 1990.

S. Ayik, K. Washiyama, and D. Lacroix. Fluctuation and dissipation dynamics in fusion reactions from a stochastic mean-field approach. *Phys. Rev. C*, 79:054606, 2009.

S. Ayik. Mean-field theory and statistical treatment of residual interactions. *Z. Phys.*, A298:83, 1980.

S. Ayik. A stochastic mean-field approach for nuclear dynamics. *Phys. Lett. B*, 658:174, 2008.

R. Balian and E. Brezin. Nonunitary Bogoliubov transformations and extension of Wick's theorem. *Nuovo Cim.*, B64:37, 1969.

R. Balian and M. Vénéroni. Extension through time smoothing of the time dependent mean field theory. *Ann. Phys.*, 135:270, 1981.

R. Balian and M. Vénéroni. Time-dependent variational principle for the expectation value of an observable: Mean-field applications. *Ann. of Phys. (NY)*, 164:334, 1985.

R. Balian. Incompleteness descriptions and relevant entropies. *Am. J. Phys.*, 67:1078, 1999.

V. Baran, M. Colonna, V. Greco, and M. Di Toro. Reaction dynamics with exotic nuclei. *Phys. Rep.*, 410:335, 2005.

M. Bender and T. Duguet. Pairing correlations beyond the mean field. *Int. J. Mod. Phys.*, E16:236, 2007.

M. Bender, P.-H. Heenen, and P.-G. Reinhard. Self-consistent mean-field models for nuclear structure. *Rev. Mod. Phys.*, 75:121, 2003.

M. Bender, P. Bonche, and P.-H. Heenen. Shape coexistence in neutron-deficient Kr isotopes: Constraints on the single-particle spectrum of self-consistent mean-field models from collective excitations. *Phys. Rev. C*, 74:024312, 2006.

M. Bender, T. Duguet, and D. Lacroix. Particle-number restoration within the energy density functional formalism. *Phys. Rev. C*, 79:044319, 2009.

M. Bender. *Private communication*, 2010.

M. G. Bertolli and T. Papenbrock. Energy functional for the three-level Lipkin model. *Phys. Rev. C*, 78:064310, 2008.

F.E. Bertrand and R.W. Peelle. Complete hydrogen and helium particle spectra from 30-to 60-MeV proton bombardment of nuclei with A= 12 to 209 and comparison with the intranuclear cascade model. *Phys. Rev. C*, 8:1045, 1973.

F. E. Bertrand, E. E. Gross, D. J. Horen, R. O. Sayer, T. P. Sjoreen, D. K. McDaniels, J. Lisantti, J. R. Tinsley, L. W. Swenson, J. B. McClelland, T. A. Carey, K. Jones, and S. J. Seestrom-Morris. Giant resonance structure in ^{208}Pb measured using the (p,p') reaction at 334 MeV. *Phys. Rev. C*, 34:45, 1986.

G.F. Bertsch and RA Broglia. *Oscillations in finite quantum systems*. Cambridge Univ Press, 1994.

G.F. Bertsch and D. Gupta. A guide to microscopic models for intermediate energy heavy ion collisions. *Phys. Rep.*, 160:189, 1988.

G. F. Bertsch, P. F. Bortignon, and R. A. Broglia. Damping of nuclear excitations. *Rev. Mod. Phys.*, 55:287, 1983.

J.P. Blaizot and G. Ripka. *Quantum Theory of Finite Systems*. MIT Press, Cambridge, Massachusetts, 1986.

C. Bloch and A. Messiah. The canonical form of an antisymmetric tensor and its application to the theory of superconductivity. *Nucl. Phys.*, 39:95, 1962.

S. K. Bogner, T. T. S. Kuo, and A. Schwenk. Model-independent low momentum nucleon interaction from phase shift equivalence. *Phys. Rep.*, 386:1, 2003.

S. K. Bogner, T. T. S. Kuo, A. Schwenk, D. R. Entem, and R. Machleidt. Towards a model-independent low momentum nucleon-nucleon interaction. *Phys. Lett. B*, 576:265, 2003.

S.K. Bogner, A. Schwenk, R.J. Furnstahl, and A. Nogga. Is nuclear matter perturbative with low-momentum interactions? *Nucl. Phys. A*, 763:59, 2005.

N. N. Bogolyubov. *J. Phys. (USSR)*, 10:256, 1946.

P. Bonche, S. Koonin, and J. W. Negele. One-dimensional nuclear dynamics in the time-dependent Hartree-Fock approximation. *Phys. Rev. C*, 13:1226, 1976.

P. Bonche. Microscopic Description of Low-Energy Nuclear Collisions: Review and Perspective. *Prog. of Theor. Phys. (Supplement)*, page 156, 2000.

H. Born and H.S. Green. A General Kinetic Theory of Liquids. I. The Molecular Distribution Functions. *Proc. Roy. Soc.*, A188:10, 1946.

W. Botermans and R. Malfliet. Quantum transport theory of nuclear matter. *Phys. Rep.*, 198:115, 1990.

H.P. Breuer and F. Petruccione. *The Theory of Open Quantum Systems*. Oxford University Press, Oxford, 2002.

H.-P. Breuer and F. Petruccione. Stochastic analysis and simulation of spin star systems. *Phys. Rev. E*, 76:016701, 2007.

H.-P. Breuer, D. Burgarth, and F. Petruccione. Non-markovian dynamics in a spin star system: Exact solution and approximation techniques. *Phys. Rev. B*, 70:045323, 2004.

H.-P. Breuer. Exact quantum jump approach to open systems in bosonic and spin baths. *Physical Review A*, 69:022115, 2004.

H.-P. Breuer. The non-markovian quantum behavior of open systems: An exact monte carlo method employing stochastic product states. *Eur.Phys.J. D*, 29:105, 2004.

K. Burke and friends. The ABC of DFT, 2003.

A. O. Caldeira and A. J. Leggett. Quantum tunneling in a dissipative system. *Ann. Phys.*, 149:374, 1983.

K. Capelle. A bird's-eye view of density-functional theory. *Brazilian Journal of Physics*, 36:1318, 2006.

H. Carmichael. *An Open Systems Approach to Quantum Optics*. Lecture Notes in Physics, Springer-Verlag, Berlin, 1993.

I. Carusotto, Y. Castin, and J. Dalibard. N-boson time-dependent problem: A reformulation with stochastic wave functions. *Phys. Rev. A*, 63:023606, 2001.

W. Cassing and U. Mosel. Many body theory of high-energy heavy ion reactions. *Prog. Part. Nucl. Phys.*, 25:235, 1990.

Yvan Castin and Klaus Mölmer. Monte carlo wave functions and nonlinear master equations. *Phys. Rev. A*, 54:5275, 1996.

R. J. Charity, M. A. McMahan, G. J. Wozniak, R. J. McDonald, L. G. Moretto, D. G. Sarantites, L. G. Sobotka, G. Guarino, A. Pantaleo, L. Fiore, A. Gobbi, and K. D. Hildenbrand. Systematics of complex fragment emission in niobium-induced reactions. *Nucl. Phys. A*, 483:371, 1988.

Ph. Chomaz, M. Colonna, and J. Randrup. Nuclear spinodal fragmentation. *Phys. Rep.*, 389:263, 2004.

Ph. Chomaz. Selected aspects of collective motions in nuclei. *Ann. Phys. Fr*, 21:669, 1996.

J. Cioslowski and K. Pernal. Constraint upon natural spin orbital functionals imposed by properties of a homogeneous electron gas. *J. Chem. Phys.*, 111:3396, 1999.

J. Cioslowski and K. Pernal. Local-density-matrix approximation: Exact asymptotic results for a high-density homogeneous electron gas. *Phys. Rev. B*, 71:113103, 2005.

J. Cioslowski, K. Pernal, and M. Buchowiecki. Approximate one-matrix functionals for the electron–electron repulsion energy from geminal theories. *J. Chem. Phys.*, 119:6443, 2003.

G. Csányi and T. A. Arias. Tensor product expansions for correlation in quantum many-body systems. *Phys. Rev. B*, 61:7348, 2000.

G. Csányi, S. Goedecker, and T. A. Arias. Improved tensor-product expansions for the two-particle density matrix. *Phys. Rev. A*, 65:032510, 2002.

J. Dalibard, Y. Castin, and K. Mølmer. Wave-function approach to dissipative processes in quantum optics. *Phys. Rev. Lett.*, 68:580, 1992.

P. Danielewicz. Quantum theory of nonequilibrium processes. ii. application to nuclear collisions. *Ann. Phys. (NY)*, 152:305, 1984.

F. V. De Blasio, W. Cassing, M. Tohyama, P. F. Bortignon, and R. A. Broglia. Nonperturbative study of the damping of giant resonances in hot nuclei. *Phys. Rev. Lett.*, 68:1663, 1992.

J. Decharge and D. Gogny. Hartree-Fock-Bogolyubov calculations with the D1 effective interactions on spherical nuclei. *Phys. Rev.*, C21:1568, 1980.

P. Deuar and P. D. Drummond. Gauge p representations for quantum-dynamical problems: Removal of boundary terms. *Phys. Rev. A*, 66:033812, 2002.

L. Diósi and W. T. Strunz. The non-Markovian stochastic Schroedinger equation for open systems. *Phys. Lett.*, A224:25, 1996.

L. Diósi, N. Gisin, and W. T. Strunz. Non-markovian quantum state diffusion. *Phys. Rev. A*, 58:1699, 1998.

P. Dirac. Note on exchange phenomena in the Thomas atom. *Proc. Cambridge Philos. Soc.*, 26:376, 1930.

L. Disi. Stochastic pure state representation for open quantum systems. *Phys. Lett. A*, 114:451, 1986.

J. Dobaczewski, M. V. Stoitsov, W. Nazarewicz, and P.-G. Reinhard. Particle-number projection and the density functional theory. *Phys. Rev. C*, 76:054315, 2007.

F. Dönau. Canonical form of transition matrix elements. *Phys. Rev. C*, 58:872, 1998.

R.M. Dreizler and E.K.U. Gross. *Density functional theory: an approach to the quantum many-body problem*. Springer-Verlag Berlin, 1990.

S. Drozdz, M. Ploszajczak, and E. Caurier. Variational approach to the Schroedinger dynamics in the Klauder's continuous representations. *Ann. Phys. (NY)*, 171:1, 1986.

T. Duguet, M. Bender, K. Bennaceur, D. Lacroix, and T. Lesinski. Particle-number restoration within the energy density functional formalism: Nonviability of terms depending on noninteger powers of the density matrices. *Phys. Rev. C*, 79:044320, 2009.

R. Dum, P. Zoller, and H. Ritsch. Monte Carlo simulation of the atomic master equation for spontaneous emission. *Phys. Rev. A*, 45:4879, 1992.

D. Durand. An event generator for the study of nuclear collisions in the Fermi energy domain (I). Formalism and first applications. *Nucl. Phys. A*, 541:266, 1992.

S. Dusuel and J. Vidal. Finite-Size Scaling Exponents of the Lipkin-Meshkov-Glick Model. *Phys. Rev. Lett.*, 93:237204, 2004.

J. Engel. Intrinsic-density functionals. *Phys. Rev. C*, 75:014306, 2007.

M. Fallot, JA Scarpaci, D. Lacroix, P. Chomaz, and J. Margueron. Coulomb versus nuclear break-up of ^{11}Be halo nucleus in a nonperturbative framework. *Nucl. Phys. A*, 700:70, 2002.

H. Feldmeier and J. Schnack. Molecular dynamics for fermions. *Rev. Mod. Phys.*, 72:655, 2000.

H. Feldmeier. Transport phenomena in dissipative heavy-ion collisions: the one-body dissipation approach. *Rep. Prog. Phys.*, 50:915, 1987.

R. P. Feynman and Jr. Vernon, F. L. The theory of a general quantum system interacting with a linear dissipative system. *Ann. Phys. (NY)*, 24:118, 1963.

C. Fiolhais, F. Nogueira, and M. Marques, editors. *A Primer in Density Functional Theory*, volume 620 of *Lecture Notes in Physics*. Springer, Berlin and Heidelberg, 2003.

H. Flocard and N. Onishi. On the restoration of symmetry in paired fermion systems. *Ann. Phys. (NY)*, 254:275, 1997.

V. Fock. *Z. Phys.*, 61:126, 1930.

V. N. Fomenko. Projection in the occupation-number space and the canonical transformation. *J. Phys. (G.B)*, A3:8, 1970.

W. Gardiner and P. Zoller. *Quantum Noise*. Springer-Verlag, Berlin-Heidelberg, 2000.

W. Gardiner. *Handbook of Stochastic Methods*. Springer-Verlag, Berlin-Heidelberg, 1985.

T. L. Gilbert. Hohenberg-kohn theorem for nonlocal external potentials. *Phys. Rev. B*, 12:2111, 1975.

B. G. Giraud. Density functionals in the laboratory frame. *Phys. Rev. C*, 77:014311, 2008.

N. Gisin and I.C. Percival. The quantum-state diffusion model applied to open systems. *J. Math. Phys.*, A25:5677, 1992.

S. Goedecker and C. J. Umrigar. Natural orbital functional for the many-electron problem. *Phys. Rev. Lett.*, 81:866, 1998.

K. Goeke and P.G. Reinhard. The generator-coordinate-method with conjugate parameters and the unification of microscopic theories for large amplitude collective motion. *Ann. of Phys. (NY)*, 124:249, 1980.

K. Goeke and P.G. Reinhard. *Time-Dependent Hartree-Fock and Beyond*. Germany, Bad Honnef, 1982.

K. Goeke, P. G. Reinhard, and D. J. Rowe. A study of collective paths in the time-dependent Hartree-Fock approach to large amplitude collective nuclear motion. *Nucl. Phys.*, A359:408, 1981.

H. Goutte, J. F. Berger, P. Casoli, and D. Gogny. Microscopic approach of fission dynamics applied to fragment kinetic energy and mass distributions in u-238. *Phys. Rev.*, C71:024316, 2005.

P. Grange, H. A. Weidenmuller, and G. Wolschin. Beyond the tdhf: A collision term from a random-matrix model. *Ann. Phys. (NY)*, 139:190, 1981.

O. Gritsenko, K. Pernal, and E.J. Baerends. An improved density matrix functional by physically motivated

repulsive corrections. *The Journal of Chemical Physics*, 122:204102, 2005.
E. K. U. Gross, L. N. Oliveira, and W. Kohn. Density-functional theory for ensembles of fractionally occupied states. i. basic formalism. *Phys. Rev. A*, 37:2809, 1988.
E. K. U. Gross, L. N. Oliveira, and W. Kohn. Rayleigh-Ritz variational principle for ensembles of fractionally occupied states. *Phys. Rev. A*, 37:2805, 1988.
A. J. Glick H. J. Lipkin, N. Meshkov. Validity of many-body approximation methods for a solvable model : (i). exact solutions and perturbation theory. *Nucl. Phys. A*, 62:188, 1965.
M.N. Harakeh, A. Woude, and A. Van Der Woude. *Giant resonances: fundamental high-frequency modes of nuclear excitation*. Oxford University Press, USA, 2001.
D. R. Hartree. The wave mechanics of an atom with a non-Coulomb central field. part I. theory and methods. *Proc. Cambridge Philos. Soc.*, 24:89, 1928.
P. Hohenberg and W. Kohn. Inhomogeneous electron gas. *Phys. Rev.*, 136:B864, 1964.
E. Joos, H.D. Zeh, C. Kiefer, D. Giulini, J. Kupsch, and I.-O. Stamatescu. *Decoherence and the Appearance of a Classical World in Quantum Theory*. Springer, New York, 2003.
O. Juillet and Ph. Chomaz. Exact stochastic mean-field approach to the fermionic many-body problem. *Phys. Rev. Lett.*, 88:142503, 2002.
O. Juillet, P. Chomaz, D. Lacroix, and F. Gulminelli. An exact stochastic mean-field approach to the fermionic many-body problem. 2001.
O. Juillet, F. Gulminelli, and Ph. Chomaz. Exact pairing correlations for one-dimensionally trapped fermions with stochastic mean-field wave functions. *Phys. Rev. Lett.*, 92:160401, 2004.
S. Kamerdzhiev, J. Lisantti, P. von Neumann-Cosel, A. Richter, G. Tertychny, and J. Wambach. Fine structure of the giant isoscalar quadrupole resonance in ^{208}Pb observed in high-resolution $(e, e^{'})$ and $(p, p^{'})$ experiments. *Phys. Rev. C*, 55:2101, 1997.
A. Kamlah. An approximation for rotation-projected expectation values of the energy for deformed nuclei and a derivation of the cranking variational equation. *Z. Phys. A*, 216:52, 1968.
S. Kehrein. *The flow equation approach to many-particle systems*. Springer, 2006.
A.K. Kerman and S.E. Koonin. Hamiltonian formulation of time-dependent variational principles for the many-body system. *Ann. of Phys. (NY)*, 100:332, 1976.
K.H. Kim, T. Otsuka, and P. Bonche. Three-dimensional TDHF calculations for reactions of unstable nuclei. *J. Phys. G*, 23:1267, 1997.
J.G. Kirkwood. Elastic Loss and Relaxation Times in Cross-Linked Polymers. *J. Chem. Phys.*, 14:51, 1946.
W. Koch and M. C. Holthausen. *A Chemist's Guide to Density Functional Theory*. Wiley-VCH, Weinheim, 2001.
W. Kohn and L. J. Sham. Self-consistent equations including exchange and correlation effects. *Phys. Rev.*, 140:A1133, 1965.
W. Kohn. Nobel lecture: Electronic structure of matter—wave functions and density functionals. *Rev. Mod. Phys.*, 71:1253, 1999.
C. Kollmar. The "JK-only" approximation in density matrix functional and wave function theory. *J. Chem. Phys.*, 121:11581, 2004.
C. Kollmar. A size extensive energy functional derived from a double configuration interaction approach: The role of N representability conditions. *J. Chem. Phys.*, 125:084108, 2006.
S. E. Koonin, D. J. Dean, and K. Langanke. Results from shell model monte carlo studies. *Ann. Rev. Nucl. Part. Sci.*, 47:463, 1997.
S.E. Koonin. Progress in particle and nuclear physics. Wilkinson, DH (ed.), Vol. 4, 1980.
O. Kuebler and H. D. Zeh. Dynamics of quantum correlations. *Ann. Phys. (NY)*, 76:405, 1973.
G. Kuhler, D. Meuer, S. Muller, A. Richter, E. Spamer, O. Titze, and W. Knupfer. Electroexcitation of ^{208}Pb, distribution of electric dipole and quadrupole strength and fragmentation of the isoscalar quadrupole giant resonance. *Phys. Lett. B*, 104:189, 1981.
D. Lacroix and P. Chomaz. Multiscale fluctuations in the nuclear response. *Phys. Rev. C*, 60:64307, 1999.
D. Lacroix and G. Hupin. Exact stochastic mean-field dynamics. (arXiv:0812.3650), Dec 2008. Proceedings series of Proceedings of FUSION08:New Aspects of Heavy Ion Collisions near the Coulomb Barrier, September 22-26, 2008, Chicago, USA.
D. Lacroix and G. Hupin. Density-matrix functionals for pairing in mesoscopic superconductors. *Arxiv preprint arXiv:1003.2860*, 2010.
D. Lacroix, Ph. Chomaz, and S. Ayik. Finite temperature nuclear response in the extended random phase approximation. *Phys. Rev. C*, 58:2154, 1998.
D. Lacroix, Ph. Chomaz, and S. Ayik. On the simulation of extended TDHF theory. *Nucl. Phys.*, A651:369, 1999.
D. Lacroix, J.A. Scarpaci, and P. Chomaz. Theoretical description of the towing mode through a time-dependent quantum calculation. *Nucl. Phys. A*, 658:273, 1999.
D. Lacroix, A. Mai, P. von Neumann-Cosel, A. Richter, and J. Wambach. Multiple scales in the fine structure of the isoscalar giant quadrupole resonance in ^{208}Pb. *Phys. Lett. B*, 479:15, 2000.
D. Lacroix, S. Ayik, and P. Chomaz. Collective response of nuclei: Comparison between experiments and

extended mean-field calculations. *Phys. Rev. C*, 63:064305, 2001.
D. Lacroix, S. Ayik, and Ph. Chomaz. Nuclear collective vibrations in extended mean-field theory. *Prog. Part. Nucl. Phys.*, 52:497, 2004.
D. Lacroix, A. Van Lauwe, and D. Durand. Event generator for nuclear collisions at intermediate energies. *Phys. Rev. C*, 69:54604, 2004.
D. Lacroix, V. Blideanu, and D. Durand. Mechanism of light cluster production in nucleon induced reactions at intermediate energy. *Phys. Rev. C*, 71:024601, 2005.
D. Lacroix, T. Duguet, and M. Bender. Configuration mixing within the energy density functional formalism: Removing spurious contributions from nondiagonal energy kernels. *Phys. Rev. C*, 79:044318, 2009.
D. Lacroix. From microscopic to macroscopic dynamics in mean-field theory: effect of neutron skin on fusion barrier and dissipation. *Arxiv preprint nucl-th/0202063*, 2002.
D. Lacroix. Macroscopic approaches for fusion reactions. *International Joliot-Curie School, Maubuisson, Sept 2002*, page 283, 2002.
D. Lacroix. Exact and approximate many-body dynamics with stochastic one-body density matrix evolution. *Phys. Rev.*, C71:064322, 2005.
D. Lacroix. Optimizing stochastic trajectories in exact quantum-jump approaches of interacting systems. *Phys. Rev. A*, 72:013805, 2005.
D. Lacroix. Quantum Monte-Carlo methods and exact treatment of the two- body problem with Hartree-Fock Bogoliubov states. 2006.
D. Lacroix. Stochastic mean-field dynamics for fermions in the weak coupling limit. *Phys. Rev.*, C73:044311, 2006.
D. Lacroix. Stochastic schroedinger equation from optimal observable evolution. *Ann. Phys. (NY)*, 322:2055, 2007.
D. Lacroix. Stochastic simulation of dissipation and non-markovian effects in open quantum systems. *Phys. Rev. E*, 77:041126, 2008.
D. Lacroix. Density matrix functional theory for the Lipkin model. *Phys. Rev. C*, 79:014301, 2009.
N. N. Lathiotakis and Miguel A. L. Marques. Benchmark calculations for reduced density-matrix functional theory, 2008.
N. N. Lathiotakis, N. Helbig, and E. K. U. Gross. Open shells in reduced-density-matrix-functional theory. *Phys. Rev. A*, 72:030501, 2005.
N. N. Lathiotakis, N. Helbig, and E. K. U. Gross. Performance of one-body reduced density-matrix functionals for the homogeneous electron gas. *Phys. Rev. B*, 75:195120, 2007.
A. J. Leggett, S. Chakravarty, A. T. Dorsey, Matthew P. A. Fisher, A. Garg, and W. Zwerger. Dynamics of the dissipative two-state system. *Rev. Mod. Phys.*, 59:1, 1987.
P. Leiva and M. Piris. Assessment of a new approach for the two-electron cumulant in natural-orbital-functional theory. *J. Chem. Phys.*, 123:214102, 2005.
S. Levit, J. W. Negele, and Z. Paltiel. Time-dependent mean-field theory and quantized bound states. *Phys. Rev. C*, 21:1603, 1980.
S. Levit. Time-dependent mean-field approximation for nuclear dynamical problems. *Phys. Rev. C*, 21:1594, 1980.
Peter C. Lichtner and James J. Griffin. Evolution of a quantum system: Lifetime of a determinant. *Phys. Rev. Lett.*, 37:1521, 1976.
V. Lima, J.A. Scarpaci, D. Lacroix, Y. Blumenfeld, C. Bourgeois, M. Chabot, P. Chomaz, P. Désesquelles, V. Duflot, J. Duprat, et al. Nuclear break-up of ^{11}Be. *Nucl. Phys. A*, 795:1, 2007.
Harry J. Lipkin. Collective motion in many-particle systems : Part 1. the violation of conservation laws. *Ann. Phys. (NY)*, 9:272, 1960.
J. Lisantti, E. J. Stephenson, A. D. Bacher, P. Li, R. Sawafta, P. Schwandt, S. P. Wells, S. W. Wissink, W. Unkelbach, and J. Wambach. Spin-flip probabilities in ^{208}Pb measured with 200 MeV protons. *Phys. Rev. C*, 44:R1233, 1991.
O. Lopez, D. Lacroix, and E. Vient. Bimodality as a signal of a liquid-gas phase transition in nuclei? *Phys. Rev Lett.*, 95:242701, 2005.
P.-O. Löwdin. Quantum Theory of Many-Particle Systems. II. Study of the Ordinary Hartree-Fock Approximation. *Phys. Rev.*, 97:1490, 1955.
H.-G. Luo, W. Cassing, and S.-J. Wang. Damping of collective nuclear motion and thermodynamic properties of nuclei beyond mean field. *Nucl. Phys.*, A652:164, 1999.
M. Marques and E. Gross. Time-dependent density functional theory. *Ann. Rev. Phys. Chem.*, 55:427, 2004.
Miguel A. L. Marques and N. N. Lathiotakis. Empirical functionals for reduced-density-matrix-functional theory. *Phys. Rev. A*, 77:032509, 2008.
M. Marques, C. Ullrich, F. Nogueira, A. Rubio, K. Burke, and EKU Gross. Time-Dependent Density Functional Theory, vol. 706/2006 of Lecture Notes in Physics, 2006.
J. A. Maruhn, P.-G. Reinhard, P. D. Stevenson, and M. R. Strayer. Spin-excitation mechanisms in skyrme-force time-dependent hartree-fock calculations. *Phys. Rev. C*, 74:027601, 2006.

Jérémie Messud, Michael Bender, and Eric Suraud. Density functional theory and Kohn-Sham scheme for self-bound systems. *Phys. Rev. C*, 80:054314, 2009.

J. Messud. Time-dependent internal density functional theory formalism and Kohn-Sham scheme for self-bound systems. *Phys. Rev. C*, 80:054614, 2009.

M. Mocko, M.B. Tsang, D. Lacroix, A. Ono, P. Danielewicz, WG Lynch, and RJ Charity. Transport model simulations of projectile fragmentation reactions at 140 MeV/nucleon. *Phys. Rev. C*, 78:24612, 2008.

H. Mori. Transport, collective motion, and brownian motion. *Prog. Theor. Phys.*, 33:423, 1965.

A. M. K. Mller. Explicit approximate relation between reduced two- and one-particle density matrices. *Phys. Lett. A*, 105:446, 1984.

T. Nakatsukasa and K. Yabana. Linear response theory in the continuum for deformed nuclei: Green's function vs time-dependent Hartree-Fock with the absorbing boundary condition. *Phys. Rev. C*, 71:024301, 2005.

J.W. Negele and H. Orland. *Quantum Many-Particle*. Frontiers in Physics, Addison-Weysley publishing company, New-York, 1988.

J. W. Negele and D. Vautherin. Density-matrix expansion for an effective nuclear hamiltonian. *Phys. Rev. C*, 5:1472, 1972.

J. W. Negele. Structure of finite nuclei in the local-density approximation. *Phys. Rev. C*, 1:1260, 1970.

J. W. Negele. The mean-field theory of nuclear structure and dynamics. *Rev. Mod. Phys.*, 54:913, 1982.

Y. Nogami. Improved superconductivity approximation for the pairing interaction in nuclei. *Phys. Rev.*, 134:B313, 1964.

L. N. Oliveira, E. K. U. Gross, and W. Kohn. Density-functional theory for ensembles of fractionally occupied states. ii. application to the he atom. *Phys. Rev. A*, 37:2821, 1988.

L. N. Oliveira, E. K. U. Gross, and W. Kohn. Density-functional theory for superconductors. *Phys. Rev. Lett.*, 60:2430, 1988.

N. Onishi and S. Yoshida. Generator coordinate method applied to nuclei in the transition region. *Nucl. Phys.*, 80:367, 1966.

A. Ono and H. Horiuchi. Antisymmetrized molecular dynamics for heavy ion collisions. *Prog. Part. Nucl. Phys.*, 53(2):501, 2004.

T. Papenbrock and A. Bhattacharyya. Density-functional theory for the pairing hamiltonian. *Phys. Rev. C*, 75:014304, 2007.

R. G. Parr and W. Yang. *Density-Functional Theory of Atoms and Molecules*. Clarendon, Oxford, 1989.

J. P. Perdew and Alex Zunger. Self-interaction correction to density-functional approximations for many-electron systems. *Phys. Rev. B*, 23:5048, 1981.

K. Pernal and J. Cioslowski. Phase dilemma in density matrix functional theory. *J. Chem. Phys.*, 120:5987, 2004.

A. Peter, W. Cassing, J. M. Hauser, and A. Pfitzner. Microscopic analysis of two-body correlations in light nuclei. *Nucl. Phys.*, A573:93, 1994.

J. Piilo, S. Maniscalco, K. Härkönen, and K.-A. Suominen. Non-markovian quantum jumps. *Phys. Rev. Lett.*, 100:180402, 2008.

M. B. Plenio and P. L. Knight. The quantum-jump approach to dissipative dynamics in quantum optics. *Rev. Mod. Phys.*, 70:101, 1998.

L. I. Plimak, M. K. Olsen, and M. J. Collett. Optimization of the positive-P representation for the anharmonic oscillator. *Phys. Rev. A*, 64:025801, 2001.

P.G. Reinhard and K. Goeke. The generator coordinate method and quantized collective motion in nuclear systems. *Rep. Prog. Phys.*, 50:1, 1987.

P. G. Reinhard and E. Suraud. Stochastic and TDHF and large fluctuations. *Nucl. Phys.*, A545:59–70, 1992.

P. G. Reinhard and E. Suraud. Stochastic TDHF and the Boltzmann-Langevin equation. *Ann. Phys.*, 216:98, 1992.

P. G. Reinhard and C. Toepffer. Correlations in nuclei and nuclear dynamics. *Int. J. of Mod. Phys. E*, 3:435, 1994.

M. Rigo and N. Gisin. Unravellings of the master equation and the emergence of a classical world. *Quantum Semiclass. Opt.*, 8:255, 1996.

P. Ring and P. Schuck. *The Nuclear Many-Body Problem*. Springer-Verlag, New-York, 1980.

L.M. Robledo. Particle number restoration: its implementation and impact in nuclear structure calculations. *Int. J. Mod. Phys.*, E16:337, 2007.

E. Runge and E. K. U. Gross. Density-functional theory for time-dependent systems. *Phys. Rev. Lett.*, 52:997, 1984.

J.A. Scarpaci, D. Beaumel, Y. Blumenfeld, P. Chomaz, N. Frascaria, J. Jongman, D. Lacroix, H. Laurent, I. Lhenry, F. Marechal, et al. A new phenomenon in heavy ion inelastic scattering: the towing mode. *Phys. Lett. B*, 428(3):241, 1998.

A. Schwierczinski, R. Frey, A. Richter, E. Spamer, H. Theissen, O. Titze, Th. Walcher, S. Krewald, and R. Rosenfelder. Multipole Assignment of the 8.9-MeV Resonance in ^{208}Pb. *Phys. Rev. Lett.*, 35:1244, 1975.

A. P. Severyukhin, M. Bender, and P.-H. Heenen. Beyond mean field study of excited states: Analysis within the Lipkin model. *Phys. Rev. C*, 74:024311, 2006.

J. Shao. *J. Chem. Phys.*, 120:5053, 2004.

J. A. Sheikh and P. Ring. Symmetry-projected Hartree-Fock-Bogoliubov equations. *Nucl. Phys. A*, 665:71, 2000.

A. Shevchenko, J. Carter, R. W. Fearick, S. V. Förtsch, H. Fujita, Y. Fujita, Y. Kalmykov, D. Lacroix, J. J. Lawrie, P. von Neumann-Cosel, R. Neveling, V. Yu. Ponomarev, A. Richter, E. Sideras-Haddad, F. D. Smit, and J. Wambach. Fine structure in the energy region of the isoscalar giant quadrupole resonance: Characteristic scales from a wavelet analysis. *Phys. Rev. Lett.*, 93:122501, 2004.

A. Shevchenko, O. Burda, J. Carter, G. R. J. Cooper, R. W. Fearick, S. V. Förtsch, H. Fujita, Y. Fujita, Y. Kalmykov, D. Lacroix, J. J. Lawrie, P. von Neumann-Cosel, R. Neveling, V. Yu. Ponomarev, A. Richter, E. Sideras-Haddad, F. D. Smit, and J. Wambach. Global investigation of the fine structure of the isoscalar giant quadrupole resonance. *Phys. Rev. C*, 79:044305, 2009.

C. Simenel and B. Avez. Time-Dependent Hartree-Fock Description of Heavy Ions Fusion. *Int. J. Mod. Phys/ E*, 17:31, 2008.

C. Simenel, Ph. Chomaz, and G. de France. Quantum calculation of the dipole excitation in fusion reactions. *Phys. Rev. Lett.*, 86:2971, 2001.

C. Simenel, B. Avez, and D. Lacroix. Microscopic approaches for nuclear Many-Body dynamics: applications to nuclear reactions. *nucl-th:0806.2714*, 2008.

T.H.R. Skyrme. The nuclear surface. *Phil. Mag*, 1:1043, 1956.

J. T. Stockburger and H. Grabert. Exact c-number representation of non-markovian quantum dissipation. *Phys. Rev. Lett.*, 88:170407, 2002.

W. T. Strunz, L. Diósi, and N. Gisin. Open system dynamics with non-markovian quantum trajectories. *Phys. Rev. Lett.*, 82:1801, 1999.

W. T. Strunz. Stochastic pure states for quantum brownian motion. *New Journ. of Phys.*, page 91, 2005.

K. Smmerer and B. Blank. EPAX version 2: a modified empirical parametrization of fragmentation cross sections. *Nucl. Phys. A*, 701:161, 2002.

N. Tajima, H. Flocard, P. Bonche, J. Dobaczewski, and P.H. Heenen. Generator coordinate kernels between zero-and two-quasiparticle bcs states. *Nucl. Phys. A*, 542:355, 1992.

D. J. Thouless. Stability conditions and nuclear rotations in the Hartree-Fock theory. *Nucl. Phys.*, 21:225, 1960.

M. Tohyama and S. Takahara. Relation between the density-matrix theory and the pairing theory. *Prog. of Theor. Phys.*, 112:499, 2004.

M. Tohyama and A. S. Umar. Dipole resonances in oxygen isotopes in time-dependent density-matrix theory. *Phys. Lett. B*, 516:415, 2001.

M. Tohyama and A. S. Umar. Fusion window problem in time-dependent hartree-fock theory revisited. *Phys. Rev. C*, 65:037601, 2002.

M. Tohyama and A. S. Umar. Quadrupole resonances in unstable oxygen isotopes in time- dependent density-matrix formalism. *Phys. Lett.*, B549:72, 2002.

A. S. Umar and V. E. Oberacker. Three-dimensional unrestricted time-dependent Hartree-Fock fusion calculations using the full Skyrme interaction. *Phys. Rev. C*, 73:054607, 2006.

S. M. Valone. Consequences of extending 1-matrix energy functionals from pure–state representable to all ensemble representable 1 matrices. *J. Chem. Phys.*, 73:1344, 1980.

S. M. Valone. A one-to-one mapping between one-particle densities and some n-particle ensembles. *J. Chem. Phys.*, 73(9):4653, 1980.

NG Van Kampen. *Stochastic processes in physics and chemistry*. North Holland, 2007.

A. Van Lauwe. *Modélisation des collisions nucléaires aux énergies de Fermi : validation à l'aide des données INDRA*. PhD thesis, Université de Caen, 2003. LPCC T 03-05.

D. Vautherin and D. M. Brink. Hartree-Fock calculations with Skyrme's interaction. 1. Spherical nuclei. *Phys. Rev.*, C5:626, 1972.

D. Vautherin. Hartree-Fock Calculations with Skyrme's Interaction. II. Axially Deformed Nuclei. *Phys. Rev. C*, 7:296, 1973.

K. Washiyama and D. Lacroix. Energy dependence of the nucleus-nucleus potential close to the Coulomb barrier. *Phys. Rev. C*, 78:024610, 2008.

K. Washiyama, S. Ayik, and D. Lacroix. Mass dispersion in transfer reactions with a stochastic mean-field theory. *Phys. Rev. C*, 80:031602, 2009.

K. Washiyama, D. Lacroix, and S. Ayik. One-body energy dissipation in fusion reactions from mean-field theory. *Phys. Rev. C*, 79:024609, 2009.

H.A. Weidenmüller. Transport theories of heavy-ion reactions. *Prog. Part. Nucl. Phys.*, page 49, 1980.

U. Weiss. *Quantum Dissipative Systems*. World Scientific, Singapore, 2nd ed., 1999.

G. C. Wick. The evaluation of the collision matrix. *Phys. Rev.*, 80:268, 1950.

C.-Y. Wong and H. H. K. Tang. Extended Time-Dependent Hartree-Fock Approximation with Particle Collisions. *Phys. Rev. Lett.*, 40:1070, 1978.

C-Y Wong and H. H. K. Tang. Dynamics of nuclear fluid. V. Extended time-dependent Hartree-Fock

approximation illuminates the approach to thermal equilibrium. *Phys. Rev. C*, 20:1419, 1979.

K. Yasuda. Local approximation of the correlation energy functional in the density matrix functional theory. *Phys. Rev. Lett.*, 88:053001, 2002.

PG Young, ED Arthur, and MB Chadwick. Comprehensive nuclear model calculations: introduction to the theory and use of the GNASH code. Technical report, LA–12343-MS, Los Alamos National Lab., NM (United States), 1992.

H. Zduńczuk, W. Satuła, J. Dobaczewski, and M. Kosmulski. Angular momentum projection of cranked Hartree-Fock states: Application to terminating bands in A∼44 nuclei. *Phys. Rev. C*, 76:044304, 2007.

Y. Zhou, Y. Yan, and J. Shao. Stochastic simulation of quantum dissipative dynamics. *Europhys. Lett.*, 3:334, 2005.

M.V. Zhukov, B.V. Danilin, D.V. Fedorov, J.M. Bang, I.J. Thompson, and J.S. Vaagen. Bound state properties of Borromean halo nuclei: ^{6}He and ^{11}Li. *Phys. Rep.*, 231:151, 1993.

G. Zumbach and K. Maschke. Density-matrix functional theory for the N-particle ground state. *J. Chem. Phys.*, 82:5604, 1985.

B. Zumino. Normal forms of complex matrices. *J. Math. Phys.*, 3:1055, 1962.